NOTE TO USERS

This reproduction is the best copy available.

UMI®

OPTIMIZATION AND MODELING OF AN
EMULSION POLYMERIZATION
REACTOR

By

Narges Ghadi

Bachelor of Chemical Engineering

Sharif University of Technology

Iran, 2000

A thesis

Presented to Ryerson University

In partial fulfillment of the

requirement for the degree of

Master of Applied Science

In the Program of

Chemical Engineering

Toronto, Ontario, Canada, 2004

Copyright © 2004 by Narges Ghadi

UMI Number: EC52949

INFORMATION TO USERS

The quality of this reproduction is dependent upon the quality of the copy submitted. Broken or indistinct print, colored or poor quality illustrations and photographs, print bleed-through, substandard margins, and improper alignment can adversely affect reproduction.

In the unlikely event that the author did not send a complete manuscript and there are missing pages, these will be noted. Also, if unauthorized copyright material had to be removed, a note will indicate the deletion.

UMI®

Borrower's Page

Ryerson University requires the signature of all persons using or photocopying this thesis. Please sign below and give address and date.

iii

Optimization and Modeling of an Emulsion Polymerization Reactor

Narges Ghadi, 2004

Master of Applied Science

Chemical Engineering Department

Ryerson University

Abstract

A mathematical model was developed to simulate emulsion polymerization in batch, semi-batch and continuous reactors for monomers with high water solubility and significant desorption such as vinyl acetate. The effects of operating conditions such as initiator and emulsifier concentration as well as reactor temperature have been studied. The simulation results revealed the sensitivity of polymer properties and monomer conversion to variation of these operating conditions. Furthermore, the impact of monomer soluble impurities on reduction of monomer conversion has been investigated. In order to control polymer molecular weight, application of chain transfer agents such as t-nonyl mercaptan was suggested. Generally, the simulation results fitted well experimental data from the literature.

Several optimization policies were considered to enhance the reaction operation for better product quality. During continuous polymerization, the reactor demonstrates oscillatory behavior throughout the operation. A new reactor train configuration was considered with the aim of damping the oscillations and producing high-quality latex.

Acknowledgments

First of all, I would like to express my sincere appreciation to my supervisors, Dr. Muhammed Fayed and Dr. Ramdhane Dhib. This work wouldn't have been recognized without their guidance and support. Dr. Fayed provided me with motivation as well as many helpful comments, advice and guidance regarding this thesis. I learned a lot from my conversations with him. His guidance was not only helpful for improvement of this work but also effective to enhance my insight towards life in general. Furthermore, I am thankful to Dr. Dhib for his extensive help and unsurpassable patience. Without his fatherly attention as well as continuous flow of ideas and improvements, I could not be able to come this far and pass all the problems.

Special thanks goes to Professor Alex Penlidis, Waterloo University, to whom I am deeply grateful for many valuable correspondence despite his busy schedule. I was really impressed by his valuable technical advice on emulsion polymerization as well as friendly manner.

Suggestions and contributions from the committee members, Dr. Philip Chan, Dr. Huu Doan and Dr. Darrick Heyd, were considerably helpful in the improvement of this thesis. I wish to extend my deepest appreciation to them as well.

I should also mention that this research would not be possible without the financial support of NSERC, School of Graduate Studies and Department of Chemical Engineering at Ryerson University.

Most importantly, I would like to thank my parents and Tirgari's family and all other relatives and friends for their understanding and support throughout these years.

Dedications

To my parents for their unconditional love and endless support during all my life

To Tirgari's family for their emotional support and invaluable assistance

Table of Contents

List of Tables

ix

List of Figures

xii

Nomenclature

$a_p(t,\tau)$ Initial particle surface area at birth, dm^2

$A_m(t)$ Total surface area of the micelles, dm^2/L-latex

$A_p(t)$ Total polymer particle surface area, dm^2/L-latex

$\overline{B}_N(t)$ Average number of long-chain branch points per polymer molecule, 1/L-latex

C_p Heat capacity, cal/g.K

$[CTA(t)]$ Chain transfer agent concentration, mol/L

$d_p(t,\tau)$ Initial particle diameter at birth, dm

$D_p(t)$ Total polymer particle diameter, dm/L-latex

DP_{max} Maximum degree of polymerization

D_w Diffusion coefficient of monomeric radicals in water phase, dm^2/s

f   Initiator efficiency

$f(t)$ Net particle generation rate, 1/L-latex.s

FT Total volumetric flow rate to the second reactor, mL/min

ΔH_r Reaction enthalpy, cal/mol

I Initiator

$I^\bullet$ Initiator Radical

I_F Initiator concentration in feed stream, mol/L

I_{R1} Initiator volumetric flow rate to R_1, mL/min

$[I(t)]$ Initiator concentration, mol/L

k_{ab} Absorption rate constant, dm/s

k_d Decomposition rate constant of initiator, 1/s

k_{de} Radical desorption coefficient, 1/s

k_{fcta}	Rate constant for transfer to chain transfer agent, L/mol.s
k_{fm}	Rate constant for transfer to monomer, L/mol.s
k_{fp}	Rate constant for transfer to polymer, L/mol.s
k_h	Specific homogeneous nucleation rate constant, 1/s
k_{h0}	Rate coefficient of homogeneous nucleation, 1/s
k_m	Rate coefficient of micellar nucleation, 1/s
k_{MI}	Rate constant for transfer to impurity, L/mol.s
k_p	Rate constant of propagation, L/mol.s
k_p^*	Rate constant of terminal double bond, L/mol.s
k_{tc}	Rate constant of termination, L/mol.s
k_{tw}	Rate constant of termination in water phase, L/mol.s
k_v	Ratio of volume of emulsion phase over the volume of aqueousphase, L- latex/L
L	Critical diffusion length of radicals, dm
m	Partition coefficient of monomeric radicals between water andparticle
M_1	Monomer flow rate to the first reactor (R_1), mL/min
M_F	Monomer concentration in feed stream, mol/L
M_{wc}	Saturation concentration of monomer in the water phase, gmole/L
MI_F	Monomer soluble impurity's concentration in feed stream, mol/L
$[M(t)]$	Monomer concentration, mol/L
$[MI(t)]$	Monomer soluble impurity's concentration, mol/L
$[MI_p(t)]$	Monomer soluble impurity's concentration in polymer phase, mol/L
Mw_M	Monomer molecular weight, gmole/mole
$\overline{M}n(t)$	Number average molecular weight, g/mole
$\overline{M}w(t)$	Weight average molecular weight, g/mole
$[M_P]$	Monomer concentration in polymer particles, mol/L
$n(t,\tau)$	Number of polymer particles born between

times τ and $\tau+d\tau$, 1/L-latex

N_A	Avogadro's number, 6.023×10^{23} molecules/mole
$N_P(t)$	Total number of polymer particles, 1/L-latex
P_r	Dead polymer with chain length r
$\bar{q}(t,\tau)$	Average number of radicals per particle associated with the class of particles, $n(t,\tau)$
r	Chain length
R	Gas constant, Cal/mol.K.
$R_I(t)$	Rate of initiation, 1/L-latex.s
$R_p(t)$	Rate of polymerization, mole/L-latex.s
$R_r^\bullet$	Live radical with chain length r
$[R_w^\bullet(t)]$	Concentration of free radicals in water phase, 1/L-latex
$[S(t)]$	Emulsifier concentration, mole/L-latex
$[S(t)]_{CMC}$	Critical micelle concentration, mole/L-latex
Sa	Area occupied by an emulsifier molecule, dm^2/molecule of soap
S_F	Emulsifier concentration in feed stream, mol/L
S_p	Flow split
S_{R1}	Emulsifier volumetric flow rate to R_1, mL/min
t	Time, s
t_f	Time corresponding to the end of stage 1, s
T	Reactor temperature, K
T_j	Cooling medium temperature, K
UA	Product of total heat transfer coefficient and area, cal/K
$v(t,\tau)$	Polymer volume associated with the class of particles $v(t,\tau)$, L-polymer/L- latex
$V_p(t)$	Total volume of polymer particles, L/L-latex
x(t)	Monomer conversion
x_c	Critical conversion

Chapter 1

Introduction

1.1 Emulsion Polymerization

Emulsion polymerization is an important industrial polymerization process for manufacturing water based polymers such as: latex paints, rubbers, coatings and adhesives. Latexes are currently undergoing extensive research and development as key replacement materials for many solvent-based systems. Emulsion polymerization is a free radical reaction carried out under heterogeneous conditions and it is mostly used for the synthesis of wide range latex polymers on a commercial scale. The advantages of emulsion polymerization include favourable kinetics, safety, environmental and compositional control, high solid level and conversion. The low viscosity of latexes allows a high rate of heat transfer during polymerization.

Four essential components are required to carry out an emulsion polymerization process: the dispersion medium which is in general water, the monomer which is often slightly soluble in water, the water soluble initiator and an emulsifier. The heterogeneous nature of the process requires the diffusion of the monomers from the emulsified droplets, through the aqueous medium into the polymer particles where the polymerization takes place. Therefore, the monomer should be soluble enough to allow effective diffusion. In fact, very hydrophobic monomers are not suitable for emulsion polymerizations. The water-soluble initiator commonly used is potassium or sodium persulfate. The polymer produced is in the form of small particles having an average diameter around 5 μm.

Emulsion polymerization can be done in batch, semi-batch and continuous stirred tanks reactors (CSTR). In commercial batch reactors, it has been found that there is an always small variation, from batch to batch in monomer conversion, particle number and size, molecular weight and polymer branching. Operation of CSTRs for emulsion polymerization offers several advantages over batch reactors, the most important of which are high production rate and better polymer quality. CSTRs may eliminate the problem

1

encountered in batch reactors and also produce polymers with narrower molecular weight distribution (MWD). End-use properties of polymers (flexibility, elasticity...) are related to molecular morphology and particle size, which strongly depend on the reactor type and operating conditions (temperature, monomer or initiator concentration, initiator type and cooling medium flow rate).

Research on modelling, optimization and control of the emulsion polymerization reactors has been expanding rapidly due to the increasing demand for new and high quality latex products. The objectives are usually to maximize the production rate and to control product properties such as polymer particle size distribution, long chain branching and crosslinking.

The success of optimization methods is highly dependent on the availability of valid dynamic models for the chemical changes occurring in this complex polymerization. In case of optimization and control, the reactor model should be detailed and precise enough to predict the effect of the main process input variables on the output variables, and to represent well the relationship between operating conditions, kinetics and final product properties. The model should also remain at a precision level allowing optimal profile determination and control law computation.

The main purpose of this thesis is to study the emulsion polymerization mechanism and try to develop a mathematical model, which can describe the process behaviour throughout the reaction. The model mainly considers the behaviour of highly water soluble monomers by application of population balance theory. After that the model should be tested and verified with experimental data over different operating conditions in order to show its capability to simulate the emulsion reaction in batch, semi-batch and continuous reactors. The verified model is then used to find optimal policies for feed and reactor temperature for the production of high quality polymer, which in turn is highly dependent on operating conditions.

Based on the objectives, the following part briefly describes the order of contents of this thesis.

2

1.2 Organization of Thesis

Chapter 2 of this study reviews studies done on emulsion polymerization. The review shows how the understanding and modeling of emulsion polymerization has gradually progressed over the years. Chapter 3 consists of two sections. The first section deals with understanding the process and the second section describes the steps of model development for emulsion polymerization processes of case 1 monomers, which can predict the rate of change of reactants through the reaction as well as product properties.

The formulated model is then tested to simulate a well-mixed reactor in different modes (batch, semi-batch and continuous), whose results fitted well experimental data from the literature (Chapter 4). In polymerization industry, it is very incentive to produce high quality polymers and achieve high monomer conversion. Therefore, in addition to simulation results. Chapter 4 includes optimization policies with the aim of achieving desired product property and high monomer conversion. The end-product properties are related to the structure of the polymer molecules, which can be described in terms of molecular weight distribution (MWD), molecular weight averages ($\overline{Mn}, \overline{Mw}$) and number of branching points ($\overline{B}_N$). Furthermore, new train configurations are presented to keep the reactor under stable conditions, which is highly desirable in industry to prevent serious implications like runaway during the high portion of the conversion oscillation. Chapter 5 summarizes the most important concluding remarks and finally Chapter 6 proposes recommendations for future studies.

3

Chapter 2
Literature Review

In recent years considerable advances have been made in the modeling of emulsion polymerization reactions. The basic mechanism for emulsion polymerization was first postulated by Harkins (1947). Smith and Ewart (1948) were the first group that quantitatively expressed Harkin's postulation in an empirical formulation. Models in 1960s and 1970s were more or less extended/modified versions of the Smith-Ewart's theory.

In general, particle nucleation phenomena as well as balances for particle size distribution (PSD) were not included in emulsion polymerization models developed before 1974. Now both homogeneous nucleation and micellar nucleation mechanisms are considered in most models. Two levels of models are used to calculate the particle size.

- The monodispersed approximation method: models the number of particles and the total particle volume assuming monodispersed particles.
- Age distribution analysis method: uses moments of these distribution equations to get the total or average properties.

Penlidis et al. (1984) worked on modeling of the continuous emulsion polymerization of vinyl chloride. Their model was able to predict monomer conversion, polymer particle size distribution, molecular weight distribution and long and short branching frequencies. New reactor train configurations were also suggested to keep the reactor operation in a stable mode. Another research group, Lu and Lin (1985), proposed a model for absolute particle size distribution in continuous emulsion polymerization of styrene based on the modified population balance theory. The effect of emulsifier and initiator concentrations as well as mean residence time on the product properties were investigated.

Later, Penlidis (1986) modified the previous models based on particle age distribution analysis and simulated dynamic behaviour of emulsion polymerization reactor

4

in different modes (batch, semi-batch and continuous) for vinyl acetate and vinyl chloride monomers. Experimental studies were also carried out to demonstrate the improved performance of the modified model. Lu and Lin (1986) found the best value for desorption coefficient by comparing theoretical predictions with experimental data. The effect of radical desorption as well as residence time on the quality of the product were analyzed.

A model predicting the behaviour of emulsion polymerization reactors on the basis of population balance equations was formulated by Rawlings and Ray (1988). Model predictions were compared with experimental data of styrene, methyl methacrylate and vinyl acetate. They were in good agreement with laboratory data and the model was capable of predicting other experimentally observed phenomena like sustained oscillations and overshoots during the continuous reactor's start-up. The effect of water soluble and monomer soluble impurities on the kinetics of emulsion polymerization reactor were carried out experimentally by Penlidis et al. (1988). The outcome of their study revealed that impurities could have an appreciable effect on both polymer particle nucleation and growth.

In a more recent study, Chiu and Lee (1997) worked on seeded soapless emulsion polymerization. Poly (methyl methacrylate) (PMMA) was considered as seeds, styrene as monomer and potassium persulfate ($K_2S_2O_8$) as initiator. They modified the core-shell model proposed in previous studies to predict the monomer conversion that fitted well with the experimental data. Meira et al. (1998) investigated a starved emulsion polymerization of styrene in order to control the molecular weights of the product. The reactor was operated under a starved feed of a mixture of monomer and chain transfer agent (tert-dodecyl and tert-nonyl mercaptans). This method produced a constant molecular weight distribution along the polymerization. For better interpretation of effect of chain transfer agent's length, a mathematical model was developed. Two batch experimental reactors were used to adjust some of the model parameters.

Nomura et al. (2001) conducted emulsion polymerization of styrene in a Couette-Taylor Vortex flow reactor (CTVFR). They developed a model by combining the empirical correlation of the mixing characteristics of a CTVFR and a CSTR. Experimental results revealed that a CTVFR is more suitable to be used as a first reactor in a reactor system for continuous emulsion polymerization. Further, Pinto et al. (2001) formulated a mathematical

model to compute dynamic evolution of molecular weight distributions (MWDs) during nonlinear emulsion polymerization reactions. The MWDs were calculated by application of an adaptive orthogonal collocation technique. The model was in agreement with experimental data of methyl methacrylate/butyl acrylate (BuA) in semi continuous and of vinyl acrylate (VA)/veova10 in continuous emulsion polymerization reactors. Both reaction systems show significant chain transfer reactions to polymer chains due to the presence of BuA and VA, respectively. The model was able to predict quite properly the kinetics and MWD of polymer samples during emulsion polymerizations.

Recently, Gao and Penlidis (2002) developed a complete computer database package for emulsion homo-/copolymerization under wide range of reaction and operation conditions (batch, semi-batch, seeded or unseeded, etc.). This comprehensive model was able to describe all important physicochemical phenomena in emulsion polymerization both qualitatively and quantitatively. The effects of particle nucleation, absorption and desorption of radicals, monomer partitioning and gel effect were also investigated.

Kiparissides and his coworkers (2002) investigated the influence of oxygen concentration on the polymerization rate and particle size distribution (PSD). Since the generated radicals due to initiator decomposition are scavenged by dissolved oxygen, a reduction of polymerization rate was observed as a consequence of increasing the oxygen concentration in the water phase. More recently, a model was reported by Doyle III et al. (2003) for emulsion polymerization of styrene under nonisothermal condition. The model was used to control particle size distributions. Sensitivity results suggested that operation of reactor under semi-batch condition rather than batch mode increases the accuracy of online measured model parameters. The nonosithermal operation of the reactor revealed that the reactor temperature could be manipulated to achieve desired final product properties.

Since emulsion homopolymerization is a very complex system, modeling of emulsion copolymerization is an even more challenging task. Therefore, more modeling is required for a better understanding of the complicated physicochemical reaction phenomena. The structure of a copolymerization model is similar to that of a homopolymerization model. However, in emulsion copolymerization, certain phenomena like monomer partitioning and radical desorption require some modifications. Broadhead et

6

al. (1985) developed a dynamic model to predict polymer particle properties such as molecular weight averages ($\overline{Mn}, \overline{Mw}$) and particle size distribution for the emulsion copolymerisation of styrene/butadiene. The model was used to design, optimize and control emulsion copolymerisation in well-mixed stirred tank reactors operated in batch, semi-batch and continuous modes for transient and steady state operations. Multicomponent free radical polymerization for solution and emulsion systems were carried out by Hamielec et al. (1987). The model was considered to be applicable to several comonomer systems such as: styrene/acrylonitrile, p-methyl styrene/acrylonitrile and styrene/butadiene. Free volume theory used to represent diffusion-controlled termination and propagation reactions.

Beside distinctive study on emulsion homopolymerization, Penlidis et al. (1996) simulated the emulsion copolymerization of acrylonitrile/ butadiene (nitrile rubber). The main objective was to predict rates of production of polymer and product properties in an industrial setting. The predicted monomer conversion was in good agreement with industrial pilot-plant data.

Industrial emulsion (co) polymerization is generally performed in large-scale semi-batch processes because of the process flexibility. During most batches, certain components such as emulsifier, chain transfer agent and monomer have to be added to control the particle size distribution and other properties of the polymer. Scholtens et al. (2001) designed a tubular continuous flow reactor, a pulsed packed column (PPC), as an alternative for semi-batch reactors. The production of copolymers of styrene and methyl acrylate was investigated to test the performance of the new reactor arrangement. The main advantage of the column is its ability to be operated under steady state condition in improved temperature control and elimination of batch-to-batch variations.

In more recent study, Doyle III et al. (2003) developed a population balance model for the particle size distribution in the emulsion copolymerization of vinyl acetate and butyl acrylate with non-ionic poly (ethylene oxide) surfactants and a redox initiator. The effects of nucleation, growth and coagulation events were accounted for in the model. The model predicts to a reasonable accuracy the experimental data on the particle size distribution.

The demand for producing polymers with special properties rose academic interest in the control and optimization of emulsion polymerization reactors. Some recent

7

contributions to the area of optimization of polymerization reactor operation are surveyed herein. Wu and co-workers (1982) were one of the first groups who studied optimization schemes for bulk polymerization of styrene both theoretically and experimentally. They found optimal temperature policies by employing boundary condition iteration method to reach the final conversion and molecular weight averages. Later on, Jang and Yang (1989) employed a mixed integration collocation method (MICO) to obtain initiator feed policies for minimizing the batch time of an emulsion polymerization reactor producing polyvinyl acetate. Constrains during their optimization were maximum polymerization rate and an upper limit on the total amount of initiator.

Furthermore, they proposed a minimum final-time initiator concentration and/or temperature policies (Jang and Lin, 1991). Previously, it was assumed that the optimal initiator policy for the operation of a batch vinyl acetate latex reactor could be approximated by a collocation polynomial. But in their new study, the discontinuous policies were found using finite-element collocation method. Since the physical and chemical properties of the latex are usually different during different stages of polymerization, the discontinuous policies were shown to be superior to continuous ones.

Other attempts were made to enhance the polymer quality and investigate benefits of applying optimal operating conditions. Liang et al. (1992) developed optimal control policies for free radical polymerization of styrene in a batch reactor. A multi objective dynamic optimization technique was employed: monomer conversion, polymer molecular weight, initiator residue level and total reaction time. The results showed the realization of optimal initiator mixture and reactor temperature can significantly improve the performance of the batch process.

Leiza et al. (1993) determined minimum amount of monomer required to initially form copolymer with desired composition in semi-batch emulsion copolymerisation reactors. Corroiu et al. (1999) worked on the optimization of a batch reactor temperature for emulsion polymerization of styrene and α-methylstyrene. They minimized the reaction final time. Constraints were imposed on the end-product latex properties and thermal limitations of the pilot plan. The optimal temperature profile was tracked using a nonlinear

8

geometric control technique, which is particu... y adapted to polymerization reactor control. Experimental results showed good agreement with model predictions.

A control strategy for a simultaneous control of microstructural properties of copolymer latex was presented by Asua et al. (2002). The implementation of the open-loop control allowed the production of MMA/n-BA emulsion copolymers of a well-defined copolymer composition and molecular weight distribution. Gao et al. (2004) reviewed several commonly used process optimization policies. Since it is highly desirable in industry to reduce the production cost and produce a high quality polymer, the reactor temperature with selective mono- or bifunctional initiators were employed to decrease batch time for pre-specified molecular weight averages.

Due to high demand of producing high quality polymers by emulsion polymerization method, this mechanism still needs to be more studied and effect of various parameters on enhancement of product property should be further investigated. Therefore this study deals with modeling and simulation of emulsion homopolymerization. Furthermore the simulation results are employed to optimize the process by calculating optimal operating condition and also keep the reactor under stable and safe condition in order to avoid any runaway problem.

Chapter 3
Development of Kinetic Model for Emulsion Polymerization Reaction

This Chapter is dedicated for explaining the detail mechanism as well as the methodology for development of model for this mechanism. It is divided to two main sections: Reaction mechanism and Model development respectively.

3.1 Reaction Mechanism

The physical picture of emulsion polymerization is based on the original qualitative mechanism of Harkins [1947] and the quantitative theory of Smith [1948]. A simplified schematic representation of an emulsion polymerization system is shown in Figure 3.1. Emulsifier dissolves into water until its concentration reaches the critical micelle concentration (CMC). When the concentration exceeds the CMC value, it will form aggregates called micelles. Typical micelles have diameters of 2-10 nm with each micelle containing 50-150 emulsifier molecules. The emulsifier molecules are self-arranged into a micelle with their hydrophilic ends pointing towards the aqueous phase and their hydrophobic ends pointing outwards.

Generally, monomers can exist inside the micelles or form large monomer droplets but since monomers are usually slightly soluble in water, the largest portion of them is dispersed as monomer droplets in the water phase. The initiator present in the water phase decomposes into initiating radicals. The most common initiators are potassium or sodium persulfate which are insoluble in organic monomers. Therefore, the micelles act as a meeting place for the monomer and the initiator.

Emulsion polymerization is considered to undergo through three intervals:

- Stage 1: Particle nucleation and increasing growth rate
- Stage 2: Constant growth rate
- Stage 3: Decreasing polymerization rate

10
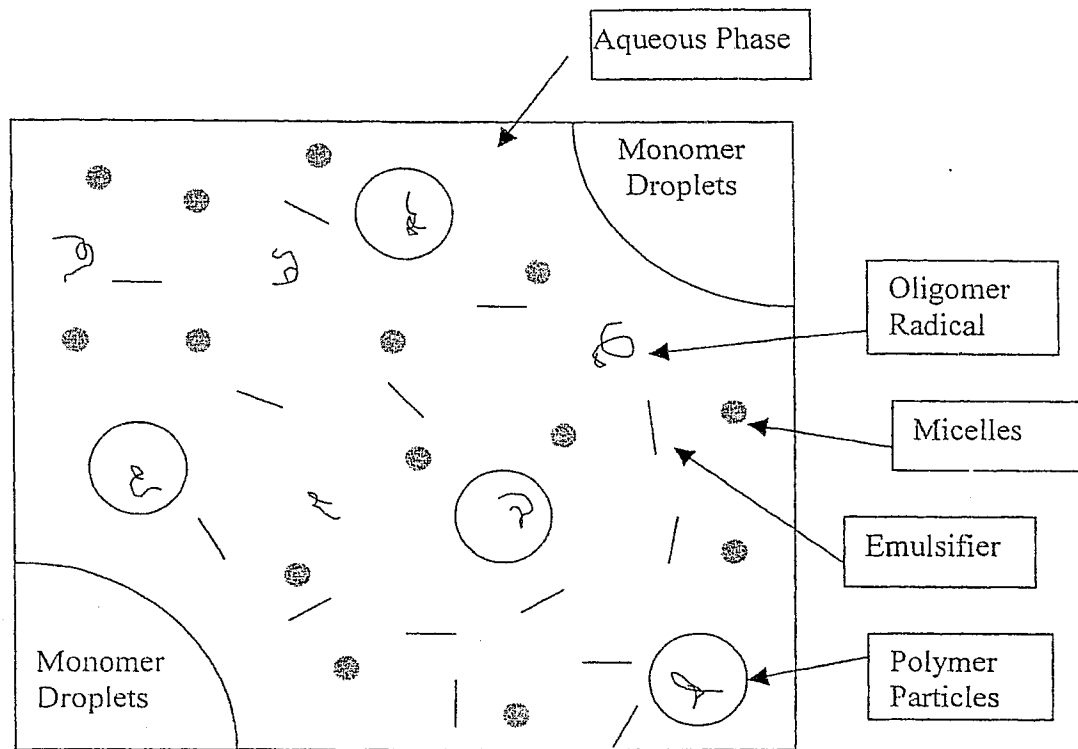
Figure 3. 1. Emulsion Polymerization Diagram (stages 1 and 2)

As the polymer particles grow in size they absorb more and more emulsifier, causing the emulsifier concentration to fall under the CMC level so the micelles will disappear. At this point the number of generated particles becomes a constant and the particle size continues to grow. In general, the number of particles increases with time in Stage 1 and then remains constant in stage 2 and 3.

The final number of polymer particles is achieved in a very short time and subsequently starts to grow during stage 2. The fall of free emulsifier concentration under the CMC level characterizes the end to stage 1. Without micelles, no new particle generation occurs. However, monomer droplets and aqueous free radicals are still present and diffuse into polymer particles.

Hence, polymer particles continue to grow in the second stage by absorbing monomer from monomer droplets. The second interval ends when all monomer droplets are consumed and after disappearance of all monomer droplets, polymer particles are the only

11

component present in the system. The final stage begins when the polymerization rate start decreasing as the monomer concentration in the polymer particles decreases. Furthermore, the number of generated particles remains the same as stage 2 because no more new generation happens in this stage. Based on these stages, the general reaction mechanism of emulsion polymerization can be described as:

3.1.1 Reaction Steps

Initiation

The first step in a polymerization reaction involves the creation of highly reactive free radicals. The initiator will decompose into two reactive free radicals, which then react with monomers to produce primary radical $R_1^{\bullet}$. The most commonly used initiator in emulsion polymerization reaction is potassium persulfate.

$$S_2O_8^{-2} \xrightarrow{\ k_d\ } 2SO_4^{-\bullet} \tag{3.1}$$

$$SO_4^{-\bullet} + M \xrightarrow{\ k_1\ } R_1^{\bullet} \tag{3.2}$$

Propagation

The second and main step of emulsion polymerization reaction starts when the generated radicals propagate with monomer. The reaction results in a live polymeric radical chain of length $r+1$.

$$R_r^{\bullet} + M \xrightarrow{\ k_p\ } R_{r+1}^{\bullet} \quad r \geq 1 \tag{3.3}$$

Termination

Live polymer radicals may terminate upon encountering each other. This termination may occur by a combination or disproportionation of live radicals:

Termination by combination

$$R_r^{\bullet} + R_s^{\bullet} \xrightarrow{\ k_{tc}\ } P_{r+s} \tag{3.4}$$

Termination by disproportionation

$$R_r^{\bullet} + R_s^{\bullet} \xrightarrow{\ k_{td}\ } P_r + P_s \tag{3.5}$$

12
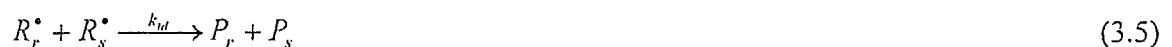
Chain transfer to monomer

In general, the case I monomers such as vinyl acetate or vinyl chloride are characterized by polar monomers with moderate solubility in water and a relatively high rate of radical chain transfer to monomer during emulsion polymerization:

$$R_r^* + M \xrightarrow{\quad k_{tpm} \quad} P_r + R_1^* \tag{3.6}$$

Chain transfer to polymer

The radicals may undergo chain transfer to polymer. In many practical circumstances this reaction is negligible.

$$R_r^* + P_s \xrightarrow{\quad k_{tp} \quad} R_s^* + P_r \tag{3.7}$$

Chain transfer to chain transfer agent

The radicals may react with a chain transfer agents:

$$R_r^* + CTA \xrightarrow{\quad k_{tcta} \quad} P_r + CTA^* \tag{3.8}$$

Chain transfer to inhibitor

Live radicals can react with impurities. Two kinds of impurities can be present in emulsion reactors: water soluble impurity and monomer soluble impurity. Oxygen is the most common impurity that consumes reactive radicals in the water phase, preventing the particle growth. Its reaction with live radicals is represented as:

$$R_r^* + IW \xrightarrow{\quad k_{IW} \quad} IW^* + P_r \tag{3.9}$$

Monomer soluble impurities may be transferred in to polymer particles during the diffusion of monomer from its droplets to micelles according to the following reaction.

$$R_r^* + MI \xrightarrow{\quad k_{MI} \quad} MI^* + P_r \tag{3.10}$$
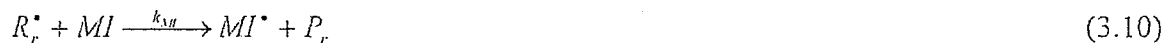
Terminal double bond polymerization

Live radicals and dead polymer may undergo reaction with terminal double bonds. This kind of reaction yields trifunctional branch points.

13

$$R_n^\bullet + P_m \xrightarrow{k_p^\bullet} R_{n+m}^\bullet \qquad (3.11)$$

The rate constants of all reactions are described in the nomenclature and their numerical values are tabulated in Table 3.1.

Feeding Cylinders
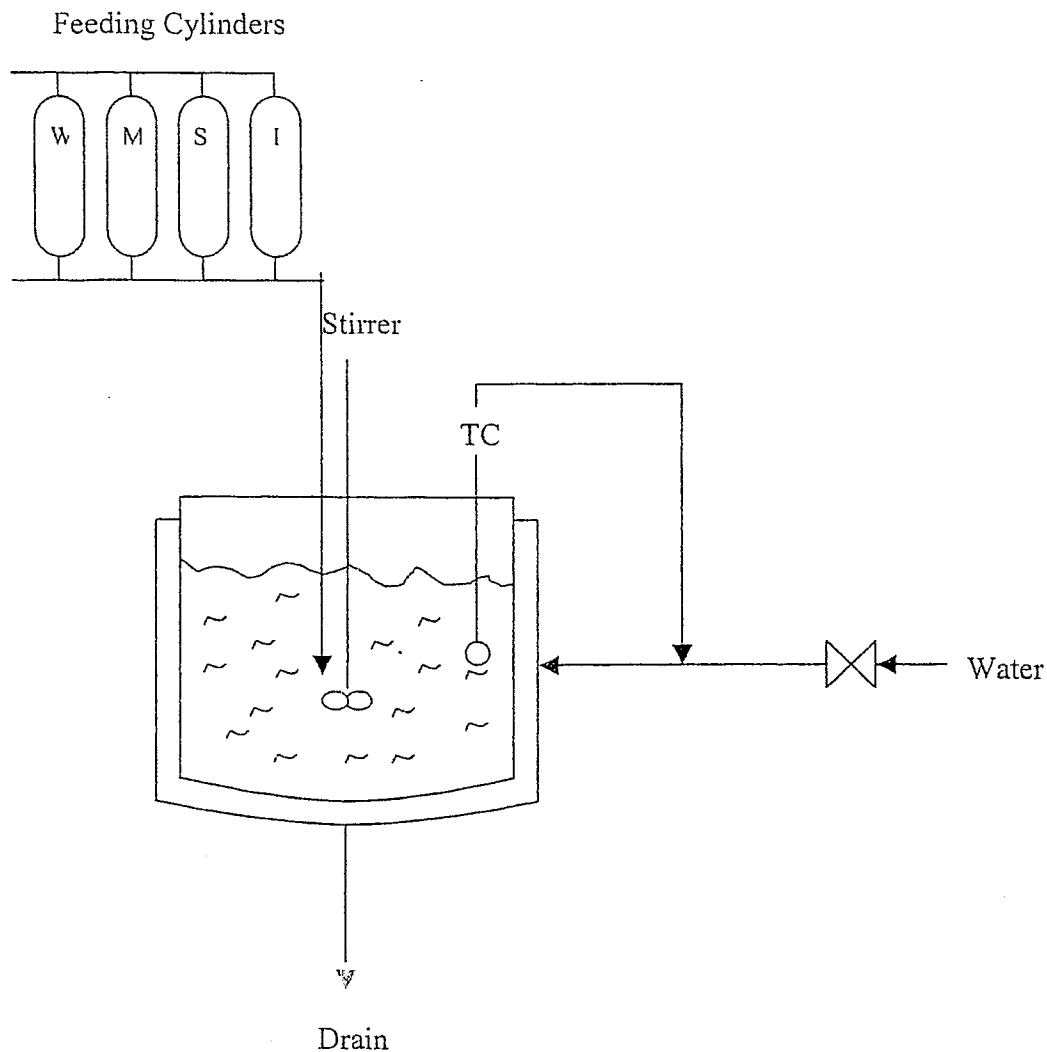
Figure 3. 2. Schematic Diagram of an Experimental Batch Reactor

Figure 3.2 shows a typical batch reactor employed for emulsion polymerization. The feed is injected through small capsules (W=Water, M=Monomer, S=Emulsifier, I=Initiator). Since the reaction is exothermic, a cooling jacket is designed to remove the generated heat during the reaction. A temperature controller (TC) is used to keep the reactor temperature constant.

14

3.2 Development of Kinetic model

Models for emulsion polymerization reactors vary greatly in their complexity (Penlidis, 1986; Odian, 1991; Kumar and Gupta, 1998). In the case of designing a controller, the reactor model should be detailed enough and precise. In order to develop the model for this process, a molar balance for each reactant, and molecular weight development equations for both linear and branched systems are included in this part. For emulsion polymerization monomers are usually classified into three categories:

- Case 1: monomers with high water solubility and significant desorption, like vinyl acetate, vinyl chloride.
- Case 2: monomers with low water solubility and negligible desorption, like styrene, butadiene.
- Case 3: monomers that exhibit significant gel effect like MMA.

The model herein is used to study the characteristics of vinyl acetate further. The main characteristics of emulsion polymerization of vinyl acetate when there is no chain transfer agent and inhibitor in the reactor are:

- The gel effect is usually not observed.
- Termination reactions are not as important as they are in bulk reactions.
- Molecular weight is mainly controlled by chain transfer reactions to monomer and polymer.
- Chain transfer to monomer is the first step in the desorption process.

In this section, the concentration of each species in the feed stream is designated by the subscript F and θ represents the average residence time of the stream in the reactor.

3.2.1 Rate of change of monomer concentration in reactor

The monomer molar balance comprises the inflow and outflow of the monomer and its consumption due to the propagation reaction. The inflow of monomer increases the rate of accumulation of the monomer while its outflow in addition to the reaction of monomer result in a decrease in $\dfrac{d[M(t)]}{dt}$.

15

$$\frac{d[M(t)]}{dt} = \frac{[M(t)]_F}{\theta} - \frac{[M(t)]}{\theta} - R_p(t) \tag{3.12}$$

3.2.2 Rate of change of monomer conversion

The molar conversion of the monomer to polymer can be calculated by the following equation:

$$x(t) = \frac{[M(t)]_F - [M(t)]}{[M(t)]_F} \tag{3.13}$$

Differentiating equation (3.13) and considering equation (3.12) yields the rate of change of monomer conversion:

$$\frac{dx(t)}{dt} = \frac{R_p(t)}{[M(t)]_F} - \frac{x(t)}{\theta} \tag{3.14}$$

3.2.3 Rate of change of initiator concentration

A molar balance can be written for the concentration of initiator as follows:

$$\frac{d[I(t)]_w}{dt} = \frac{[I(t)]_F}{\theta} - \frac{[I(t)]_w}{\theta} - k_d[I(t)]_w \tag{3.15}$$

Where the subscript, w, represents the water phase

3.2.4 Rate of change of emulsifier concentration

The emulsifier may exist in micelles, monomer droplets, polymer particles and aqueous phase. Generally the molar balance on this component can be written as:

$$\frac{d[S(t)]}{dt} = \frac{[S(t)]_F}{\theta} - \frac{[S(t)]}{\theta} \tag{3.16}$$

3.2.5 Radical concentration balance

Radicals captured in the micellar nucleation of polymer particles are assumed to obey the collision theory. They are produced by initiation in water phase ($\rho_i(t)$) and desorption from polymer particles ($\rho_{des}(t)$). These generated radicals may be captured by micelles and particles or terminate by meeting other radicals. They can also undergo homogenous nucleation.

16

$$\frac{d[R_w^\bullet(t)]}{dt} = \frac{[R_w^\bullet(t)]_F}{\theta} - \frac{[R_w^\bullet(t)]}{\cdot \theta} + (\rho_i(t) + \rho_{des}(t))N_A$$

$$- k_m A_m(t)[R_w^\bullet(t)]k_v - k_h[R_w^\bullet(t)] - k_{ah}A_p(t)[R_w^\bullet(t)]k_v - k_{tw}[R_w^\bullet(t)]^2(k_v/N_A) \qquad (3.17)$$

In driving equation (3.17) it is assumed that the rate of radical capture is proportional to the total surface available for radical capture. The forth term on the right of equation (3.17) represents the rate at which radicals are captured by micelles. $A_m(t)$ is the free micellar area and k_m is the rate coefficient of micellar nucleation.

The next term in equation (3.17) represents the rate of homogeneous nucleation of particles, which means polymer particles can be generated even though the micelles do not exist. ·

The term $k_{ah}A_p(t)[R_w^\bullet(t)]k_v$ stands for the rate at which radicals are captured by polymer particles, and it is proportional to the total particle area, $A_p(t)$, and the radical concentration, $[R_w^\bullet(t)]$. k_{ah} is an overall transport coefficient for radical transfer from the aqueous phase into polymer particles and the constant k_v is the volume of emulsion phase over the volume of aqueous phase . The last term shows termination of radical in the water phase in which k_{tw} is the rate constant for termination in water phase.

Application of the steady state hypothesis for live radical concentration as well as neglecting radical termination in water phase gives:

$$[R_w^\bullet(t)] = \frac{(\rho_i(t) + \rho_{des}(t))N_A}{k_m A_m(t)k_v + k_h + k_{ah}A_p(t)k_v} = \frac{\rho(t)}{k_m A_m(t)k_v + k_h + k_{ah}A_p(t)k_v} \qquad (3.18)$$

where $\rho(t)$ is rate of production of radical and defined as:

$$\rho(t) = (\rho_i(t) + \rho_{des}(t))N_A \qquad (3.19)$$

3.2.6 Rate of generation of polymer particles

The rate of generation of new polymer particles changes due to micellar and homogenous particle nucleation.

$$\frac{dN_p(t)}{dt} = \frac{N_p(t)_F}{\theta} - \frac{N_p(t)}{\theta} + f(t) \qquad (3.20)$$

Where $f(t)$ denotes the particle generation and can be written as:

17

$$f(t) = k_m A_m(t)[R_w^\bullet(t)]k_v + k_h[R_w^\bullet(t)] \qquad (3.21)$$

The first part is due to micellar nucleation and the second part is considered due to homogenous nucleation.

Substitution of equation (3.18) in equation (3.20) yields:

$$f(t) = \rho(t)\frac{k_m A_m(t)k_v + k_h}{k_m A_m(t)k_v + k_h + k_{ah}A_p(t)[R_w^\bullet]k_v} \qquad (3.22)$$

$A_m(t)$ can be calculated as:

$$A_m(t) = ([S(t)] - [S(t)]_{CMC})S_a N_A - A_p(t) \qquad (3.23)$$

As the area of polymer particles increase, the radical capture rate by the existing polymer particles becomes greater than the rate of initiation of new radicals, therefore the homogeneous rate constant, k_h, decreases towards zero, since there is a higher probability for an oligomer to be captured by a pre-existing particle.

According to Fitch and Tsai (1971):

$$k_h = k_{h_0}\left(1 - LA_p(t)k_v / 4\right) \qquad (3.24)$$

L is defined as the critical radical diffusion length. It shows the distance which a growing radical will diffuse before it participate out to form a primary particle and is given by Einstein's diffusion law:

$$L = \left(2D_w\frac{DP_{max}}{k_p M_{wc}}\right)^{1/2} \qquad (3.25)$$

where D_w is the diffusion coefficient of monomeric radicals in the water phase, DP_{max} is the maximum degree of polymerization and M_{wc} is the saturation concentration of monomer in the water phase.

By defining the ratios:

$$\mu = \frac{k_{h_0}}{k_m} \quad \text{and} \quad \varepsilon = \frac{k_{ah}}{k_m} \qquad (3.26)$$

The rate of particle nucleation can be written as:

$$f(t) = \rho(t)\frac{A_m(t)k_v + \mu\left(1 - LA_p(t)k_v / 4\right)}{A_m(t)k_v + \mu\left(1 - LA_p(t)k_v / 4\right) + \varepsilon A_p(t)k_v} \qquad (3.27)$$

18

3.2.7 Total population balance theory

Polymer model is based on the population balance strategy. In this approach, a phase space is defined for particles whose coordinates describe its location as well as its quality. This method is useful for all mechanisms in which the value of each phase coordinate changes with time. In the present analysis the birth time of the polymer particles in the reactor vessel,τ, is the phase coordinate. $n(t,\tau)$ shows the class of particles in the reactor at time t which were born in time τ. Therefore, the number density of particles in the phase space, $n(t,\tau)d\tau$, can be defined as the class of particles in the reactor at time t which were born between times τ and $\tau + d\tau$. Integration of $n(t,\tau)d\tau$ over the time period t will give the total number of particles in the reactor at time t. Based on this definition, any physical property, $p(t,\tau)$, of particles in the polymer reactor (e.g. the average diameter or area of a particle), can be calculated by summing up the $p(t,\tau)$ over all classes of particles in the reactor.

$$P(t) = \int_0^t p(t,\tau)n(t,\tau)d\tau \tag{3.28}$$

Differentiating equation (3.28) with respect to time leads to obtaining the evolution of the total property with time, which can be treated via Leibnitz's rule that is stated as:

$$\frac{d}{dx}\int_A^B f(x,t)dt = \int_A^B \frac{\partial f(x,t)}{\partial x}dt + f(x,B)\frac{dB}{dx} - f(x,A)\frac{dA}{dx} \tag{3.29}$$

Application of this rule to equation (3.28) yields:

$$\frac{d}{dt}\int_0^t p(t,\tau)n(t,\tau)d\tau = \int_0^t \frac{\partial(p(t,\tau)n(t,\tau))}{\partial t}d\tau + p(t,t)n(t,t)\frac{dt}{dt} \tag{3.30}$$

$$\frac{dP(t)}{dt} = \int_0^t \frac{\partial(p(t,\tau)n(t,\tau))}{\partial t}d\tau + P(t,t)n(t,t) \tag{3.31}$$

$$\frac{dP(t)}{dt} = \frac{P_{in}(t)}{\theta} - \frac{P(t)}{\theta} + \int_0^t \frac{\partial p(t,\tau)}{\partial t}n(t,\tau)d\tau + P(t,t)f(t) \tag{3.32}$$

The last equation states that the rate of change of total property equals to the total property inflow minus the total property outflow plus the growth and the nucleation terms.

19

3.2.8 Rate of change of polymer volume

Polymer particles grow continuously in the first two stages. Therefore, the rate of change of polymer volume in a particle born at given time τ, now being at time t, is stated as:

$$\frac{dv(t,\tau)}{dt} = R_p(t,\tau)\frac{Mw_M}{\rho_p} \qquad (3.33)$$

In similar way to bulk and solution polymerization ($R_p = k_p[M]\lambda_0$, Odian, 1991), where λ_0 is the total radical concentration (defined in 3.6), the rate of polymerization in emulsion polymerization can be written as:

$$R_p(t,\tau) = \frac{k_p[M]_p}{N_A}\bar{q}(t,\tau) \qquad (3.34)$$

where k_p is the rate constant for propagation, $[M]_p$ is the monomer concentration in the polymer particles, $\bar{q}$ is the average number of radicals per particle and N_A is Avogadro's number.

In stages one and two, the polymer particle composition is assumed to remain relatively constant, hence it is reasonable to assume that the monomer concentration also remains invariant.

The concentration of monomer in the polymer particle phase can be expressed as:

$$[M]_p = \frac{N_M}{V_p} \qquad (3.35)$$

where N_m is the number of monomer particles and V_p is the total volume of all polymer particles. The following equation can be used to calculate V_p.

$$V_p = \left(\frac{x_c}{\rho_p} + \frac{1-x_c}{\rho_m}\right)N_{M_u}Mw_M \qquad (3.36)$$

Equation (3.36) consists of two parts, the first part shows the amount of monomer consumed and the second part expresses the amount of unreacted monomer present in the reactor. As discussed before, at the end of stage 2, all monomer droplets are consumed. In particular, the critical conversion, x_c, is defined as the conversion at which all monomer

20

droplets disappear. The number of moles of monomer is expressed as $N_M = N_{M_0}(1-x)$, where N_{M_0} is the initial number of moles of monomer present in the reactor and finally equation (3.35) is rewritten as:

$$[M]_p = \phi(t)\frac{\rho_m}{Mw_M} \tag{3.37}$$

where:

$$\phi(t) = \frac{1-x_c}{1-x_c\left(1-\dfrac{\rho_m}{\rho_p}\right)} \qquad x(t) < x_c \tag{3.38}$$

$$\phi(t) = \frac{1-x(t)}{1-x(t)\left(1-\dfrac{\rho_m}{\rho_p}\right)} \qquad x_c < x(t) < 1 \tag{3.39}$$

Equation (3.33) becomes:

$$\frac{dv(t,\tau)}{dt} = \frac{k_p \rho_m}{N_A \rho_p}\phi(t)\overline{q}(t,\tau) \tag{3.40}$$

3.2.9 Average number of radicals per particle

With steady-state hypothesis assumption, the formation and disappearance rates of radicals for a particle are the same. Therefore,

$$\rho(t,\tau) = \overline{q}(t,\tau)k_{dc}(t,\tau)n(t,\tau)d\tau \tag{3.41}$$

In the same manner, application of the hypothesis for the whole system leads to:

$$R_I\frac{A_n(t,\tau)}{A_p(t)} = 2\rho(t,\tau)\overline{q}(t,\tau) \tag{3.42}$$

where:

$$A_n(t,\tau)d\tau = a_p(t,\tau)n(t,\tau)d\tau \tag{3.43}$$

$$\overline{q}(t,\tau) = \left(\frac{R_I(t)}{2k_{dc}(t,\tau)}\right)^{1/2}\left(\frac{a_p(t,\tau)}{A_p(t)}\right)^{1/2} \tag{3.44}$$

$$a_p(t,\tau) = \pi d_p^2(t,\tau) \tag{3.45}$$

$$R_I(t) = 2fk_d[I(t)]_w N_A \tag{3.46}$$

21

Expression for k_{des} has been developed by a number of research groups. Harada et al. (1971) showed that:

$$k_{de}(t,\tau) = \left(\bar{q}(t,\tau) + \frac{k_p[M]_p \, m d_p^2(t,\tau)}{12 D_w \delta} \right)^{-1} \left(\frac{k_{fm}}{k_p} + \frac{k_{fcta}[CTA]}{k_p[M]_p} + \frac{R_I(1-\bar{q}(t,\tau))}{N_p(t)k_p[M]_p \, \bar{q}(t,\tau)} \right) k_p[M]_p \qquad (3.47)$$

In order to simplify the equation, it can be assumed that the last term in the second bracket representing desorption of initial radicals can be neglected since an initiator radical would be reactive enough to polymerize monomer molecules before escaping and is much smaller in comparison with the second term of the same bracket. Therefore,

$$k_{de}(t,\tau) = \left(\bar{q}(t,\tau) + \frac{k_p[M]_p \, m d_p^2(t,\tau)}{12 D_w \delta} \right)^{-1} \left(\frac{k_{fm}}{k_p} + \frac{k_{fcta}[CTA]}{k_p[M]_p} \right) k_p[M]_p \qquad (3.48)$$

Where m is called a partition coefficient defined as the ratio of monomer concentration in polymer phase and water phase. The lumped diffusion coefficient δ is given by the following expression:

$$\delta = \left(1 + \frac{6 D_w}{m D_p} \right)^{-1} \qquad (3.49)$$

If the expression for k_{de} is substituted in equation (3.44), the following equation is obtained for the average number of radicals per particle:

$$\bar{q}(t,\tau) = \left(\frac{f k_d m N_A}{12 \pi D_w \delta \left(\frac{k_{fm}}{k_p} + \frac{k_{fcta}[CTA]}{k_p[M_p]} \right)} \right)^{1/2} \left(\frac{I_w(t)}{A_p(t)} \right)^{1/2} a_p(t,\tau) \qquad (3.50)$$

Recalling equation (3.33), new expression can be found for the rate of polymer volume change in a particle:

$$\frac{dv(t,\tau)}{dt} = \left(\frac{k_p P_m}{N_A \rho_p} \right) \left(\frac{f k_d m N_A}{12 \pi D_w \delta \left(\frac{k_{fm}}{k_p} + \frac{k_{fcta}[CTA]}{k_p[M_p]} \right)} \right)^{1/2} \left(\frac{I_w(t)}{A_p(t)} \right)^{1/2} \phi(t) a_p(t,\tau) \qquad (3.51)$$

Or

$$\frac{dv(t,\tau)}{dt} = \lambda \phi(t) a_p(t,\tau) \left(\frac{I_w(t)}{A_p(t)} \right)^{1/2} \qquad (3.52)$$

22

where

$$\lambda = \left(\frac{k_p \rho_m}{N_A \rho_p}\right)\left(\frac{f k_d m N_A}{12\pi D_w \delta \left(\dfrac{k_{fm}}{k_p} + \dfrac{k_{fcta}[CTA]}{k_p[M_p]}\right)}\right)^{\frac{1}{2}} \qquad (3.53)$$

Since $\phi(t)$ is the monomer volume over particle volume and $(1-\phi(t))$ is the polymer volume over particle volume, the particle volume can be calculated by:

$$v_p(t,\tau) = \frac{v(t,\tau)}{1-\phi(t)} \qquad (3.54)$$

where $v(t,\tau)$ is the volume occupied by polymer.

Therefore, the rate of change of particle volume is obtained by differentiating equation (3. 54) with respect to time.

$$\frac{dv_p(t,\tau)}{dt} = \frac{1}{1-\phi(t)}\frac{dv(t,\tau)}{dt} + \frac{v(t,\tau)}{(1-\phi(t))^2}\frac{d\phi(t)}{dt} \qquad (3.55)$$

$$\frac{d\phi(t)}{dt} = 0 \qquad\Rightarrow\qquad \frac{dv_p(t,\tau)}{dt} = \lambda\xi(t)a_p(t,\tau) \qquad\qquad x(t) < x_c \qquad (3.56)$$

$$\frac{d\phi(t)}{dt} = \frac{c-1}{(1-cx(t))^2}\frac{dx(t)}{dt} \qquad\Rightarrow\qquad \frac{dv_p(t,\tau)}{dt} = \lambda\xi(t)a_p(t,\tau) + v_p(t,\tau)\varepsilon(t) \qquad x_c < x(t) < 1 \qquad (3.57)$$

where

$$c = \left(1 - \frac{\rho_m}{\rho_p}\right) \qquad\qquad \rho_m < \rho_p \qquad\qquad \therefore \quad c > 0 \qquad (3.58)$$

$$\varepsilon(t) = \frac{1}{1-\phi(t)}\frac{c-1}{(1-cx(t))^2}\frac{dx(t)}{dt} \qquad (3.59)$$

$$\xi(t) = \frac{\phi(t)}{1-\phi(t)}\left(\frac{[I(t)]_w}{A_p(t)}\right)^{\frac{1}{2}} \qquad (3.60)$$

The general property balance for total particle volume in the reactor can be written as:

$$\frac{dV_p(t)}{dt} = \frac{V_{P_f}}{\theta} - \frac{V_p(t)}{\theta} + \int_0^t \frac{dv_p(t,\tau)}{dt}n(t,\tau)d\tau + v_p(t,\tau)f(t) \qquad (3.61)$$

Substituting equation (3.57) in equation (3.61) results:

23

$$\frac{dV_P(t)}{dt} = \frac{V_{P_F}}{\theta} - \frac{V_P(t)}{\theta} + \int_0^t (\lambda\xi(t)a_P(t,\tau) + v_P(t,\tau)\varepsilon(t))n(t,\tau)d\tau + v_P(t,t)f(t) \tag{3.62}$$

Finally,

$$\frac{dV_P(t)}{dt} = \frac{V_{P_F}}{\theta} - \frac{V_P(t)}{\theta} + \lambda\xi(t)A_P(t) + v_P(t,t)f(t) + \varepsilon(t)V_P(t) \tag{3.63}$$

When there is no transfer agent present in the reactor, the discussed equations will be simplified as follows:

$$k_{de}(t,\tau) = \left(\frac{12D_W\delta}{md_P^2(t,\tau)}\right)\frac{k_{fm}}{k_P} \tag{3.64}$$

Therefore,

$$\overline{q}(t,\tau) = \left(\frac{fk_d mk_P N_A}{12\pi D_w \delta k_{fm}}\right)^{\frac{1}{2}}\left(\frac{I_w(t)}{A_P(t)}\right)^{\frac{1}{2}} a_P(t,\tau) \tag{3.65}$$

$$\frac{dv(t,\tau)}{dt} = \left(\frac{k_P\rho_m}{N_A\rho_P}\right)\left(\frac{fk_d mk_P N_A}{12\pi D_w \delta k_{fm}}\right)^{\frac{1}{2}}\left(\frac{I_w(t)}{A_P(t)}\right)^{\frac{1}{2}} \phi(t)a_P(t,\tau) \tag{3.66}$$

where

$$\lambda = \left(\frac{k_P\rho_m}{N_A\rho_P}\right)\left(\frac{fk_d mk_P N_A}{12\pi D_w \delta k_{fm}}\right)^{\frac{1}{2}} \tag{3.67}$$

3.2.10 Effect of monomer soluble impurities on reactor model

On modifying the model to account for impurities, the live radical balance including the reaction with monomer soluble impurities must be redrived. The rate of radical generation in the water phase (section 3.2.5) can be written as:

$$\rho(t,\tau) = \rho_{des}(t,\tau) + R_I(t)\frac{A_n(t,\tau)d\tau}{A_p(t)} \tag{3.68}$$

where

$$\rho_{des}(t,\tau) = k_{de}(t,\tau)\overline{q}(t,\tau)n(t,\tau)d\tau \tag{3.69}$$

The stationary radical balance for the whole class, equation (3.42), is rewritten as:

$$R_I\frac{A_n(t,\tau)d\tau}{A_p(t)} = 2[\rho(t,\tau) - \rho_{MI}(t,\tau)]\overline{q}(t,\tau) + \rho_{MI}(t,\tau) \tag{3.70}$$

24

In equation (3.70), $\rho_{MI}(t,\tau)$ represents the rate of consumption of live radicals in polymer particles by reaction with impurities and is given by:

$$\rho_{MI}(t,\tau) = k_{MI}[MI_p(t)]\overline{q}(t,\tau)n(t,\tau)d\tau \tag{3.71}$$

k_{MI} is the rate constant for the reaction of live radicals with impurities and $[MI_p(t)]$ is the concentration of impurities inside the polymer particles. $[MI_p(t)]$ over $[MI(t)]$ gives the ratio k_{MISI}:

$$k_{MISI} = \frac{[MI_p(t)]}{[MI(t)]} \tag{3.72}$$

Due to the absence of experimental data, k_{MISI} is chosen to be equal to $\phi(t)$, the monomer volume fraction in the polymer particles. k_{MISI} is constant up to the critical conversion as in equation (3.72). When the conversion passes its critical point, $[MI_p(t)]$ starts decreasing. Combination of equations (3.68), (3.70) and (3.71) gives a new expression for $\overline{q}(t,\tau)$.

$$\overline{q}(t,\tau) = \frac{-2R_I(t)\dfrac{a_p(t,\tau)}{A_p(t,\tau)} - k_{MI}[MI_p(t)]}{4\big(k_{de}(t,\tau) - k_{MI}[MI_p(t)]\big)} +$$

$$\frac{\sqrt{R_I^2(t)\dfrac{a_p^2(t,\tau)}{A_p^2(t,\tau)} + k_{MI}^2[MI_p(t)]^2 + 4R_I^2(t)\dfrac{a_p(t,\tau)}{A_p(t,\tau)}\Big[2k_{de}(t,\tau) - k_{MI}[MI_p(t)]\Big]}}{4\big(k_{de}(t,\tau) - k_{MI}[MI_p(t)]\big)} \tag{3.73}$$

The expression for $\overline{q}(t,\tau)$ is quite complicated. Since usually the desorption of radicals is dominant over the term ($R_I(t)\dfrac{A_n(t,\tau)d\tau}{A_p(t)}$), equation (3.73) is simplified as:

$$\overline{q}(t,\tau) = \psi(t,\tau)a_p(t,\tau) \tag{3.74}$$

$$\psi(t,\tau) = \frac{-k_{MI}[M_p(t)]}{4\pi A} + \frac{1}{4\pi A}\left[k_{MI}^2[MI_p^2(t)] + 8\frac{\pi A R_I(t)}{A_p(t)}\right]^{1/2} \tag{3.75}$$

$$A = \left(\frac{12D_w\,\delta k_{fm}}{mk_p}\right) \tag{3.76}$$

25

Finally the molar balance for monomer soluble impurities can be written as:

$$\frac{d[MI(t)]}{dt} = \frac{[MI(t)]_{F}}{\theta} - \frac{[MI(t)]}{\theta} - \frac{k_{MI}[MI_p(t)]N_p(t)\bar{q}(t)}{N_A}$$ (3.77)

The last term in equation (3.77) is because of the reaction between inhibitor and live radicals (reaction (3.10)). The rate of reaction is written in similar way to the rate of propagation reaction.

3.2.11 Total particle diameter

The volume of a particle is related to its diameter by:

$$v_p(t,\tau) = \frac{1}{6}\pi d_p^3(t,\tau)$$ (3.78)

By differentiating this equation with respect to time:

$$\frac{d}{dt}\left(d_p(t,\tau)\right) = 2\lambda\xi(t) + \frac{1}{3}\varepsilon(t)d_p(t,\tau)$$ (3.79)

Application of the property balance equation, defined in equation (3.32), for total particle diameter yields:

$$\frac{dD_p(t)}{dt} = \frac{D_{P_F}}{\theta} - \frac{D_P(t)}{\theta} + \int_0^t \frac{d\left(d_p(t,\tau)\right)}{dt}n(t,\tau)d\tau + d_p(t,t)f(t)$$ (3.80)

Substituting equation (3.79) in equation (3.80) results:

$$\frac{dD_p(t)}{dt} = \frac{D_{P_F}}{\theta} - \frac{D_p(t)}{\theta} + \int_0^t \left(2\lambda\xi(t) + \frac{1}{3}d_p(t,\tau)\varepsilon(t)\right)n(t,\tau)d\tau + d_p(t,t)f(t)$$ (3.81)

Finally,

$$\frac{dD_p(t)}{dt} = \frac{D_{P_F}}{\theta} - \frac{D_p(t)}{\theta} + 2\lambda\xi(t)N_p(t) + d_p(t,t)f(t) + \frac{1}{3}\varepsilon(t)D_p(t)$$ (3.82)

3.2.12 Total particle area

Since

$$a_p(t,\tau) = \pi d_p^2(t,\tau)$$ (3.83)

$$\frac{da_p(t,\tau)}{dt} = 4\lambda\xi(t)d_p(t,\tau) + \frac{2}{3}\varepsilon(t)a_p(t,\tau)$$ (3.84)

26

By substituting equation (3.84) in equation (3.32), the rate of change of total particle surface area is obtained as follows:

$$\frac{dA_p(t)}{dt} = \frac{A_{p_k}}{\theta} - \frac{A_p(t)}{\theta} + 4\pi\lambda\xi(t)D_p(t) + a_p(t,t)f(t) + \frac{2}{3}\varepsilon(t)A_p(t) \tag{3.85}$$

3.2.13 Population balance

Since the molecular weight of a polymer sample is not exactly known, the concept of moment is used in order to find an average molecular weight for a polymer sample. The ith moments for live polymer and dead polymer are defined respectively as:

$$\lambda_i(t,\tau) = \sum_{r=1}^{\infty} r^i [R_r^\bullet(t,\tau)] \tag{3.86}$$

$$\mu_i(t,\tau) = \sum_{r=1}^{\infty} r^i [P_r(t,\tau)] \tag{3.87}$$

These definitions can be related to mechanic as the zeroth moments represent the weight of sample, the first moments show the moment of weight and the second moments express the moment of inertia.

Live polymer balance:

The detailed molar balance can be written for live radicals generated and consumed by different reaction (Ghadi, 2004).

For $r = 1$,

$$\frac{dR_1^\bullet}{dt} = -k_p[M]_p[R_1^\bullet] + k_{fm}[M]_p\lambda_0 - k_{fp}[R_1^\bullet]\mu_1 - k_p^\bullet[R_1^\bullet]\mu_0 + k_{fp}[P_1]\lambda_0 \tag{3.88}$$

For $r \geq 2$,

$$\frac{dR_r^\bullet}{dt} = k_p[M]_p[R_{r-1}^\bullet] - (k_{fm}[M]_p + k_{fp}\mu_1 + k_p^\bullet\mu_0 + k_p[M]_p)[R_r^\bullet] + k_p^\bullet\sum_{s=1}^{r-1}[R_s^\bullet][P_{r-s}]$$

$$+ k_{fp}r[P_r]\lambda_0 \tag{3.89}$$

$$\frac{d\lambda_0}{dt} = -k_p[M]_p\lambda_0 + k_p[M]_p\sum_{r=2}^{\infty}[R_{r-1}^\bullet] - k_p^\bullet\mu_0\lambda_0 + k_p^\bullet\sum_{r=2}^{\infty}\sum_{s=1}^{r-1}[R_s^\bullet][P_{r-s}] \tag{3.90}$$

Since:

27

$$\sum_{r=2}^{\infty}[R_{r-1}^{\bullet}] = \sum_{s=1}^{\infty}[R_s^{\bullet}] = \lambda_0 \tag{3.91}$$

$$\sum_{r=2}^{\infty}\sum_{s=1}^{r-1}[P_{r-s}][R_s^{\bullet}] = \lambda_0\mu_0 \tag{3.92}$$

Therefore after simplification, equation (3.90) becomes:

$$\frac{d\lambda_0}{dt} = 0 \tag{3.93}$$

The total number of radicals per litter of latex can be calculated by summing the product of average number of particles, which are present in the system and number of particles generated during time $d\tau$ over total time t.

$$\lambda_{0_{tot}}(t) = \int_0^t \overline{q}(t,\tau)n(t,\tau)d\tau \tag{3.94}$$

Substituting (3.50) in (3.94):

$$\lambda_{0_{tot}}(t) = \int_0^t \left(\frac{fk_d m k_p N_A}{12\pi D_w \delta k_{fm}}\right)^{\frac{1}{2}}\left(\frac{I_w(t)}{A_p(t)}\right)^{\frac{1}{2}} \cdot a_p(t,\tau)n(t,\tau)d\tau \tag{3.95}$$

$$\lambda_{0_{tot}}(t) = \left(\frac{fk_d m k_p N_A}{12\pi D_w \delta k_{fm}}\right)^{\frac{1}{2}}\left(\frac{I_w(t)}{A_p(t)}\right)^{\frac{1}{2}} A_p(t) \tag{3.96}$$

Where

$$A_p(t) = \int_0^t a_p(t,\tau)n(t,\tau)d\tau \tag{3.97}$$

Or in other words:

$$\lambda_{0_{tot}}(t) = \lambda\xi(t)\left(\frac{\rho_p}{K_p\rho_m}\right)\left(\frac{\phi(t)}{1-\phi(t)}\right)A_p(t) \tag{3.98}$$

Using the same method, first and second live polymer moments are derived (Ghadi, 2004) for computing $\overline{Mn}$ and $\overline{Mw}$ of the polymer and also required in the polymer model further (equations 3.104-3.106).

$$\frac{d\lambda_1}{dt} = k_p[M]_p\lambda_0 + k_{fm}[M]_p(\lambda_0 - \lambda_1) + k_{fp}(\lambda_0\mu_2 - \mu_1\lambda_1) + k_p^*\mu_1\lambda_0 - k_{fcta}[CTA]\lambda_1 \tag{3.99}$$

28

$$\frac{d\lambda_2}{dt} = k_p[M]_p(\lambda_0 + 2\lambda_1) + k_{fm}[M]_p(\lambda_0 - \lambda_2) + k_{fp}(\lambda_0\mu_3 - \mu_1\lambda_2) + k_p^*(\mu_2\lambda_0 + 2\lambda_1\mu_1)$$
$$-k_{fcta}[CTA]\lambda_2 \tag{3.100}$$

Assuming steady state hypothesis for live radical concentrations (3.99) yields:

$$\frac{\lambda_1(t,\tau)}{\lambda_0(t,\tau)} = \frac{k_p[M]_p + k_{fm}[M]_p + k_{fp}\mu_2(t,\tau) + k_p^*\mu_1(t,\tau)}{k_{fm}[M]_p + k_{fp}\mu_1(t,\tau) + k_{fcta}[CTA]\lambda_1} \tag{3.101}$$

Similarly for equation (3.100):

$$\frac{\lambda_2(t,\tau)}{\lambda_0(t,\tau)} = \frac{k_p[M]_p + k_{fm}[M]_p + k_{fp}\mu_3(t,\tau) + k_p^*\mu_2(t,\tau) + 2\left(k_p[M]_p + k_p^*\mu_1(t,\tau)\right)(\frac{\lambda_1(t,\tau)}{\lambda_0(t,\tau)})}{k_{fm}[M]_p + k_{fp}\mu_1(t,\tau) + k_{fcta}[CTA]\lambda_2} \tag{3.102}$$

Dead polymer balance:

A molar balance can also be written for dead polymers (Ghadi, 2004):

$$\frac{d[P_r]}{dt} = k_{fm}[M]_p[R_r^*] - k_p^*[P_r]\sum_{s=1}^{\infty}[R_s^*] + k_{fp}[R_r^*]\sum_{s=1}^{\infty}s[P_s] - k_{fp}r[P_r]\sum_{s=1}^{\infty}[R_s^*] + k_{fcta}[CTA][R_r^*] \tag{3.103}$$

$$\frac{d\mu_0(t,\tau)}{dt} = k_{fm}[M]_p\lambda_0(t,\tau) - k_p^*\mu_0(t,\tau)\lambda_0(t,\tau) + k_{fcta}[CTA]\lambda_0(t,\tau) \tag{3.104}$$

$$\frac{d\mu_1(t,\tau)}{dt} = k_{fm}[M]_p\lambda_1(t,\tau) - k_p^*\mu_1(t,\tau)\lambda_0(t,\tau) + k_{fp}\lambda_1(t,\tau)\mu_1(t,\tau)$$
$$-k_{fp}\lambda_0(t,\tau)\mu_2(t,\tau) + k_{fcta}[CTA]\lambda_1(t,\tau) \tag{3.105}$$

$$\frac{d\mu_2(t,\tau)}{dt} = k_{fm}[M]_p\lambda_2(t,\tau) - k_p^*\mu_2(t,\tau)\lambda_0(t,\tau) + k_{fp}\lambda_2(t,\tau)\mu_1(t,\tau)$$
$$-k_{fp}\lambda_0(t,\tau)\mu_3(t,\tau) + k_{fcta}[CTA]\lambda_2(t,\tau) \tag{3.106}$$

Application of equations (3.101)-(3.102) yields:

$$\frac{d\mu_0(t,\tau)}{dt} = k_{fm}[M]_p\lambda_0(t,\tau) - k_p^*\mu_0(t,\tau)\lambda_0(t,\tau) + k_{fcta}[CTA]\lambda_0(t,\tau) \tag{3.107}$$

$$\frac{d\mu_1(t,\tau)}{dt} = k_{fm}[M]_p\lambda_0(t,\tau) + k_p[M]_p\lambda_0(t,\tau) \tag{3.108}$$

$$\frac{d\mu_2(t,\tau)}{dt} = (k_{fm}[M]_p + k_p[M]_p)\lambda_0(t,\tau) + \left(\frac{2\lambda_0(t,\tau)\left(k_p[M]_p + k_p^*\mu_1(t,\tau)\right)}{k_{fm}[M]_p + k_{fp}\mu_1(t,\tau) + k_{fcta}[CTA]}\right)$$
$$\left(k_p[M]_p + k_{fm}[M]_p + k_{fp}\mu_2(t,\tau) + k_p^*\mu_1(t,\tau)\right) \tag{3.109}$$

Equations for the moments of dead polymers are re-arranged as:

29

$$\frac{d\mu_0(t,\tau)}{dt} = k_p[M]_p \lambda_{ave}(t) v_p(t,\tau)(C_m + C_{fcta}\frac{[CTA]}{[M]_p} - k\frac{\mu_0(t,\tau)}{[M]_p})$$ (3.110)

$$\frac{d\mu_1(t,\tau)}{dt} = k_p[M]_p \lambda_{ave}(t)(1 + C_m)v_p(t,\tau)$$ (3.111)

$$\frac{d\mu_2(t,\tau)}{dt} = k_p[M]_p \lambda_{ave}(t)v_p(t,\tau)$$

$$* \left(1 + C_m + 2 \left(\frac{1 + \frac{k\overline{\mu}_1(t)}{[M]_p}}{C_m + C_{fcta}\frac{[CTA]}{[M]_p} + \frac{C_p\overline{\mu}_1(t)}{[M]_p}} \right) * \left(1 + C_m + \frac{C_p\mu_2(t,\tau)}{[M]_p} + \frac{k\mu_1(t,\tau)}{[M]_p} \right) \right)$$ (3.112)

where

$$C_m = \frac{k_{fm}}{k_p}, C_p = \frac{k_{fp}}{k_p}, C_{fcta} = \frac{k_{fcta}}{k_p}, k = \frac{k_p^*}{k_p}$$ (3.113)

$$\lambda_{ave}(t) = \frac{\lambda_{0_m}(t)}{V_p(t)} = \frac{\lambda_0(t,\tau)}{v_p(t,\tau)}$$ (3.114)

$$\overline{\mu}_1(t) = \frac{\mu_1(t)}{V_p(t)} = \frac{\mu_1(t,\tau)}{v_p(t,\tau)}$$ (3.115)

Application of general property balance yields to the expressions for the total moments of dead radicals in CSTRs.

$$\frac{d\mu_0(t)}{dt} = \frac{\mu_{0_f}(t)}{\theta} - \frac{\mu_0(t)}{\theta} + k_p[M]_p \lambda_{ave}(t)\left(C_m V_p(t) + C_{fcta}\frac{[CTA]}{[M]_p} - k\frac{\mu_0(t)}{[M]_p} \right)$$ (3.116)

$$\frac{d\mu_1(t)}{dt} = \frac{\mu_{1_f}(t)}{\theta} - \frac{\mu_1(t)}{\theta} + k_p[M]_p \lambda_{ave}(t)(1 + C_m)V_p(t)$$ (3.117)

$$\frac{d\mu_2(t)}{dt} = \frac{\mu_{1_f}(t)}{\theta} - \frac{\mu_1(t)}{\theta} + k_p[M]_p \lambda_{ave}(t)$$

$$* \left((1 + C_m)V_p(t) + 2 \left(\frac{1 + \frac{k\overline{\mu}_1(t)}{[M]_p}}{C_m + C_{fcta}\frac{[CTA]}{[M]_p} + \frac{C_p\overline{\mu}_1(t)}{[M]_p}} \right) * \left((1 + C_m)V_p(t) + \frac{C_p\mu_2(t)}{[M]_p} + \frac{k\mu_1(t)}{[M]_p} \right) \right)$$ (3.118)

30

Branch point balance

If $B_N(t)$ denotes branch points per polymer molecule, then

$$\frac{d\left(\mu_{0B_N}(t,\tau)\right)}{dt} = (k_{fp}\mu_1(t,\tau) + k_p^*\mu_0(t,\tau))\lambda_0(t,\tau) \tag{3.119}$$

For a CSTR, the branch point moments are:

$$\frac{d\left(\mu_{0B_N}(t)\right)}{dt} = \frac{\mu_{0B_{N_f}}(t)}{\theta} - \frac{\mu_{0B_N}(t)}{\theta} + k_p\lambda_{ave}(t)\left(C_p\mu_1(t) + k\mu_0(t)\right) \tag{3.120}$$

Now, the number average and weight average molecular weights are defined by the following equations:

$$\overline{Mn}(t) = Mw_M \frac{\mu_1(t)}{\mu_0(t)} \tag{3.121}$$

$$\overline{Mw}(t) = Mw_M \frac{\mu_2(t)}{\mu_1(t)} \tag{3.122}$$

Similarly, the average number of long-chain branch points per polymer molecule is defined as:

$$\overline{B}_N(t) = \frac{\mu_{0B_N}(t)}{\mu_0(t)} \tag{3.123}$$

The distribution of sizes in a polymer chain is not completely defined by its central tendency. The breadth and the shape of the distribution curve must also be known and this is determined most efficiently with the parameters defined from the moments of the distribution. The ratio of $\dfrac{\overline{Mw}(t)}{\overline{Mn}(t)}$ is defined to measure the polydispersity of a sample. Friis and Hamielec (1975) showed that logarithmic normal distribution can adequately describe the MWD of polymer chains in emulsion polymerization of vinyl acetate.

$$W\left(\ln(M)\right) = \frac{\exp\left(-\left\{\ln(M) - \ln(\overline{M})\right\}^2 \Big/ (2\sigma^2)\right)}{\sigma\sqrt{2\pi}} \tag{3.124}$$

Where

$$\sigma^2 = \ln\left(\frac{\overline{Mw}}{\overline{Mn}}\right) \tag{3.125}$$

31

$$\bar{M} = \bar{M}n \exp\left(\frac{\sigma^2}{2}\right) \tag{3.126}$$

The two parameters σ^2 and $\bar{M}$ are only functions of molecular weight averages only, thus equation (3.124) in conjunction with equations (3.121)-(3.122) can predict the molecular weight distribution for different amount of molecular weight averages which are functions of conversion.

3.2.14 Reactor energy balance

Reactor temperature varies during the polymerization reaction due to exothermic nature of the process. Therefore, an energy balance can be written around the reactor.

$$\frac{dT}{dt} = \frac{T_F}{\theta} - \frac{T}{\theta} + \frac{R_p(-\Delta H_r)V_p}{Mw_m C_p} - \frac{UA(T-T_j)}{Mw_m C_p} \tag{3.127}$$

where, T_j is the cooling medium temperature.

According to the described reaction mechanisms, numerical values required for modelling the emulsion polymerization of vinyl acetate are listed in Table 3.1 (Penlidis, 1986). Table 3.1 contains the expressions for the various kinetic rate constants used in the model (e.g. initiator decomposition rate constant, propagation rate constant, etc.).

Table 3. 1 Kinetic Rate Constants

Properties	Values
k_p	$1.8669 \times 10^7 \exp(-5609/RT)$
k_{fm}	$3.7237 \times 10^6 \exp(-9895/RT)$
k_{fp}	$1.4183 \times 10^6 \exp(-8947/RT)$
k^*_p	$(k^*_p)_0 \exp(-(A_1 x(t) + A_2 x^2(t) + A_3 x^3(t)/2))$
$(k^*_p)_0$	$9.0963 \times 10^6 \exp(-5510/RT)$
A_1	$-6.8782+0.01961T$
A_2	$64.733-0.185T$
A_3	$-149.099+0.43044T$
k_d	$0.2540 \times 10^{18} \exp(-33320/RT)$

32

The required numerical values for physical properties of vinyl acetate as the used monomer are listed in Table 3.2. These values and expression are obtained by many researchers experimentally but the data from Penlidis (1986) is presented in this table.

Table 3. 2 Numerical Values of Model Constants

Properties	Values	Units
C_p	0.46	Cal/g. K
$d_p(t,\tau)$	50e-9	dm
ρ_M	930	g/L
ρ_P	1150	g/L
f	0.7	
L	8e-5	dm
m	27.1	
Mw_m	86	g/mol
N_A	6.02e-23	mole/L
S_{CMC}	3.2e-3	mole/L
S_a	5e-17	dm^2/molecule
x_c	0.2	
δ	0.5	
μ	0.55	dm^{-1}
ΔH_r	21300	Cal/mole

33

Chapter 4

Results and Discussion

4.1 Simulation Results

The proposed model has been solved and integrated in Matlab environmen
Different operating conditions have been considered for different kinds of reactors (batcl
semi-batch and CSTR) to test the model's validity. The effect of operating condition on th
properties of final product has been investigated. All the recipes/conditions used during thi
simulation is listed in Table 4.1.

Table 4. 1 Emulsion Reactor Operating Conditions

Case No.	M_F (mol/L)	I_F (mol/L)	S_F (mol/L)	MI_F (ppm)	T (°C)	Description
1	4.32	0.00222	0.0417	0	50	Batch, Isotherma Reactor
2	4.35	0.0026	0.182	Variable	50	Batch, Isotherma Reactor
3	4.35	0.01	0.01	0	50	CSTR, Isotherma Reactor,θ=30 mii

4.1.1 Batch emulsion polymerization reactor

Figure 4.1 shows plots of total polymer diameter, surface area and volume versu
batch time. The ability of the model to account for particle volume shrinkage in stage 3 i
clearly shown. This shrinkage is due to the difference in densities of monomer and polyme
particles and occurs after 20 minutes of reaction. Normally the polymer density is highe
than the density of monomer as it is stated in Table 3.2. Based on equation (3.57), befor
the critical conversion, the second term on the right hand side of the equation equals zer
and the polymer density doesn't have great effect on its size since there are still mor

34

monomer droplets present in the system in comparison with polymer particles. When the monomer passes the critical value, the second term becomes active and according to equation (3.58), parameter c is a constant number less than one because the polymer density is more than monomer density. If one substitutes all the parameters in equation (3.63) and does all the simplifications, the fifth term on the right hand side of this equation will be always less than zero and that is the reason for the shrinkage in size after completion of the second stage. After the second stage there won't be any monomer droplet in the system and based on the density's definition when the density increases the volume of that particle decreases because of their inverse relationship. Figure 4.2 shows conversion results. The critical conversion (for vinyl acetate=20%) is shown in this Figure. After this point the rate of polymerization starts decreasing due to gradual disappearance of monomer droplets.

Figure 4.3 plots the total number of polymer particles versus conversion. A total number of particles of about 13×10^{17} particle/L-latex was predicted. Therefore, the number of polymer particles grows very quickly in stage one and reaches a final constant from about 5% up to full conversion. This observation proves the nucleation theory discussed in Chapter 3. Thus, all properties of the final product depending on the number and size of particles are defined in stage 1 which is generally the shortest of the three stages.

The particle number remains constant in both stage 2 and 3. As the polymer particles grow in size, they still contain monomer particles. They absorb more and more surfactant in order to maintain physical stability. By the end of stage 1, almost all the surfactant in the system has been absorbed. The water soluble monomers such as vinyl acetate tend to end stage 1 much faster than the less water soluble ones. This is mainly a consequence of the significant extent of homogenous nucleation occurring simultaneously with micellar nucleation results in achieving the steady state particle number sooner.

Figures 4.4 and 4.5 show the predictions of number and weight average molecular weights, respectively, with conversion. Generally it is known that the polymer produced in emulsion polymerization has very high molecular weights compared with bulk/solution polymerization. The variation of polydispersity index (PDI) with conversion is displayed in Figure 4.6. When the conversion increases, the PDI also increases since it is a function of

35

molecular weight averages, which in turn become greater as the reaction proceeds. The average number of long chain branching is plotted in the Figure 4.7. Equation (3.123) has been used to calculate this property. Mainly, reaction (3.11) is responsible for the generation of branch points.

A large number of properties depend on the molecular weight distribution (MWD) of polymer chain, which is calculated using equation (3.124) and result of which are plotted in Figure 4.8, for different final conversions. The higher the conversion, the wider the distribution. This phenomenon is due to an increase in the number of branchings at higher conversion. Some research groups worked on this characteristic of the polymer product and its sensitivity to the operating conditions (Tobita 1994; Choi and Crowley 1997).

Variations of the polymerization rate with conversion depend on the relative rates of initiation, propagation and termination, which are in turn functions of the operating conditions. Since the generation of particles proliferate with time in stage 1, polymerization rate (R_p) also increases during this stage.

In stage 2, the monomer concentration in the particles is maintained at the saturation level by diffusion of monomer from solution and dissolution of monomer from the monomer droplets. Stage 2 ends when the monomer droplets disappear and during stage 3 the monomer concentration decreases and consequently R_p goes down in this stage. Due to high water solubility of vinyl acetate the transition from stage 2 to stage 3 occurs at conversion around 20%-30%. Therefore, stage 2 has a very short time for this monomer. The simulation result (Figure 4.9) also agrees with this theory and the model is able to account for polymerization rate reduction throughout the third stage.

In the next step of this study, the effects of the operating conditions have been studied. In the first sets of runs, the emulsifier concentration was set to 0.0417 mol/L, while varying initiator level. Model testing results are shown in Figures 4.10-4.16. The higher concentration of initiator, the higher the rates of polymerization and conversion. Figure 4.11 shows that with higher initiator concentration, the reaction speeds up because more radicals are present in the system and as a result the monomer conversion goes to completion in a shorter time. Figure 4.10 also confirms this trend. The initiator concentration does not have great influence on the size of particles but the particle size

36

shrinks much sooner with higher initiator concentration which is again the result of shorter nucleation time (stage 1) and constant growth rate of monomer-polymer particles (stage 2). Based on the model prediction for polymer particle diameter during the emulsion polymerization of vinyl acetate under case 1 operating condition (Figure 4.10, part (a)), stage 2 lasts 20 minutes after adding the initiator to the system, while in higher concentration of initiator the monomer droplets disappear in about 5 minutes. Furthermore, higher initiator concentration yields in higher molecular weights and increases the branching points of the polymer (figures 4.13-4.16).

The same study has been done on the effect of emulsifier concentration on batch emulsion polymerization of vinyl acetate. The model predictions are plotted in Figures 4.17-4.23. When the emulsifier concentration increases, more micelles will be available in the system. Therefore, the rate of polymerization increases and polyvinyl acetate with higher molecular weight is produced. An important point, which should be stressed, is the number of branching points. Feeding more initiator and emulsifier to the system favours more branching points at the end of reaction time. Sometimes polymer with high number of branching is desired while in some other circumstances, it is not. Therefore, based on the desired property of the product, the concentration of initiator and emulsifier can be identified.

The third series of runs were conducted at fixed emulsifier and initiator concentrations but the varying operating temperature between 40°C and 80°C. The results are shown in Figures 4.24-4.30. Figure 4.25 shows that with a constant temperature of 80°C, a conversion of about 90% is achieved in about ten minutes. The increase in the rate of polymerization and also final product property is due to high sensitivity of the rate constants to temperature. Higher temperature results in higher reaction rate so, polymerization completes in shorter time. Some research groups, particularly Lovell et al. (1998) studied the effect of chain transfer to polymer in free radical bulk and emulsion polymerization of vinyl acetate using NMR spectroscopy. They stated out that in both bulk and emulsion polymerization, the mole percent of branching increases steadily with overall conversion. Further, their experiments revealed that since the emulsion polymerisation proceeds exclusively within the latex particles and at high instantaneous conversion, the level of branching in the poly-vinyl acetate produced in emulsion is higher than bulk

37

polymerization. They also studied the effect of temperature on increasing the mole percent of the branch points. The simulation results of the current study for the number of branching point, and also its sensitivity to the operation conditions are in good agreement with the studies found in literature.

In all the performed runs, it was assumed that the reactor temperature is constant during the reaction, which means that the cooling medium can do its duty very well that the temperature of the system will be kept on a desired value. But in fact due to the exothermic nature of polymerization reactions, it is not very easy to keep the temperature at a constant value throughout the reaction.

In the next part of this study, the variation effect of temperature has been investigated and results are presented in Figures 4.31-4.37. The results compare the isothermal and nonisothermal cases. For similar feed condition, first the reactor is run under isothermal condition in which it is assumed that reactor temperature remains constant at some desired value (T=50°C) while in nonisothermal condition, the reactor's initial temperature is set at T=50 C and after that the cooling jacket is employed to keep the reactor temperature constant. Due the exothermic nature of reaction, it is not possible to keep the temperature constant throughout the reaction which is the main reason to have different final values for monomer conversion and molecular weight averages. Figure 4.36 plots the variation of rector temperature throughout the reaction. Running the reactor under nonisothermal condition yields in lower conversion due to lower rate of polymerization. Final properties of the product such as molecular weight averages and number of branch points are also decreased by application in nonisothermal operations.

Consequently, the significant effect of the initiator, emulsifier concentrations and the temperature show the necessity of designing good control strategies to keep the operating conditions on the desired value because a minor variation in operating condition may results in deviation from the desired properties.

It is known that emulsion polymerization method produces polymers with high molecular weight, compared to bulk/solution methods. Therefore, another control policy to control physical properties of the final product is addition of chain transfer agents (CTA) to the reactor. Based on dead polymer molar balances, (equations (3.116-3.118)), CTA decreases the molecular weight averages of the product. When a polymer with lower

38

molecular weight is desired, chain transfer agents such as: t-nonyl mercaptan, n-dodecyl or mercaptan will be employed. Some researchers worked on molecular weight control in emulsion polymerization (Meira et al., 1998).

The influence of different CTA differs not only because of their dissimilar chemical structures but of their diffusivity. CTAs with more carbon units have lower water solubility. When the reaction starts, a CTA with low water solubility remains in the monomer droplets but it expected to diffuse out to polymer particles as the reaction proceeds. Normally, a CTA with lower water solubility diffuses to the water phase much slower than that with high water solubility therefore the CTA affects the polymer property differently. Figures 4.38-4.39 display the effect of t-nonyl mercaptan with nine carbon atoms ($C_{fcta} = 0.0325$ at $T = 70^\circ C$, Meira et al, 1998) on average molecular weight and number of branch points. The prediction of molecular weight average is quite satisfactory and higher concentration of CTA produces shorter polymer chains as more mercaptan is abstracted. Hence, lower average molecular weight is predicted.

In order to validate the model the results should be compared with experimental data. Unfortunately, there have not been many studies done on emulsion polymerization of vinyl acetate with similar conditions. The only experimental data were found from Penlidis (1986). Plots in Figures 4.40-4.45 compare model predictions with experimental data. There is a good agreement between the model predictions and the data. Figure 4.41 shows plots of the conversion in two different temperatures; as expected, higher temperature speeds up the reaction and the conversion goes to completion in shorter time. Figure 4.42 presents monomer conversion at two different levels of emulsifier. The simulation results successfully follow the conversion points throughout the entire runs. In overall, the model gives also a good prediction of the effect of emulsifier and reactor temperature on the emulsion polymerization.

Most studies neglect the presence of impurities in the polymerization reactor. Since most industrial scale processes use either unpurified, partially purified monomers or monomer recycle streams, predictions may diverge from real process data. Figure 4.46-4.56 shows the model predictions of several variables for different impurity levels in a batch emulsion polymerization of Vinyl Acetate. Plots of conversion versus time show little difference for low concentration of impurities but much larger effect at higher

39

concentration of impurities (100-200 ppm). The validity of the model observed comparing the results with experimental data (Figures 4.51-4.56). As it was discussed in chapter 3, it was assumed that the rate constant for changing to inhibitor is equal to rate constant of propagation. Based on the operating condition shown in Figure 4.56 where $K_{MI} = 0.84 K_p$, there is a good agreement between the experimental data and the model prediction, so it means that a reasonable assumption was made for K_{MI} value.
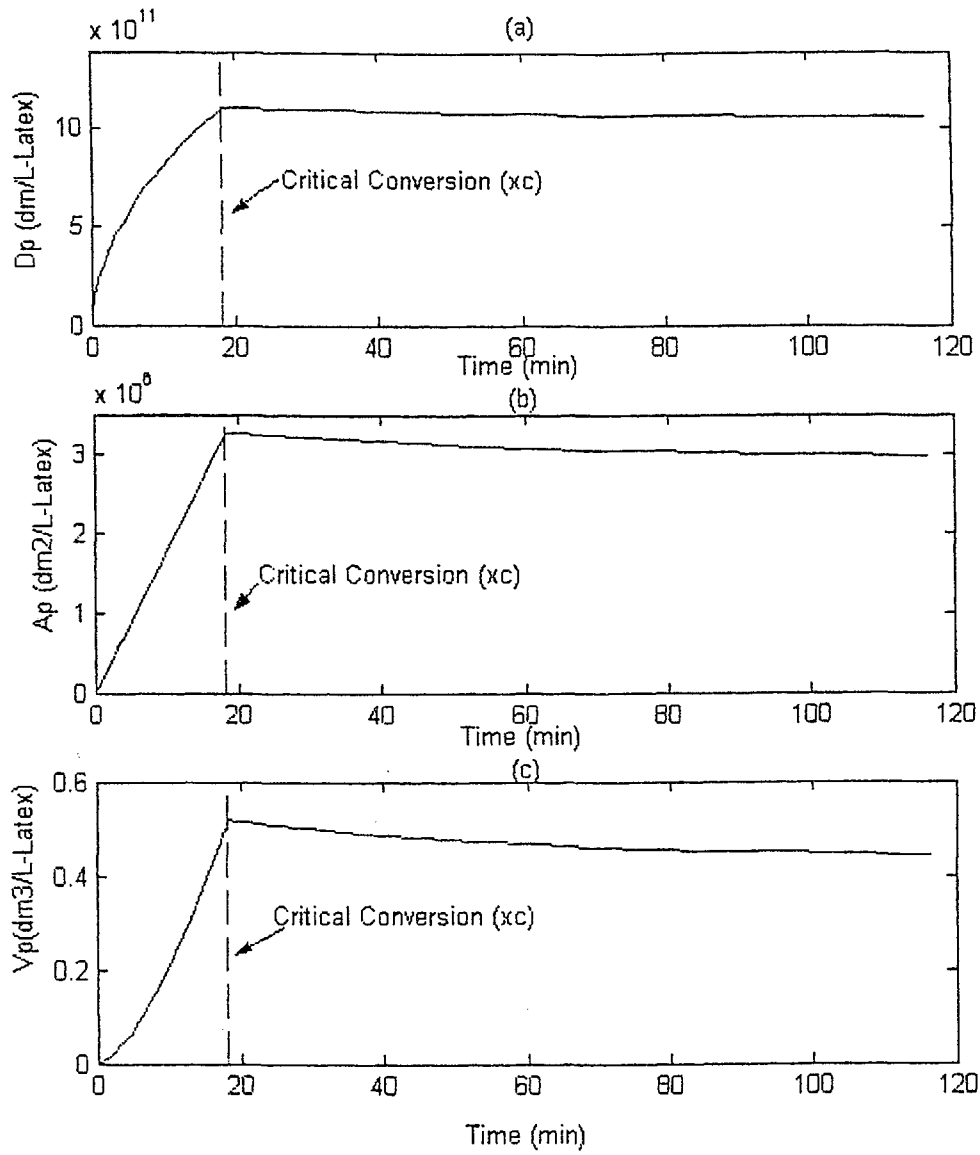
Figure 4. 1. Case 1. Particle (a) Diameter, (b) Surface Area, (c) Volume Versus a Batch

Time

41
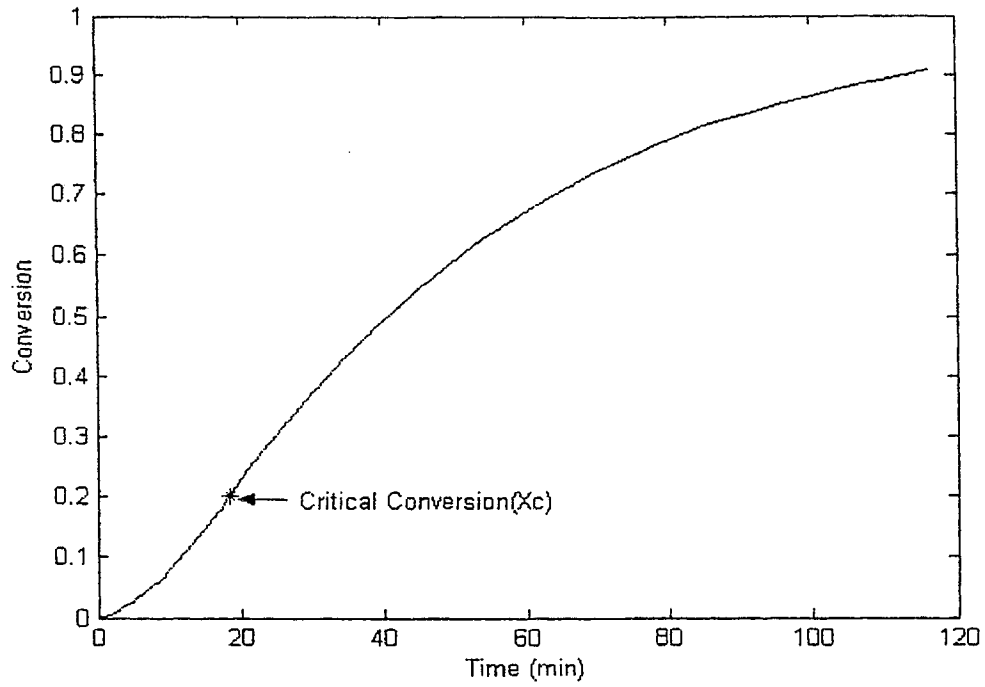
Figure 4. 2. Case 1. Conversion Versus Time
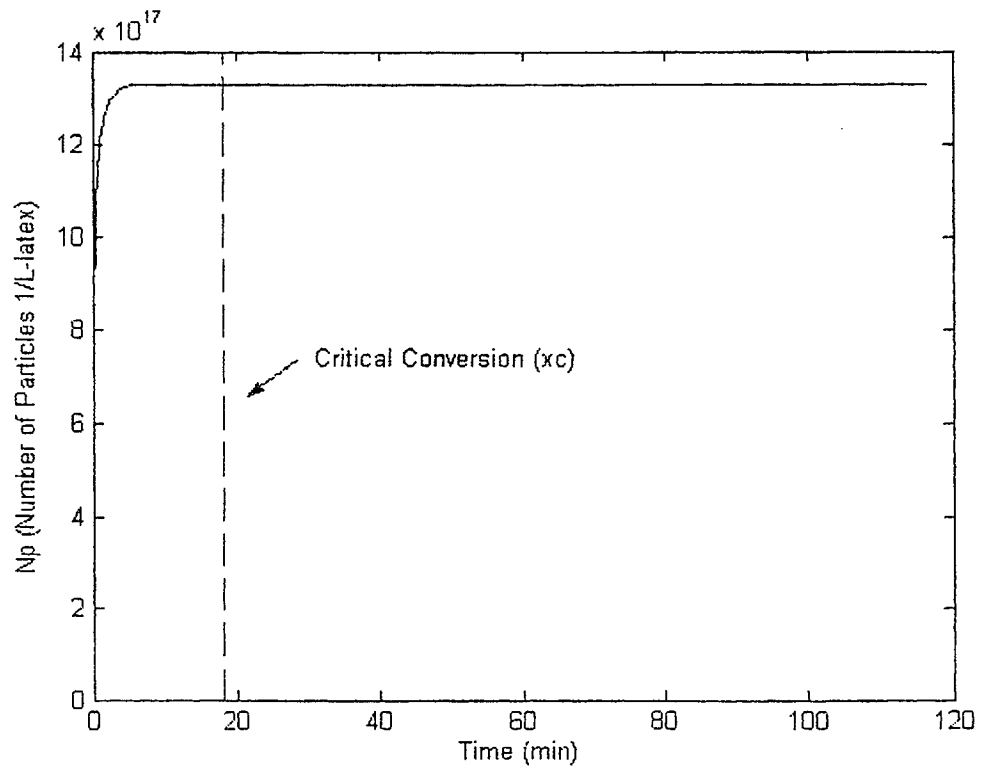
Figure 4. 3. Case 1. Number of Particles Versus Time

42
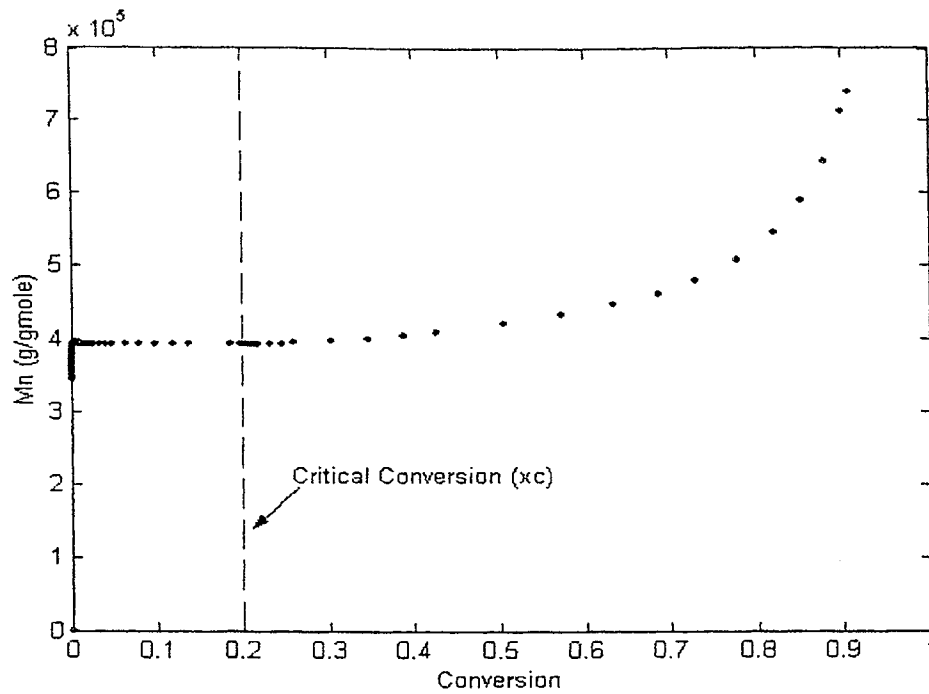
Figure 4. 4. Case 1. Number of Average Molecular Weight Versus Conversion
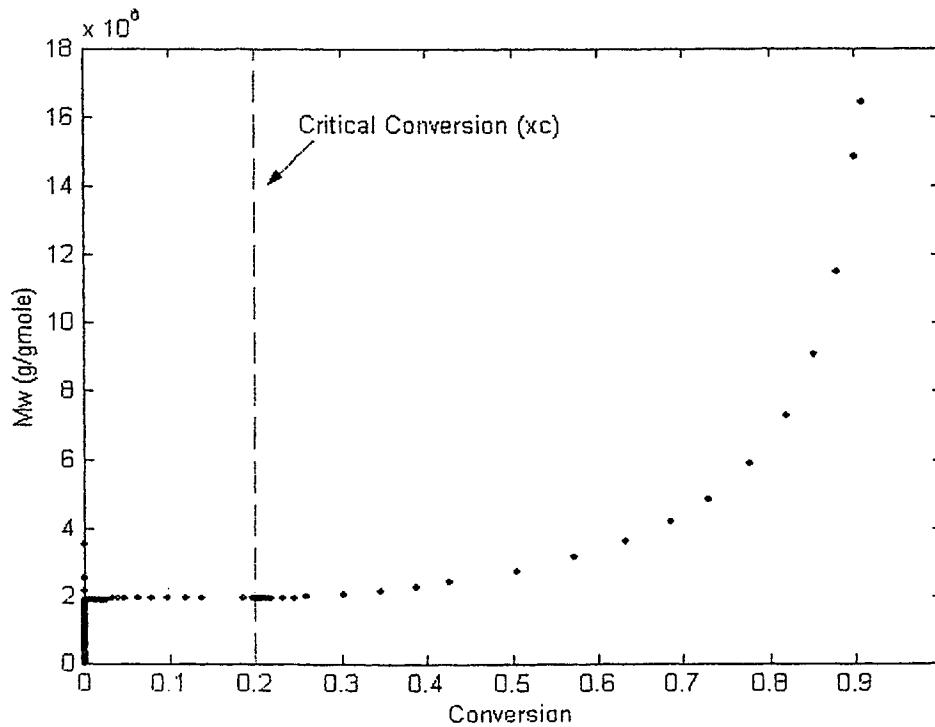
Figure 4. 5. Case 1. Average Molecular Weight Versus Conversion

43
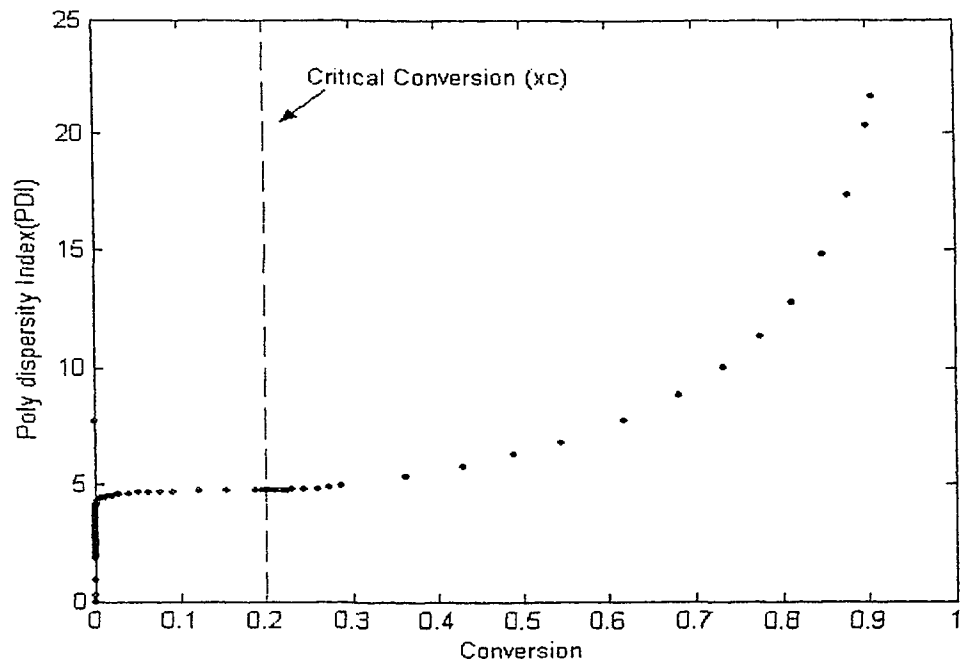
Figure 4. 6. Case 1. Polydispersity Index Versus Conversion
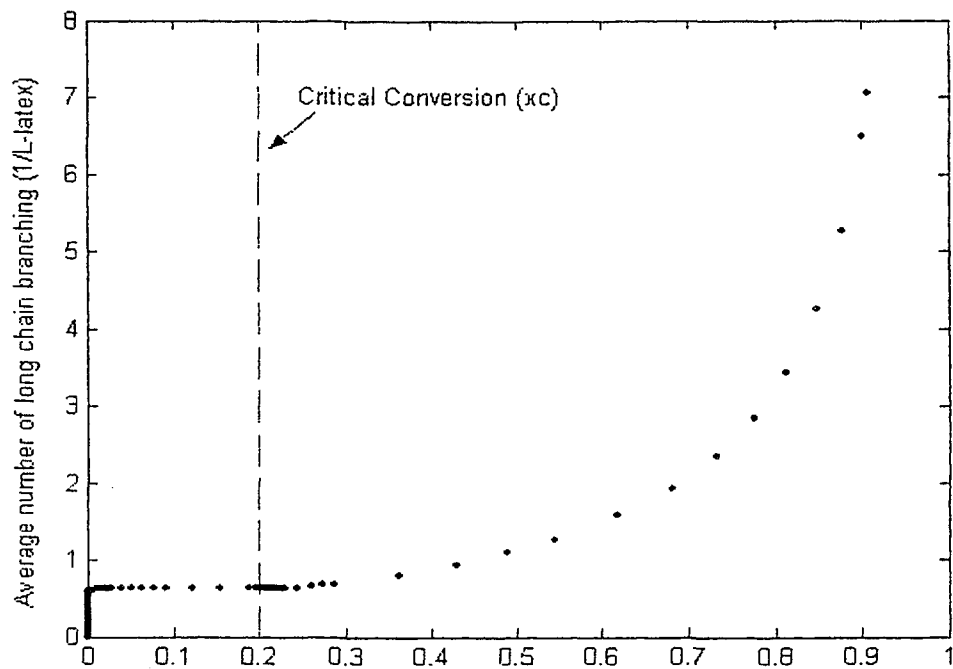
Figure 4. 7. Case 1. Number of Branching Points Versus Conversion

44
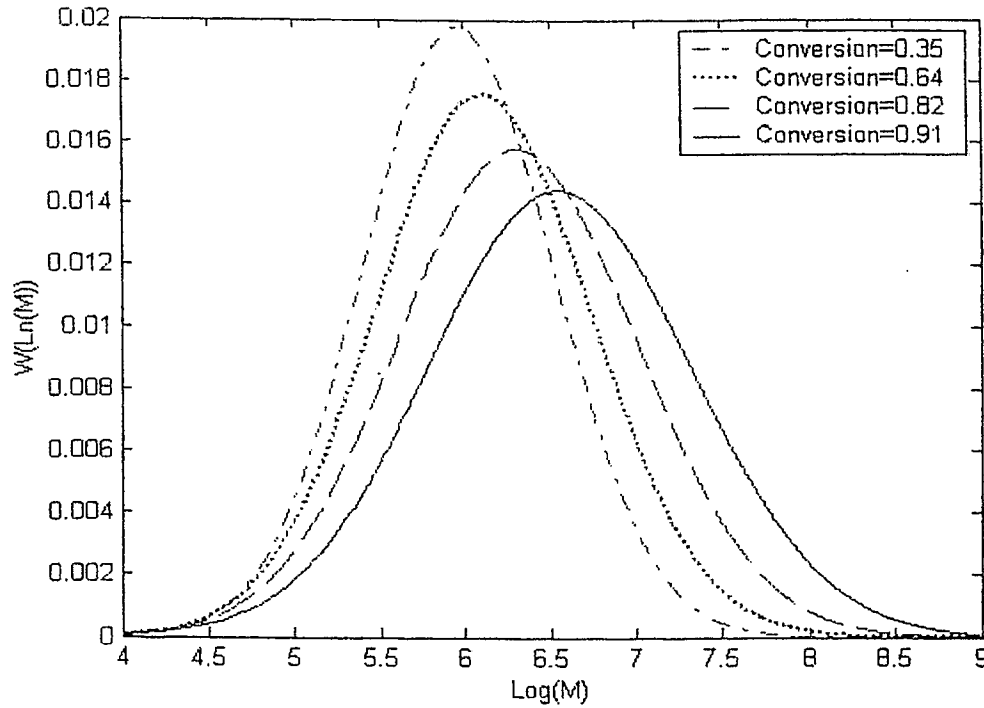
Figure 4. 8. Case 1. Molecular Weight Distribution for Different Conversion Levels
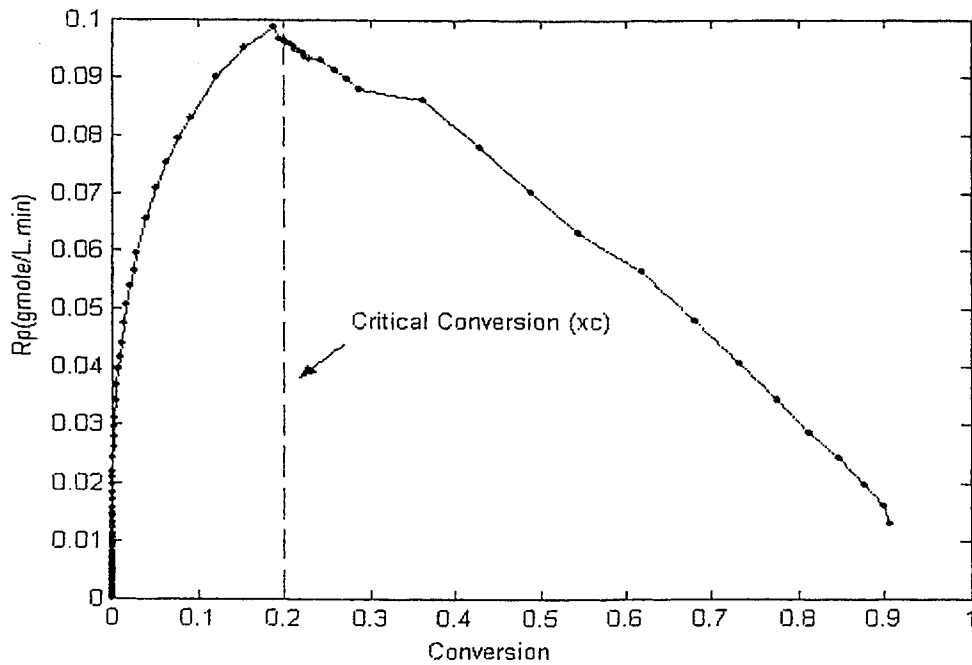
Figure 4. 9. Case 1. Rate of Polymerization Versus Conversion

45
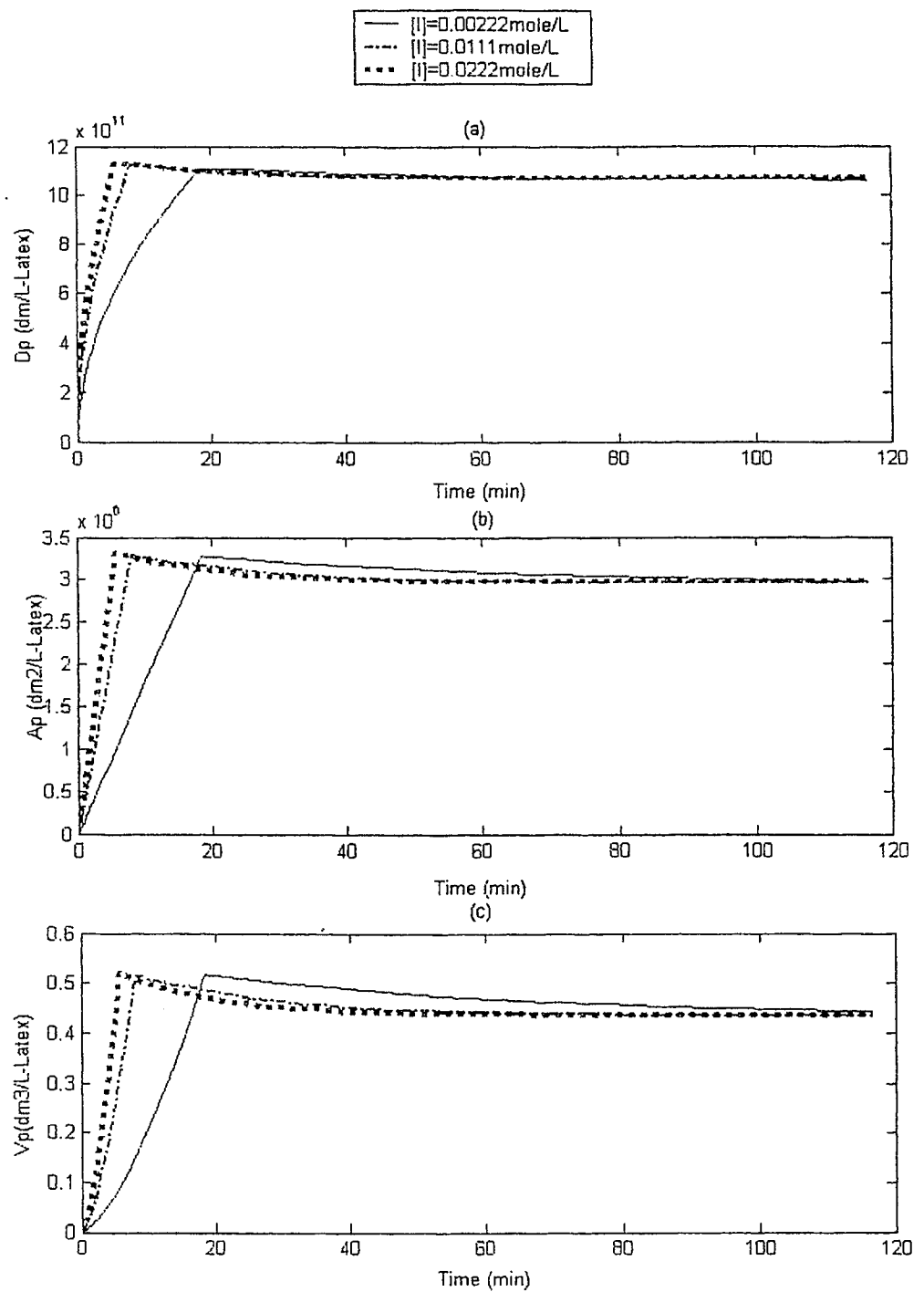
Figure 4. 10. Case 1. Effect of Initiator Concentration on Particle (a) Diameter, (b) Surface Area, and (c) Volume

46
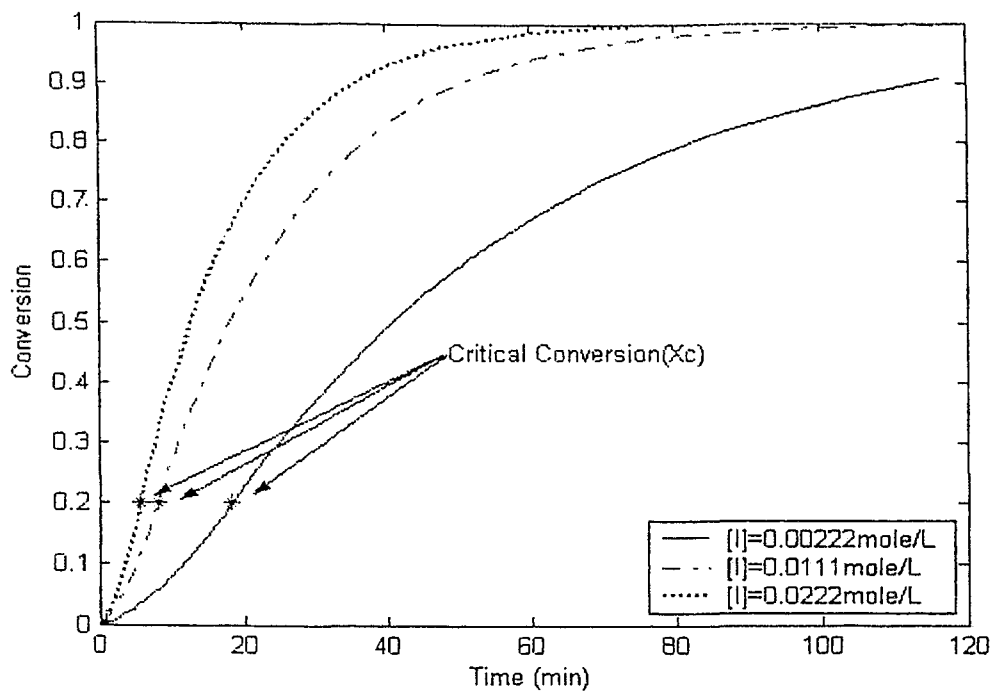
Figure 4. 11. Case 1. Effect of Initiator Concentration on Conversion
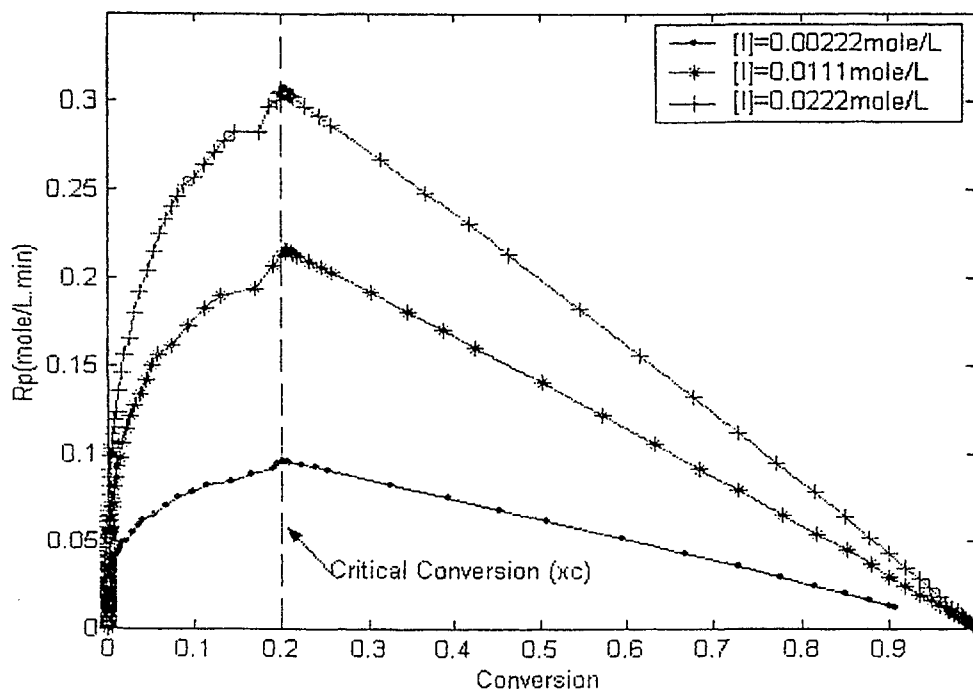
Figure 4. 12. Case 1. Effect of Initiator Concentration on Rp

47
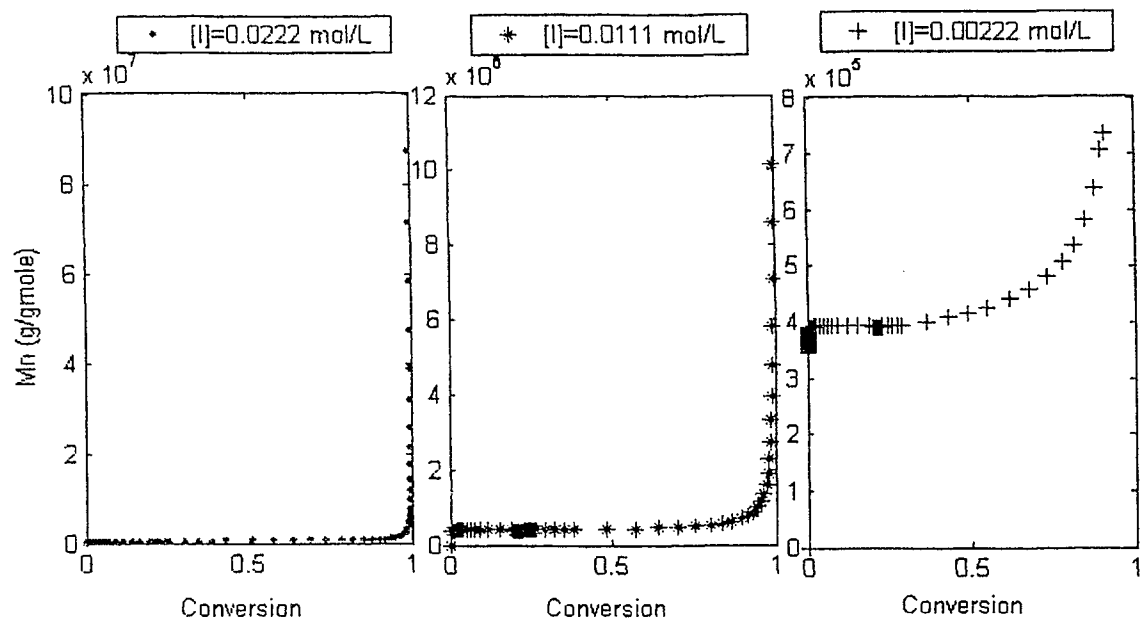
Figure 4. 13. Case 1. Effect of Initiator Concentration on Mn
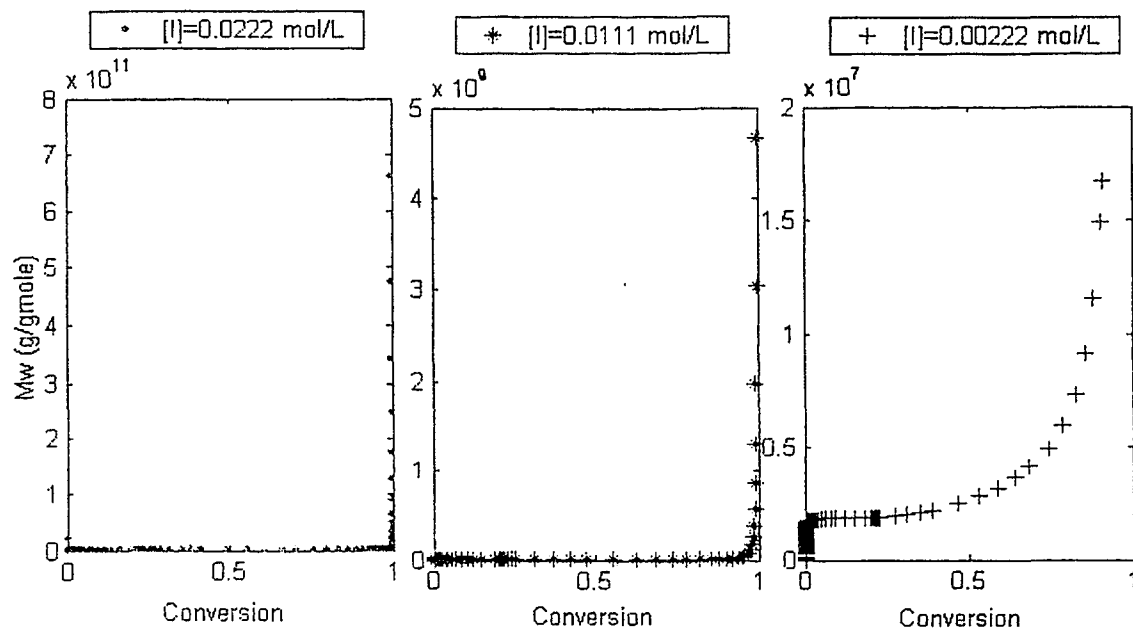
Figure 4. 14. Case 1. Effect of Initiator Concentration on Mw

48
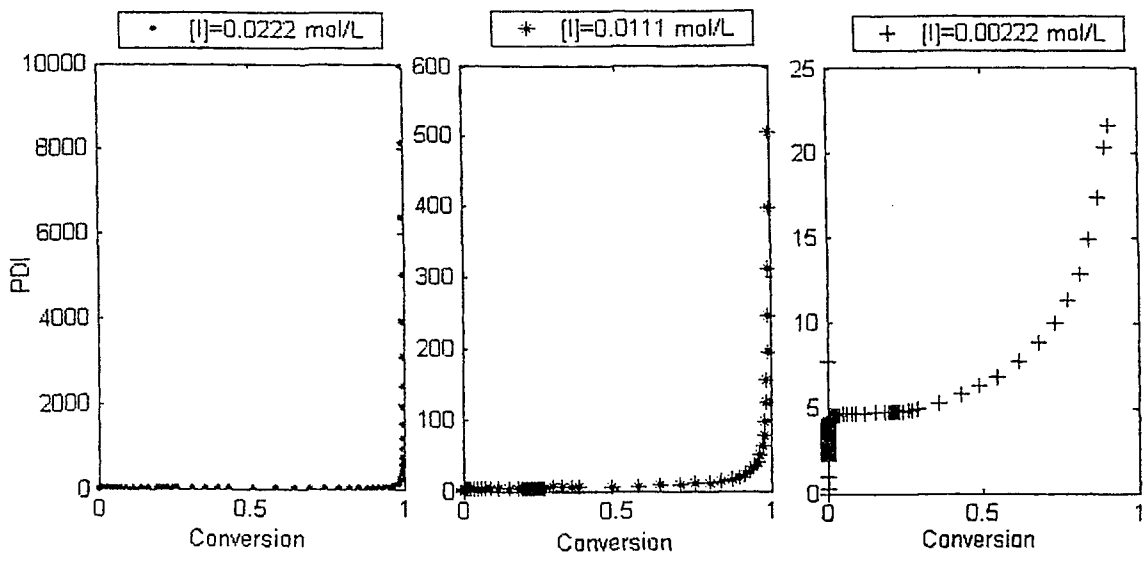
Figure 4. 15. Case 1. Effect of Initiator Concentration on PDI
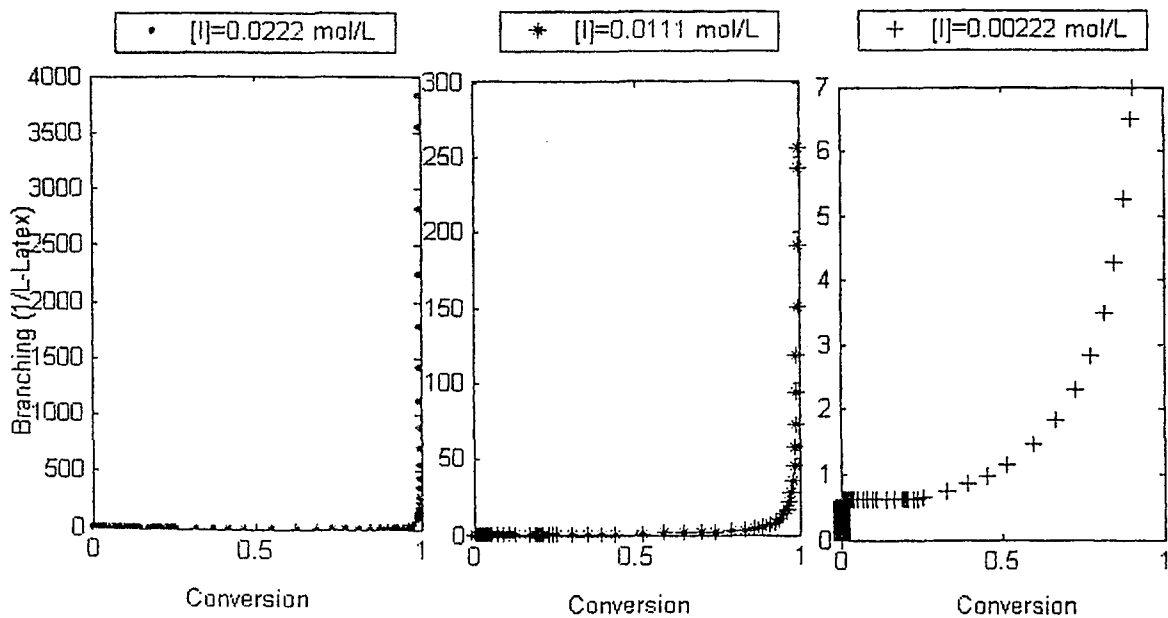
Figure 4. 16. Case 1. Effect of Initiator Concentration on Number of Branch Points

49
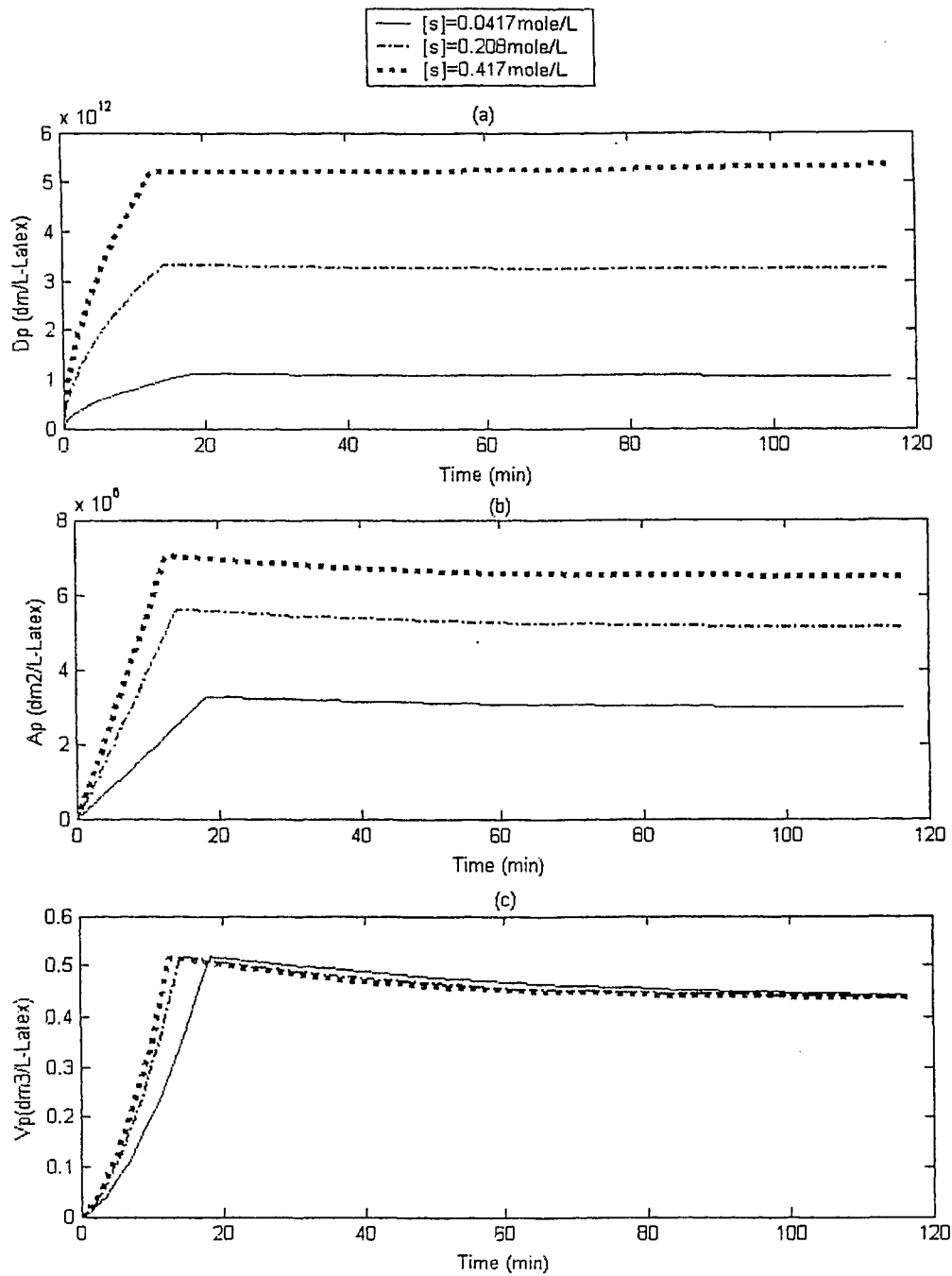
Figure 4. 17. Case 1. Effect of Emulsifier Concentration on Particle (a) Diameter, (b) Surface Area, and (c) Volume

50
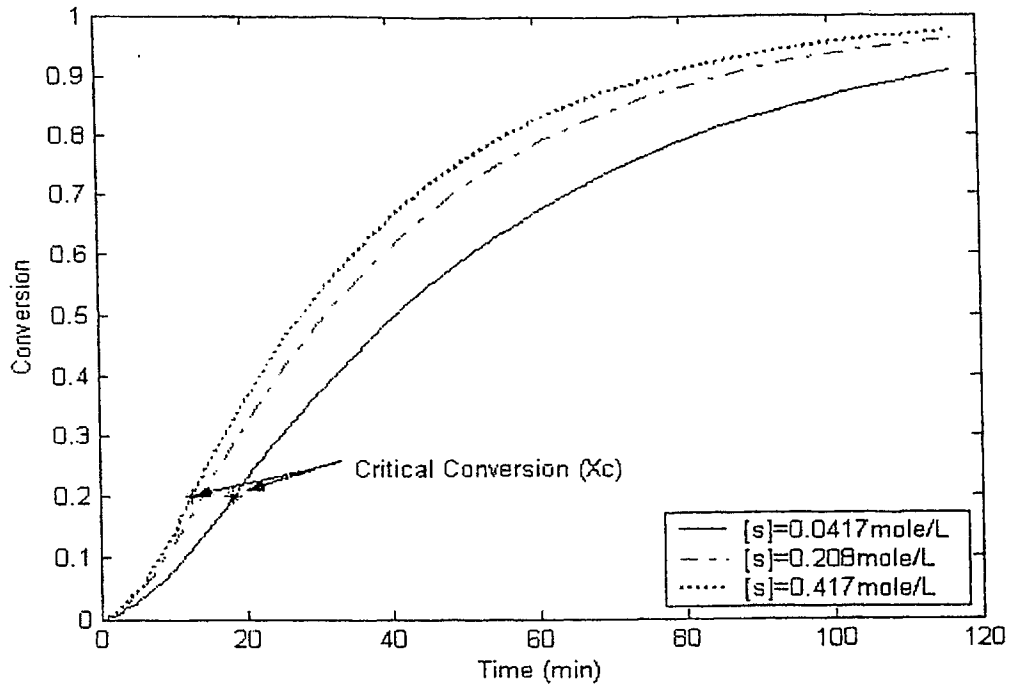
Figure 4. 18. Case 1. Effect of Emulsifier Concentration on Conversion
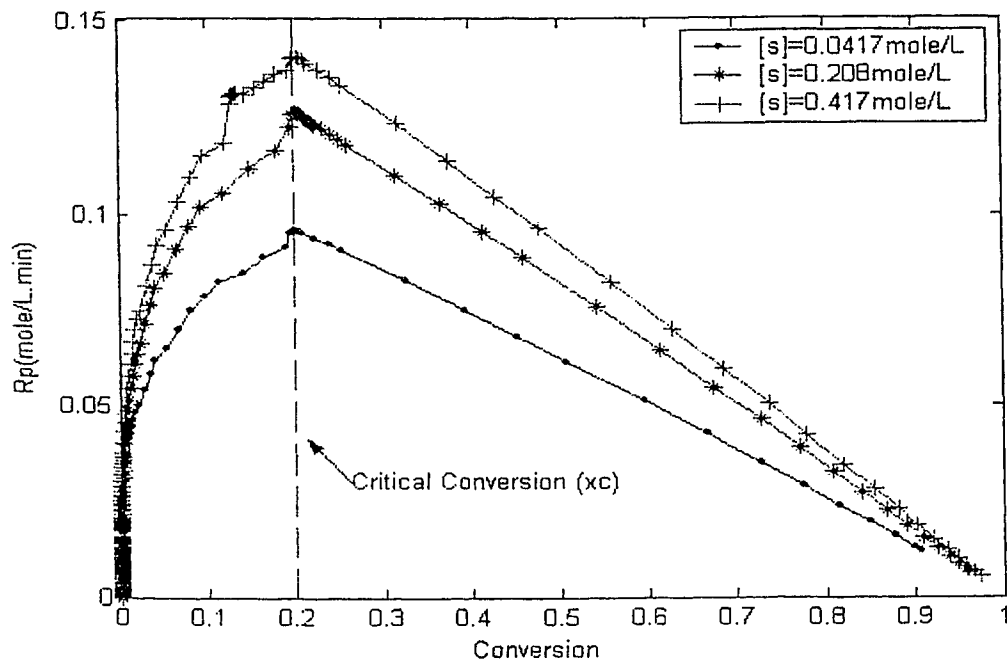
Figure 4. 19. Case 1. Effect of Emulsifier Concentration on Rp

51
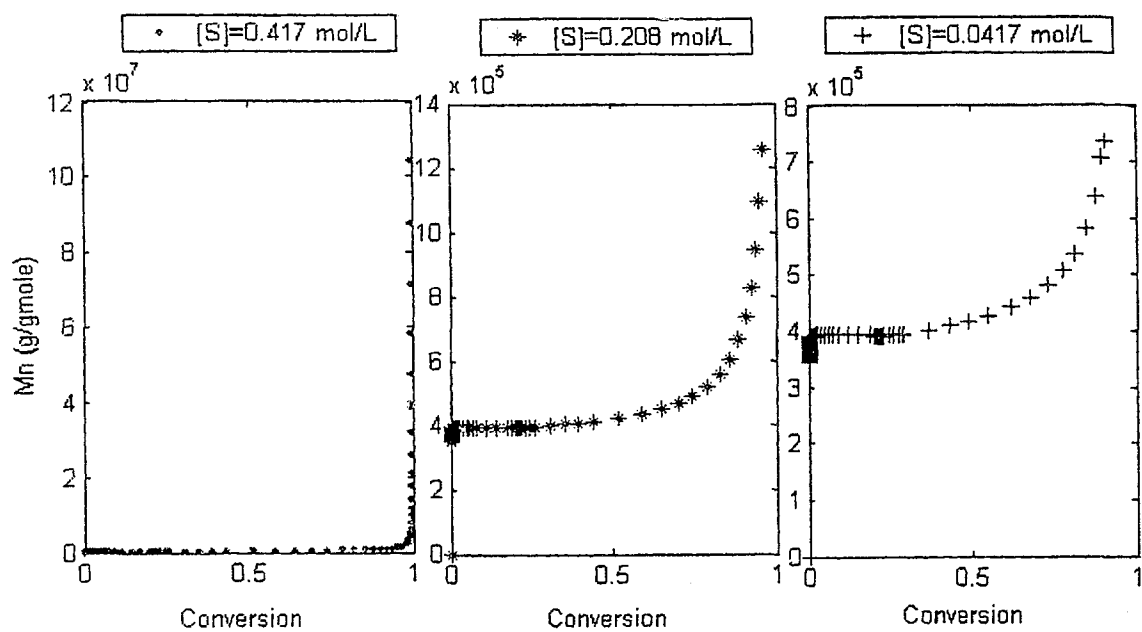
Figure 4. 20. Case 1. Effect of Emulsifier Concentration on Mn
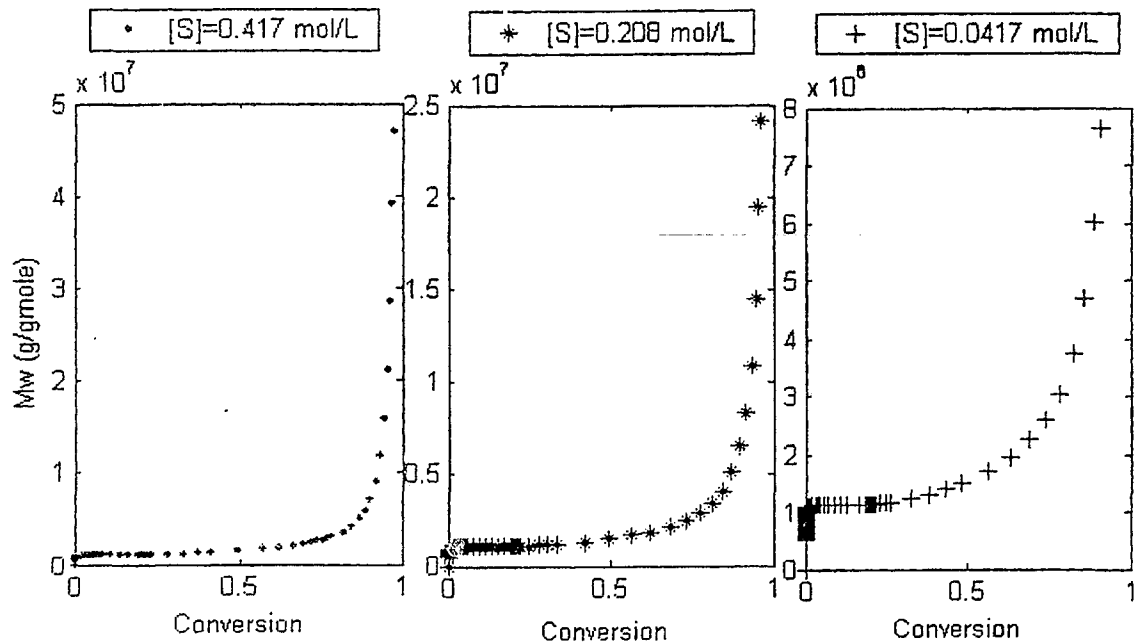
Figure 4. 21. Case 1. Effect of Emulsifier Concentration on Mw

52
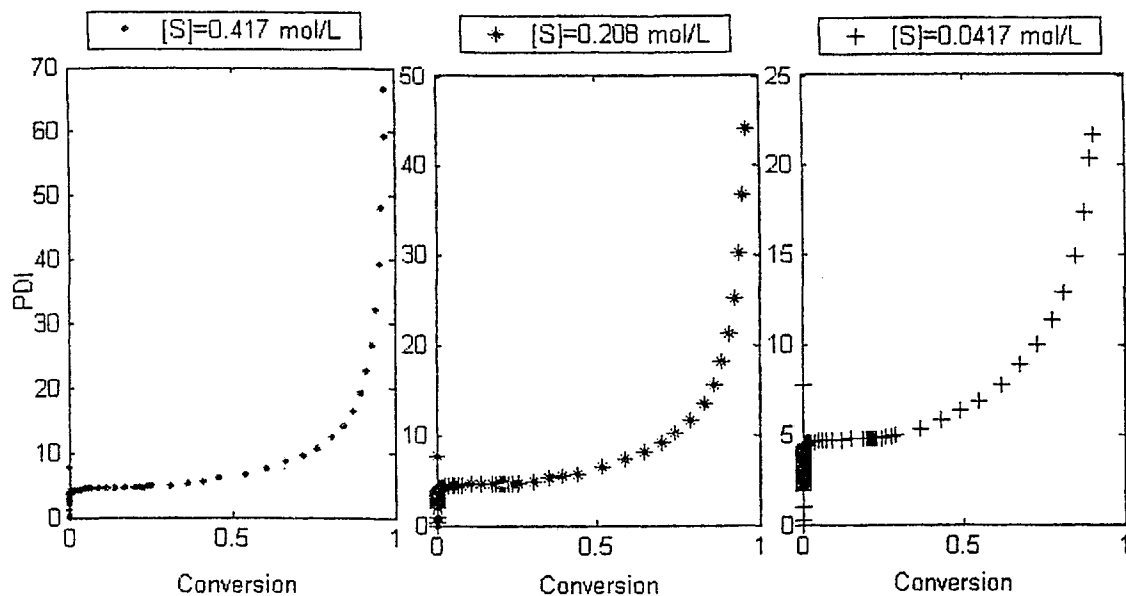
Figure 4. 22. Case 1. Effect of Emulsifier Concentration on PDI
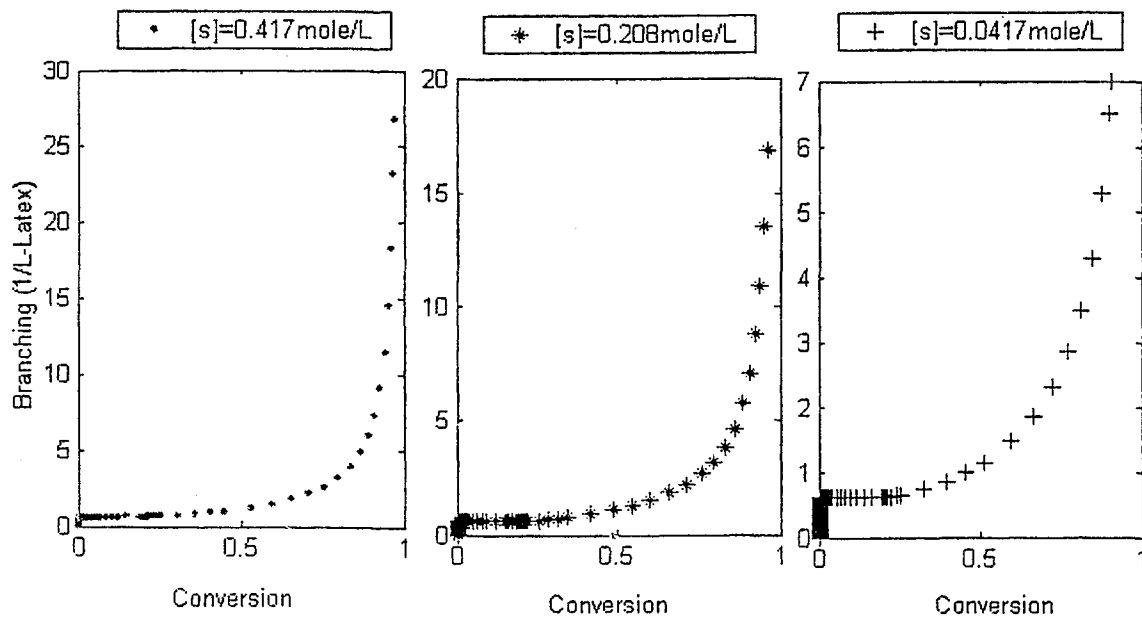
Figure 4. 23. Case 1. Effect of Emulsifier Concentration on Number of Branch Points

53
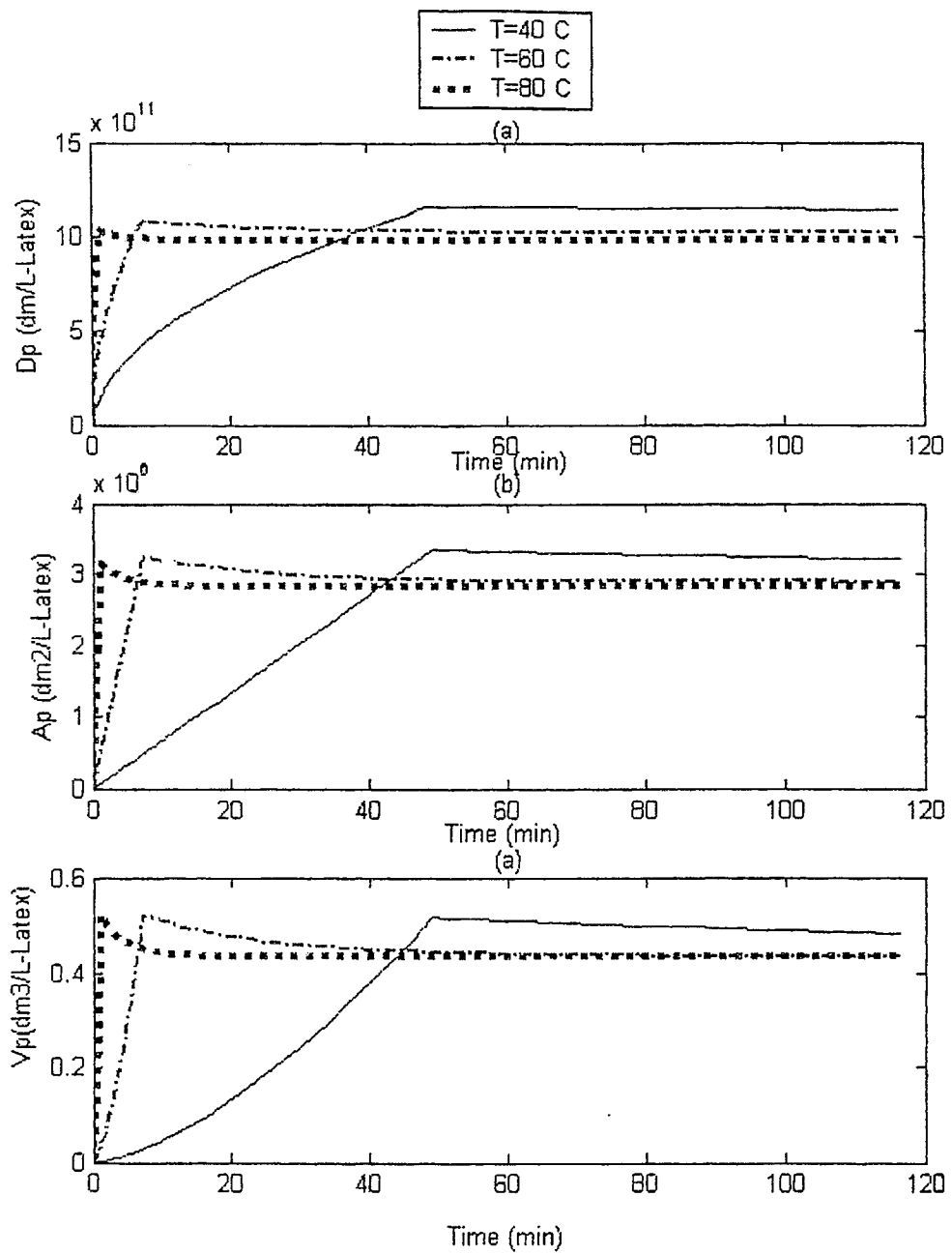
Figure 4. 24. Case 1. Effect of Reactor Temperature on Particle (a) Diameter, (b) Surface Area, and (c) Volume

54
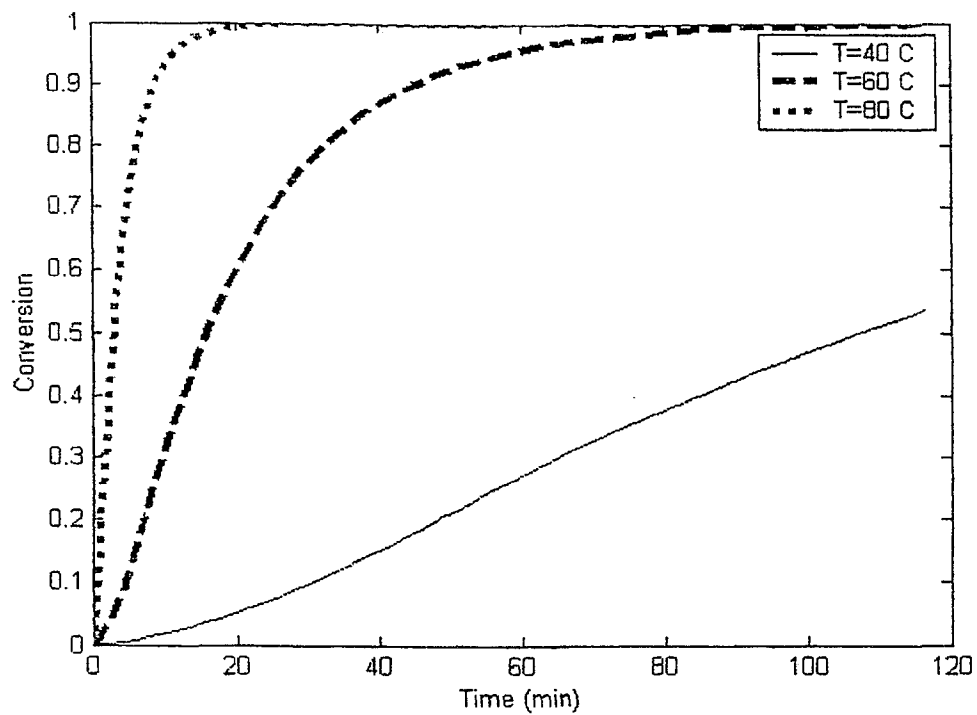
Figure 4. 25. Case 1. Effect of Reactor Temperature on Conversion
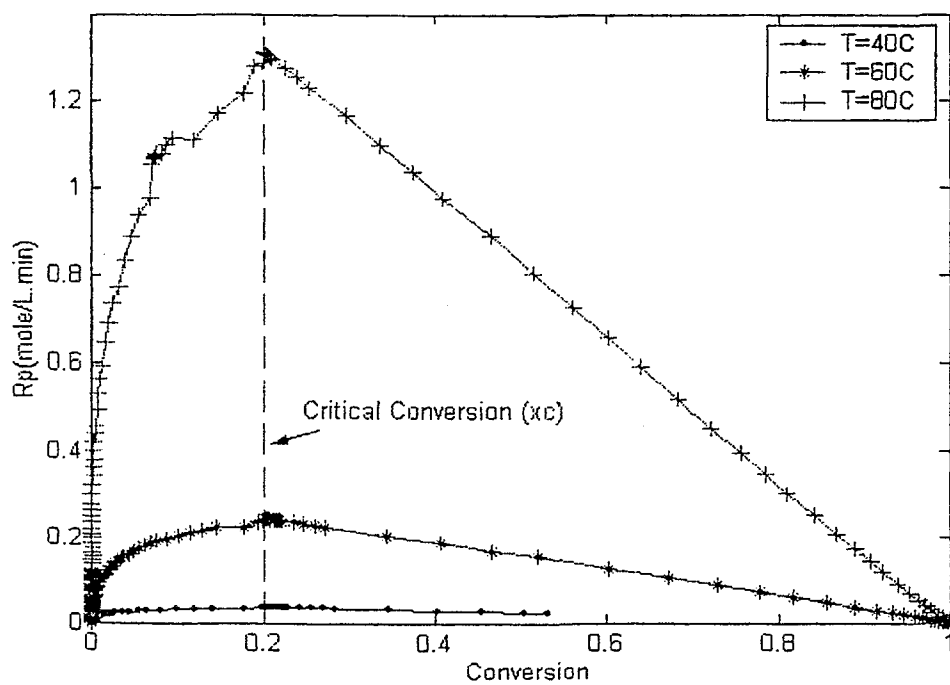
Figure 4. 26. Case 1. Effect of Reactor Temperature on Rp

55
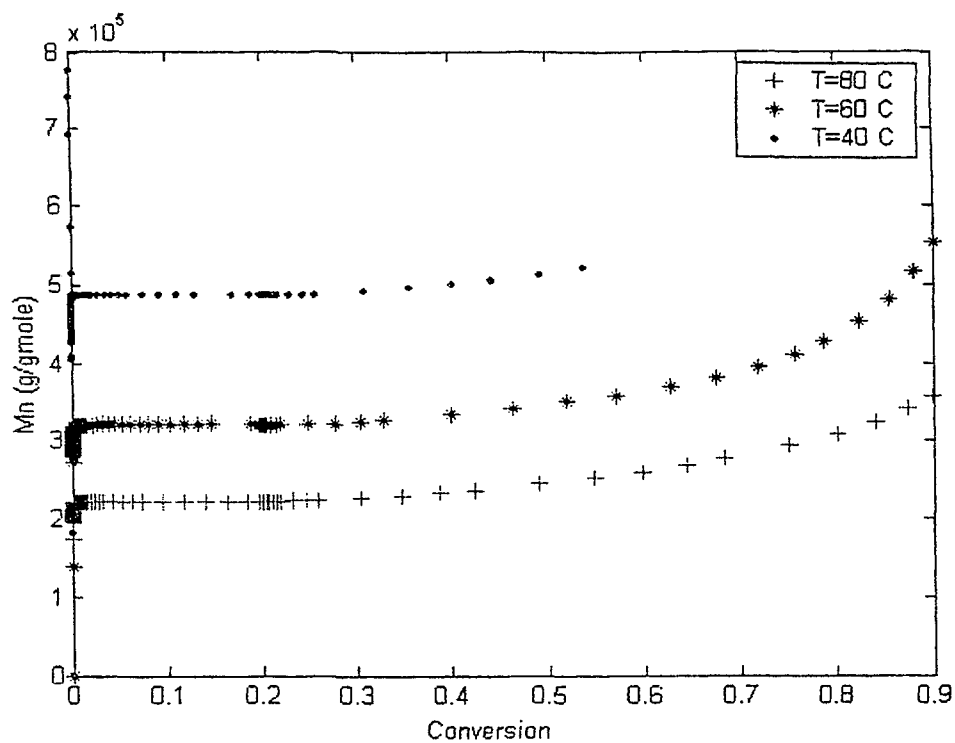
Figure 4. 27. Case 1. Effect of Reactor Temperature on Mn
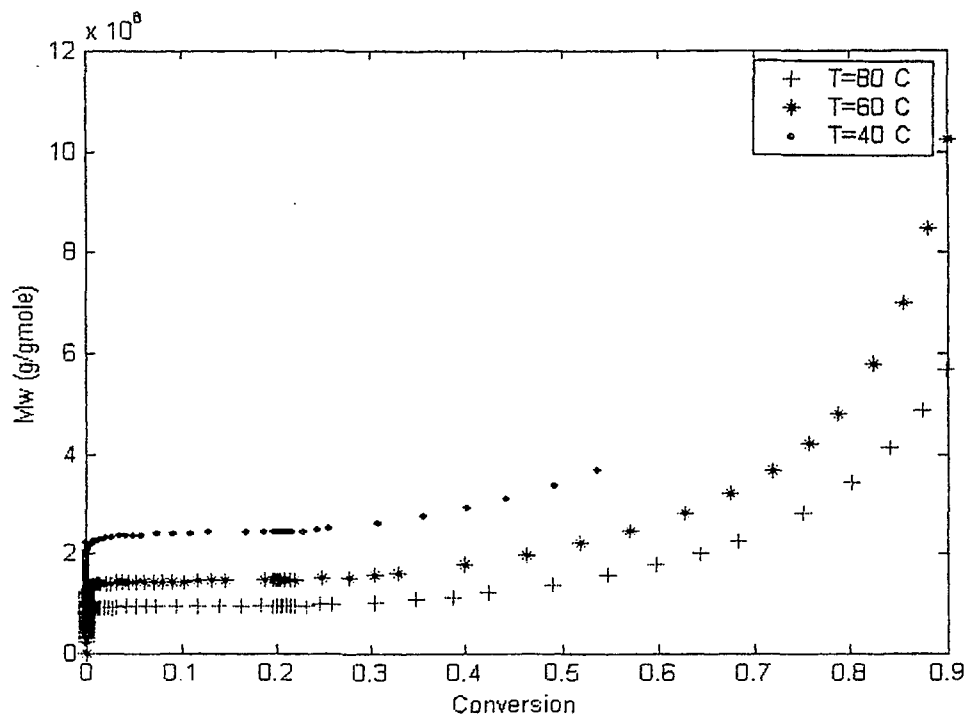
Figure 4. 28. Case 1. Effect of Reactor Temperature on Mw

56
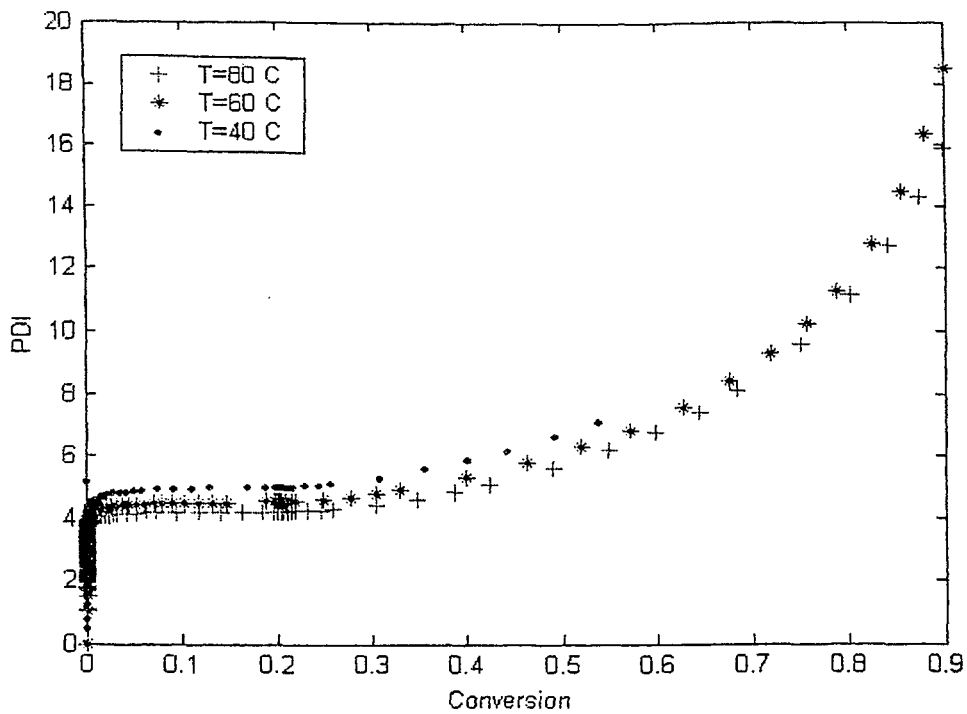
Figure 4. 29. Case 1. Effect of Reactor Temperature on PDI
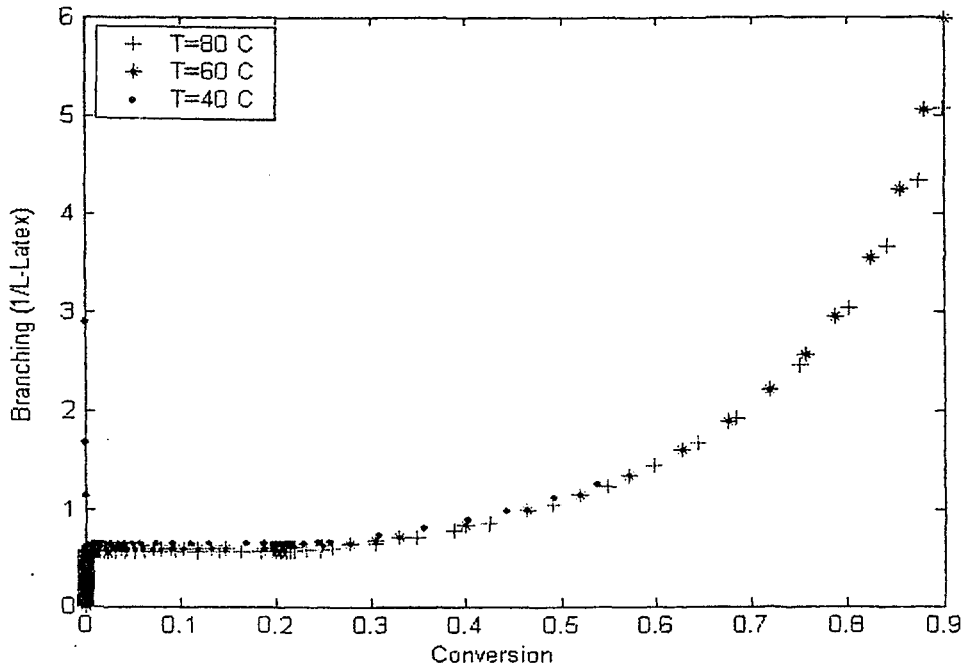
Figure 4. 30. Case 1. Effect of Reactor Temperature on Number of Branch Points

57
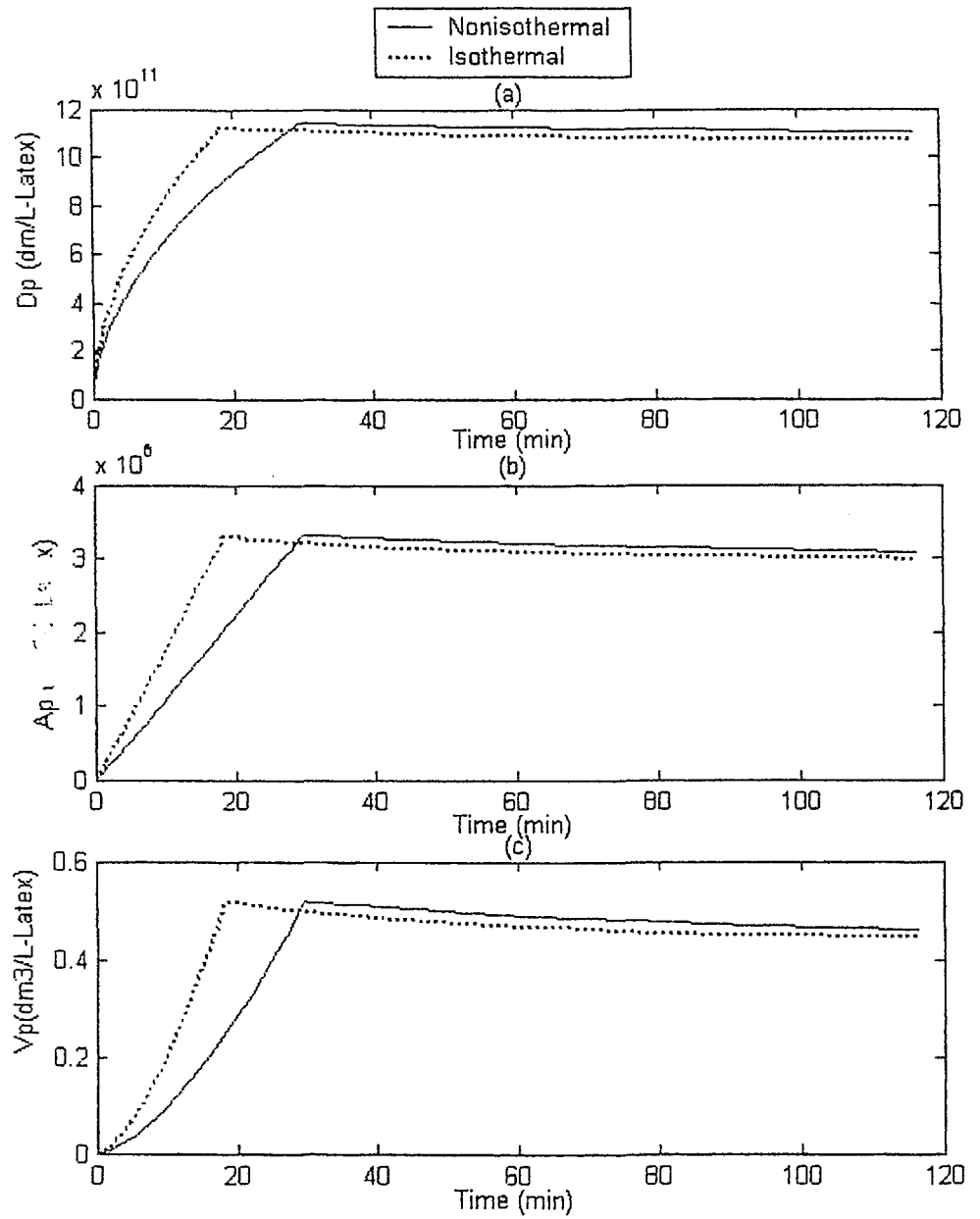
Figure 4. 31. Case 1. Effect of Nonisothermal Condition on Particle (a) Diameter, (b) Surface Area, and (c) Volume

58
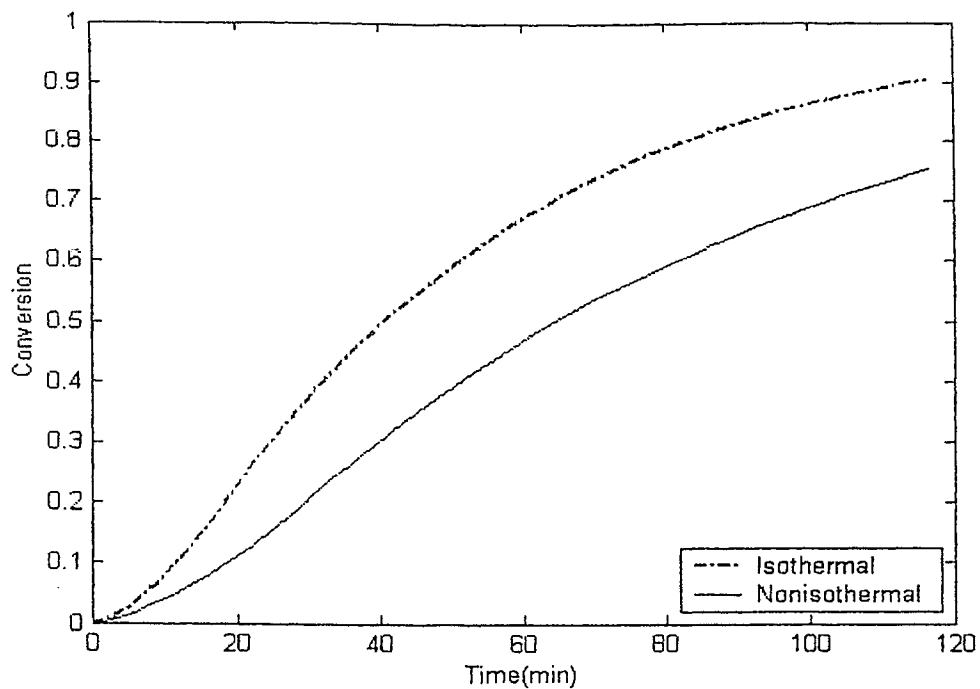
Figure 4. 32. Case 1. Effect of Nonisothermal Condition on Conversion
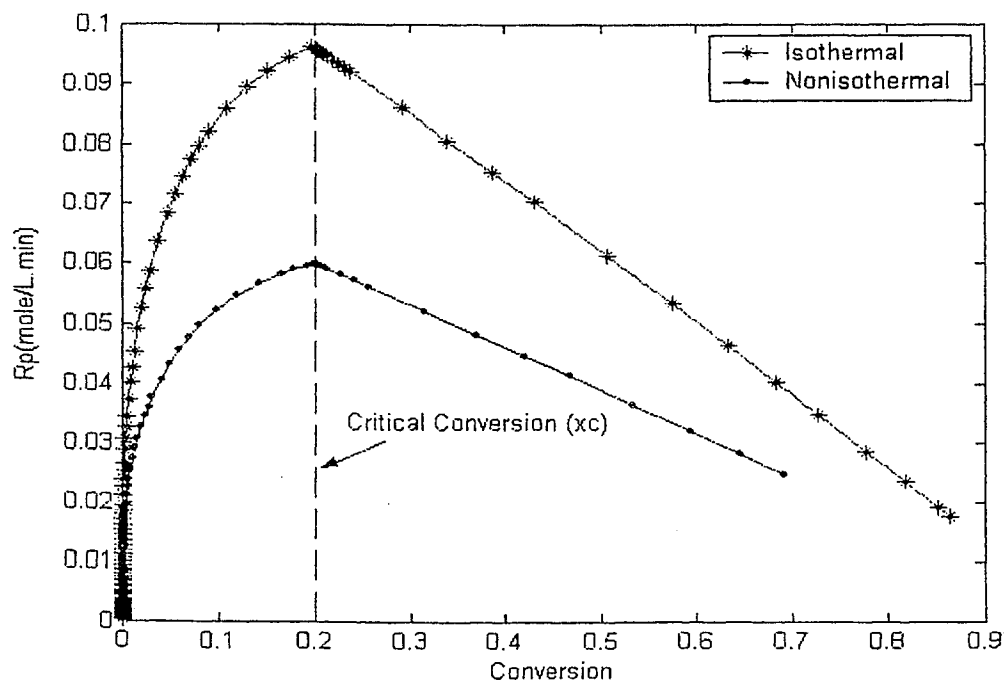
Figure 4. 33. Case 1. Effect of Nonisothermal Condition on Rp

59
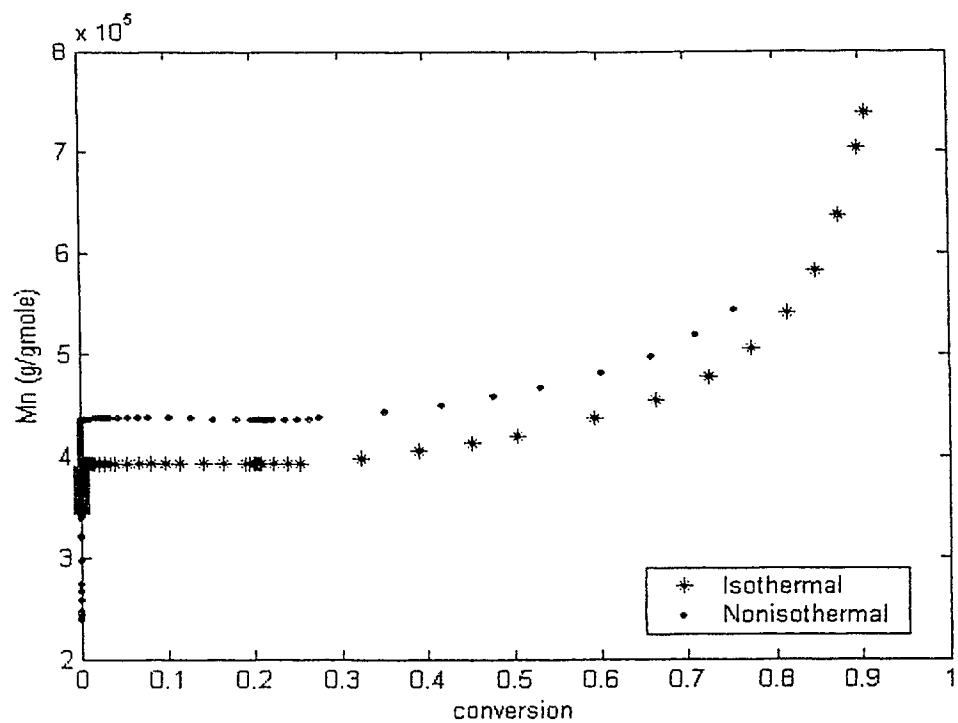
Figure 4. 34. Case 1. Effect of Nonisothermal Condition on Mn
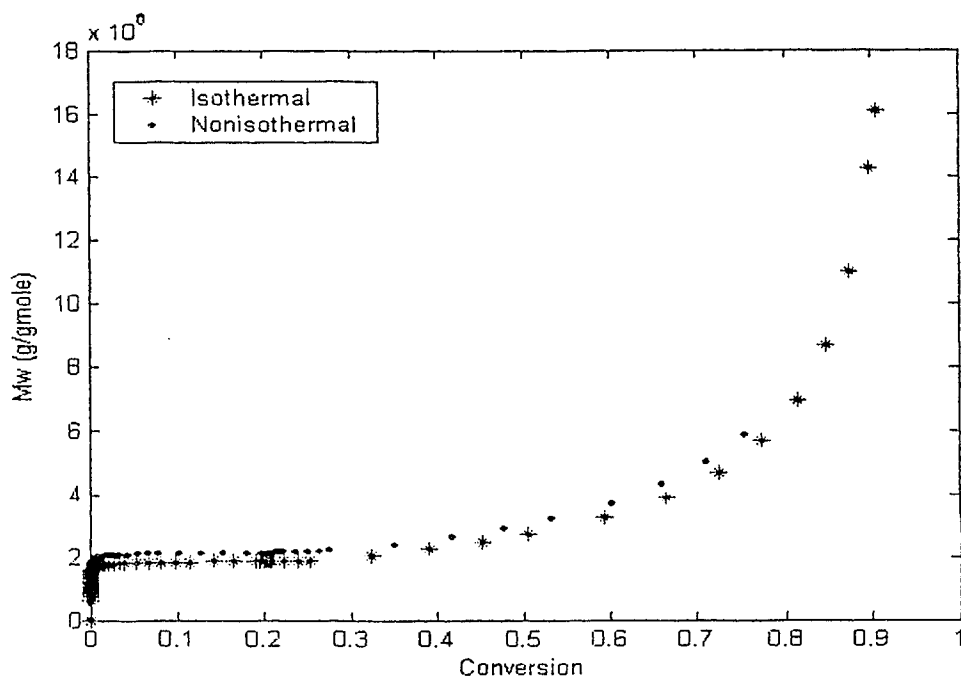
Figure 4. 35. Case 1. Effect of Nonisothermal Condition on Mw

60
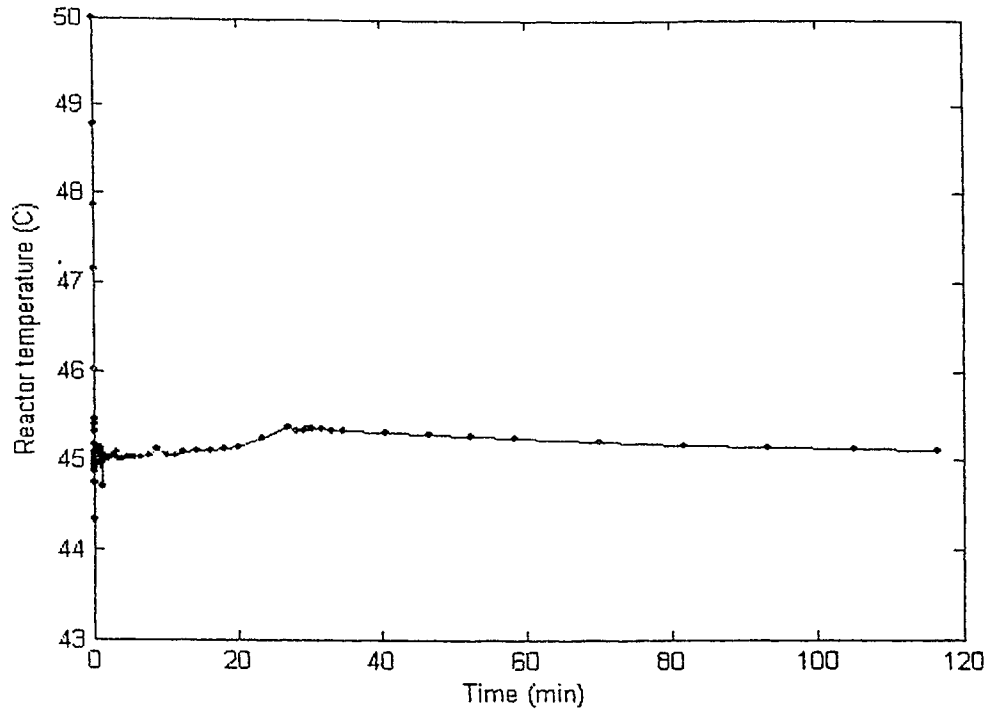
Figure 4. 36. Case 1. Variation of Reactor Temperature under Nonisothermal Condition
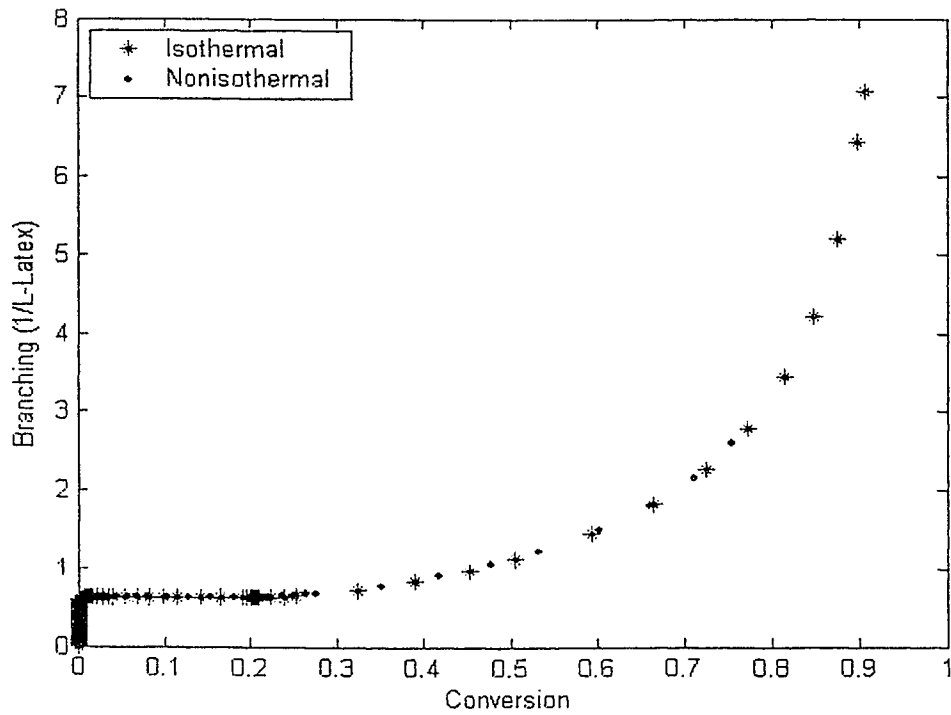
Figure 4. 37. Case 1. Effect of Nonisothermal Condition on Number of Branch Points

61
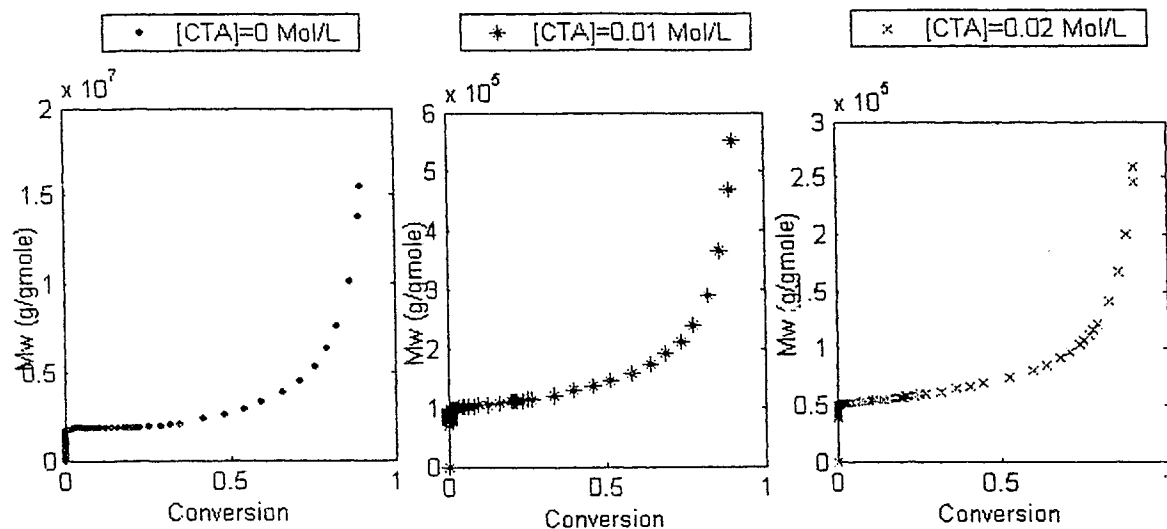
Figure 4. 38. Case 1. Effect of Chain Transfer Agent on Mw
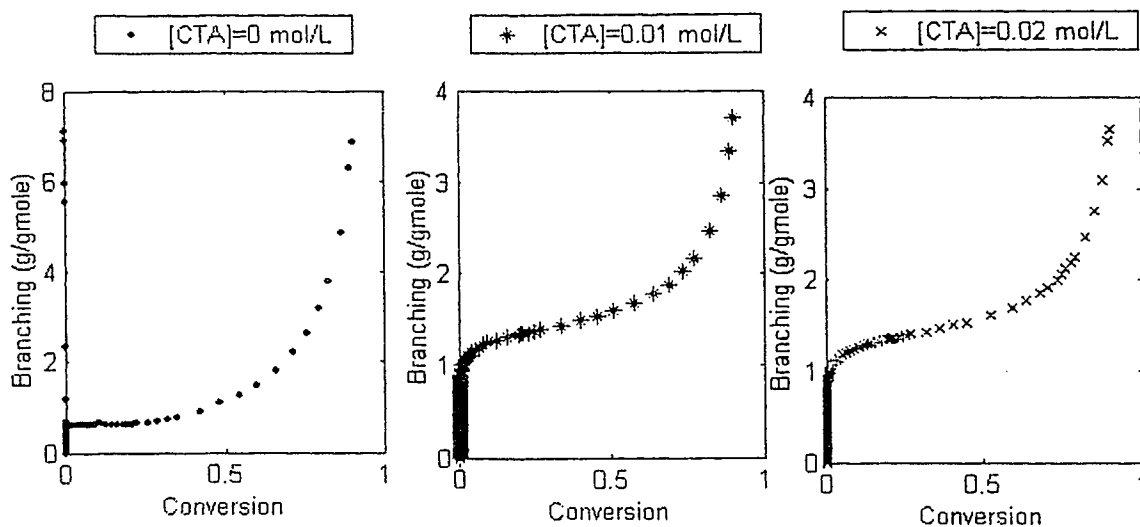
Figure 4. 39. Case 1. Effect of Chain Transfer Agent on Number of Branch Points

62
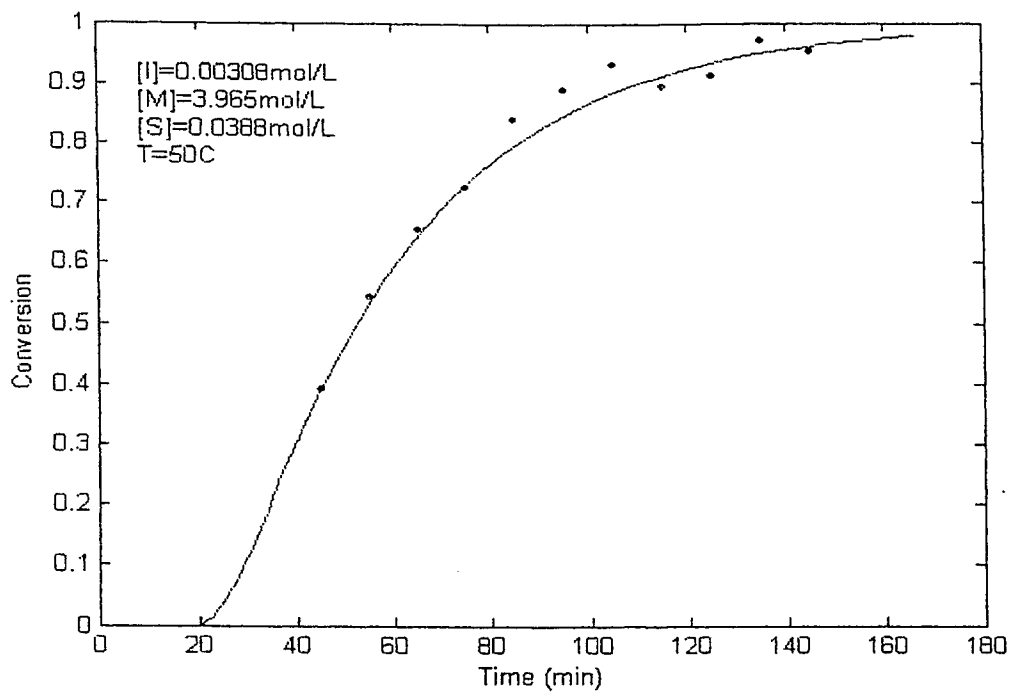
Figure 4. 40. Comparison of Model Prediction and Experimental Data
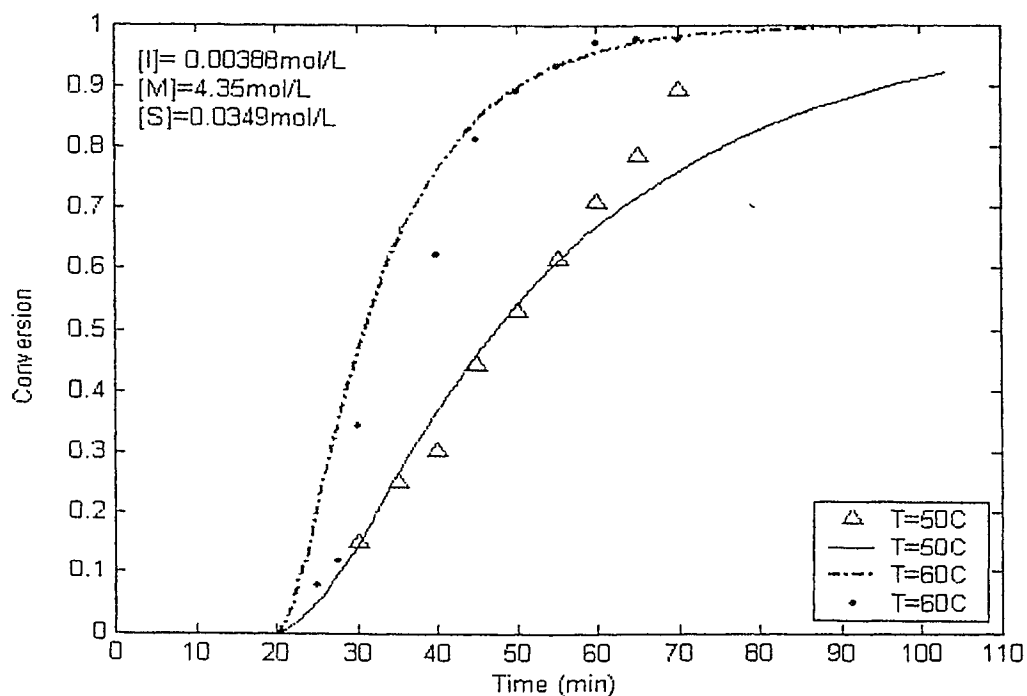
Figure 4. 41. Comparison of Model Prediction and Experimental Data

63
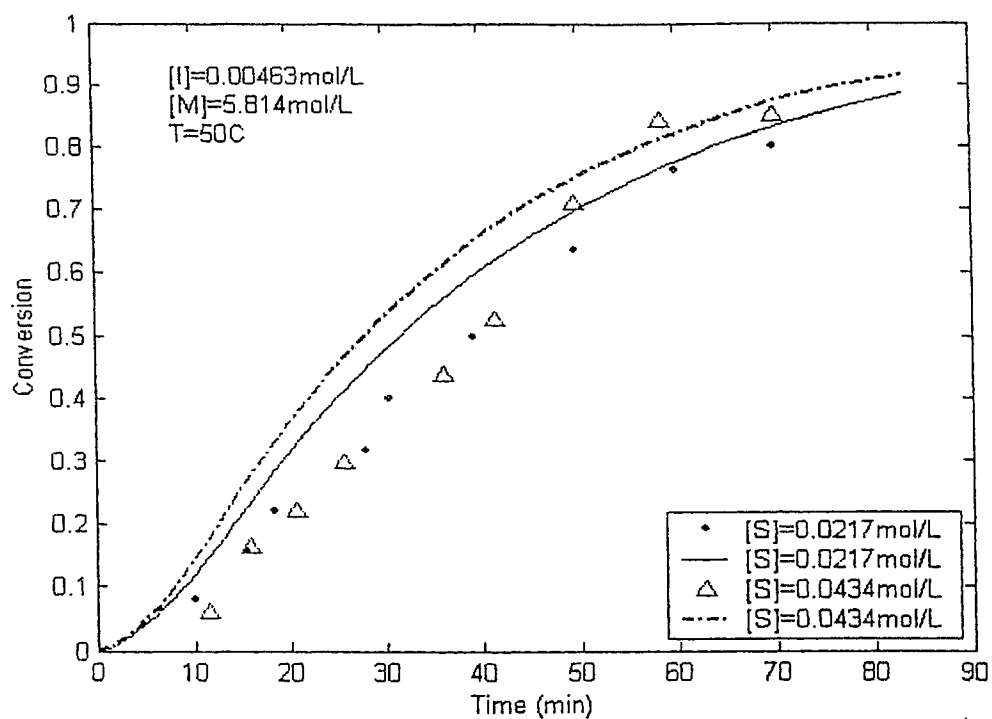
Figure 4. 42. Comparison of Model Prediction and Experimental Data
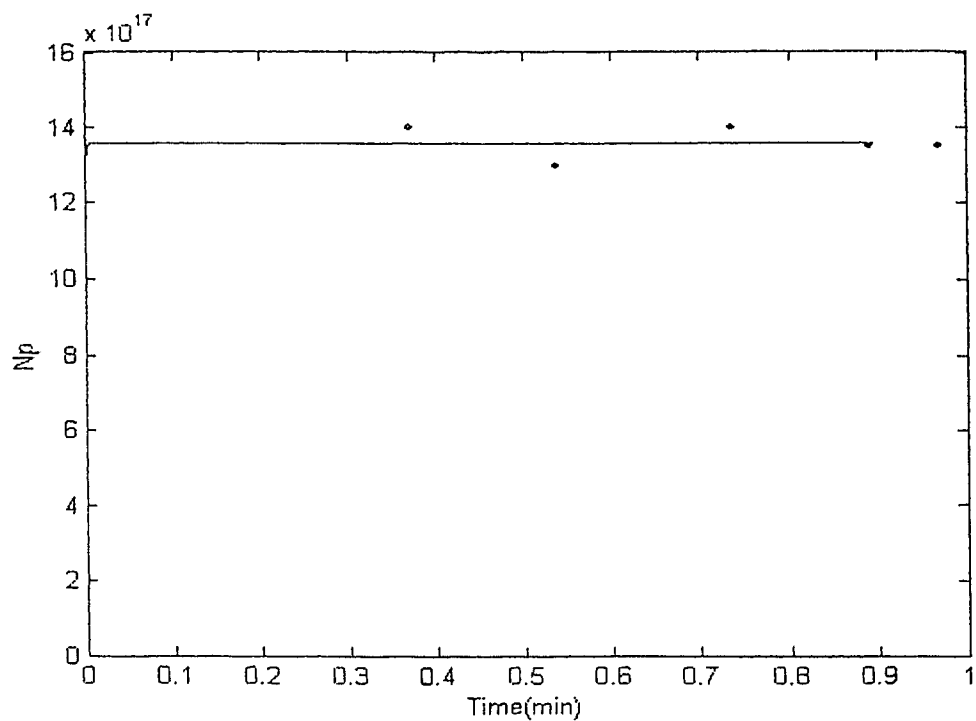
Figure 4. 43. Case 1. Comparison of Model Prediction and Experimental Data

64
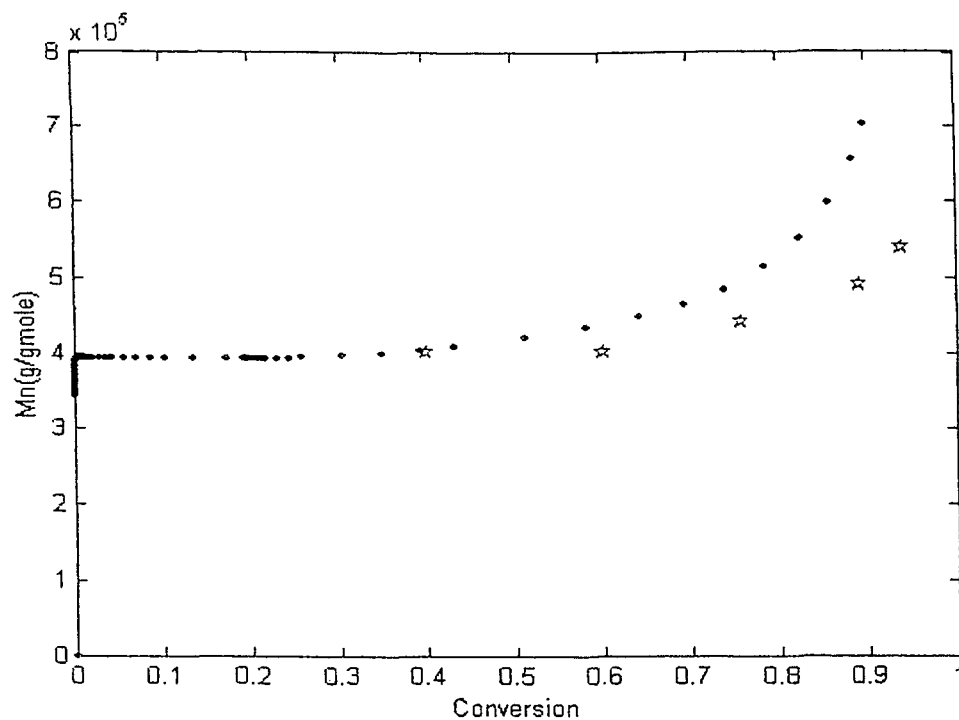
Figure 4. 44. Case 1. Comparison of Model Prediction and Experimental Data
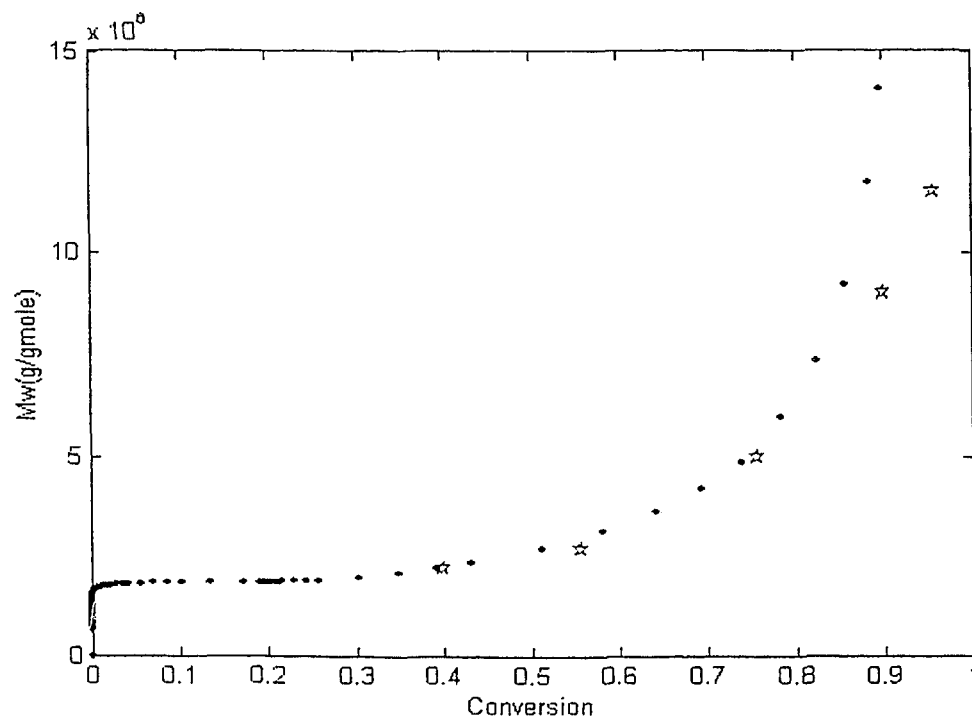
Figure 4. 45. Case 1. Comparison of Model Prediction and Experimental Data

65
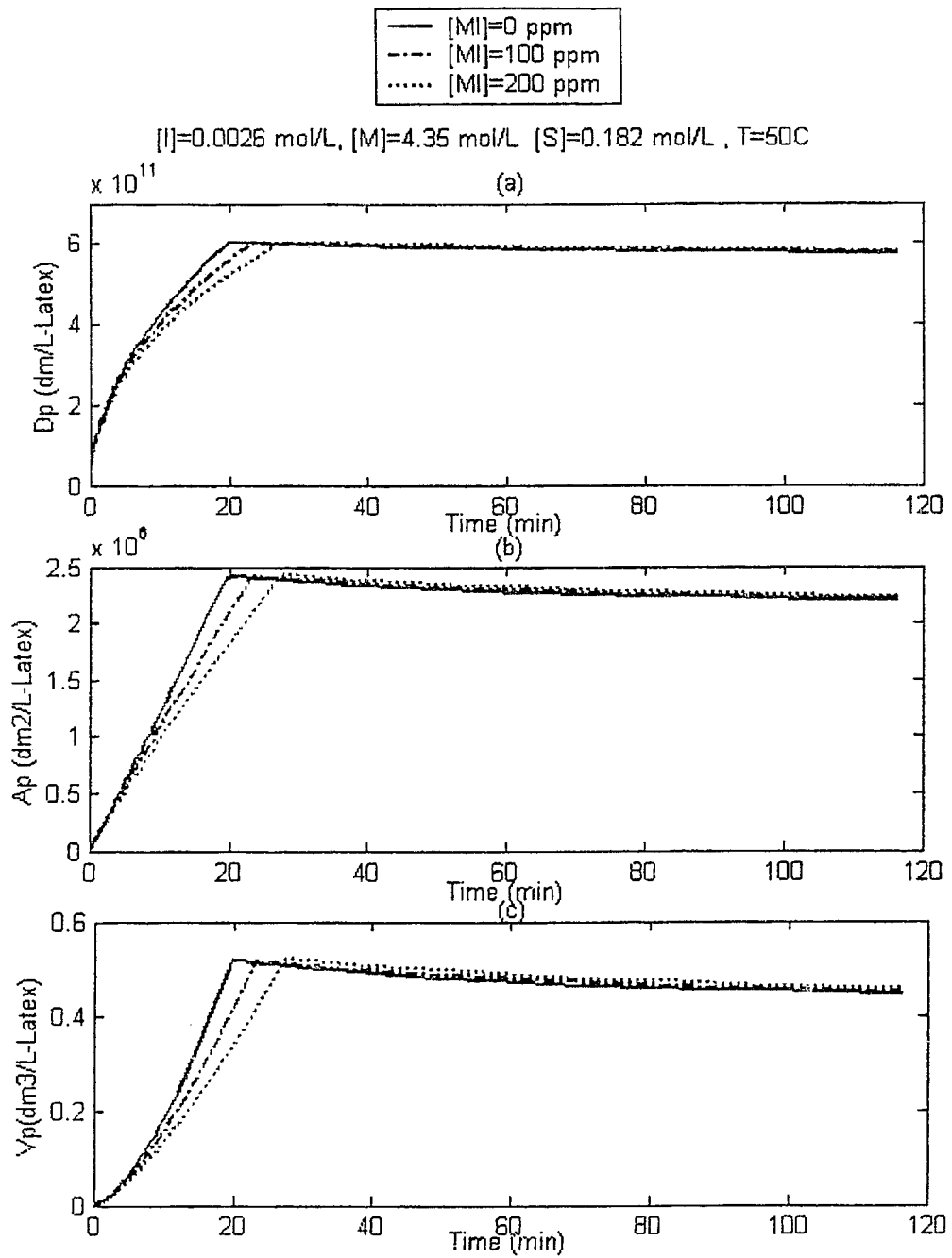
Figure 4. 46. Case 2. Effect of Impurity on Particle (a) Diameter, (b) Surface Area, and

(c) Volume

66
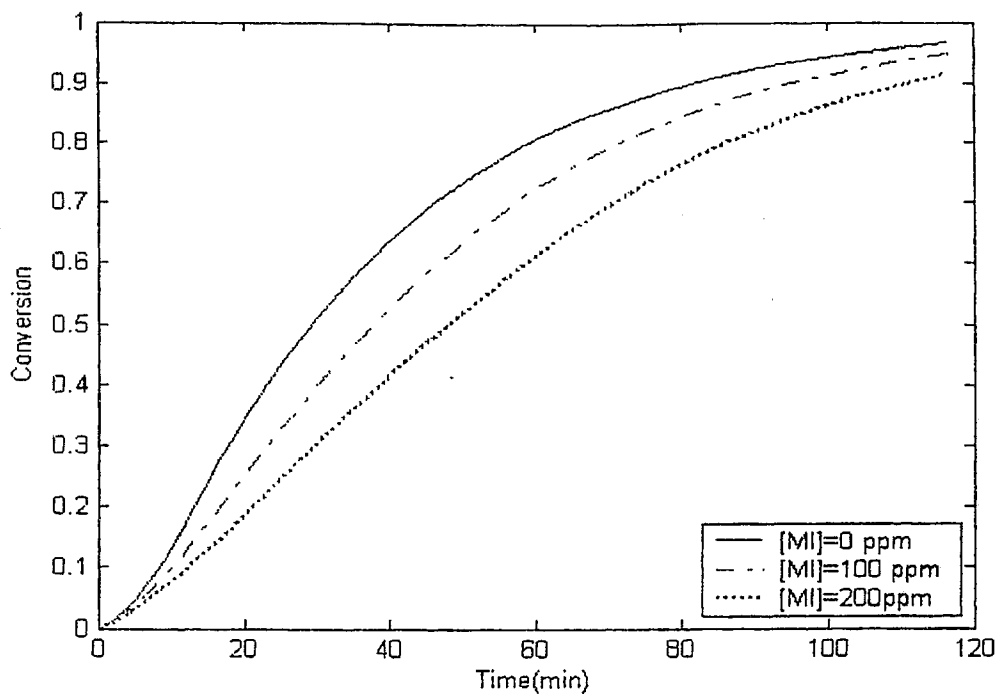
Figure 4. 47. Case 2 Effect of Impurity on Conversion
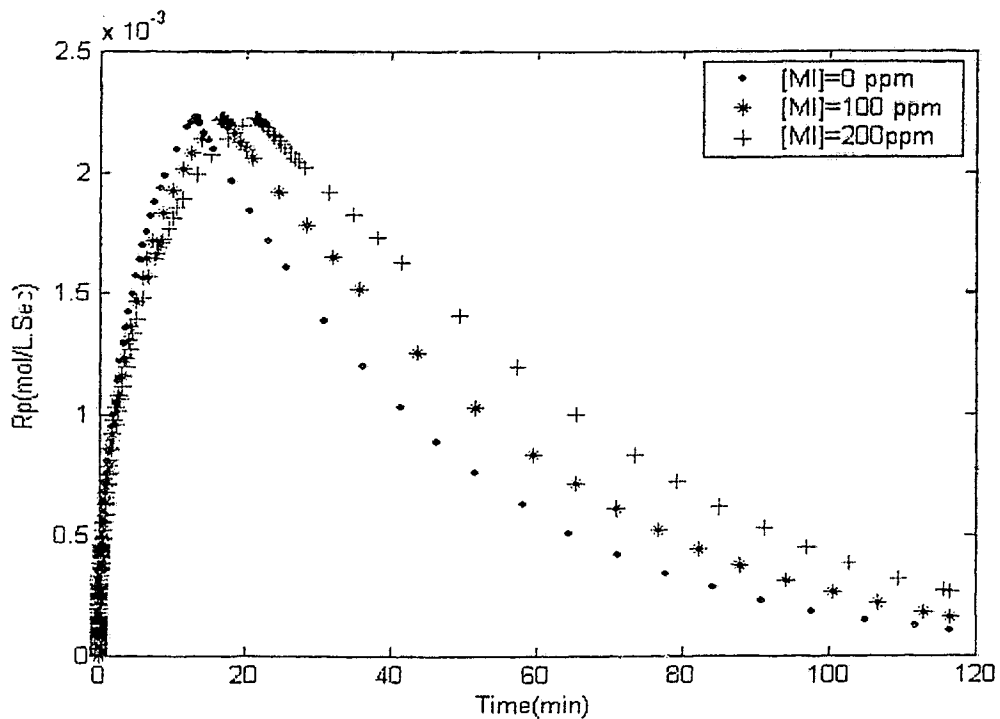
Figure 4. 48. Case 2. Effect of Impurity on Rp

67
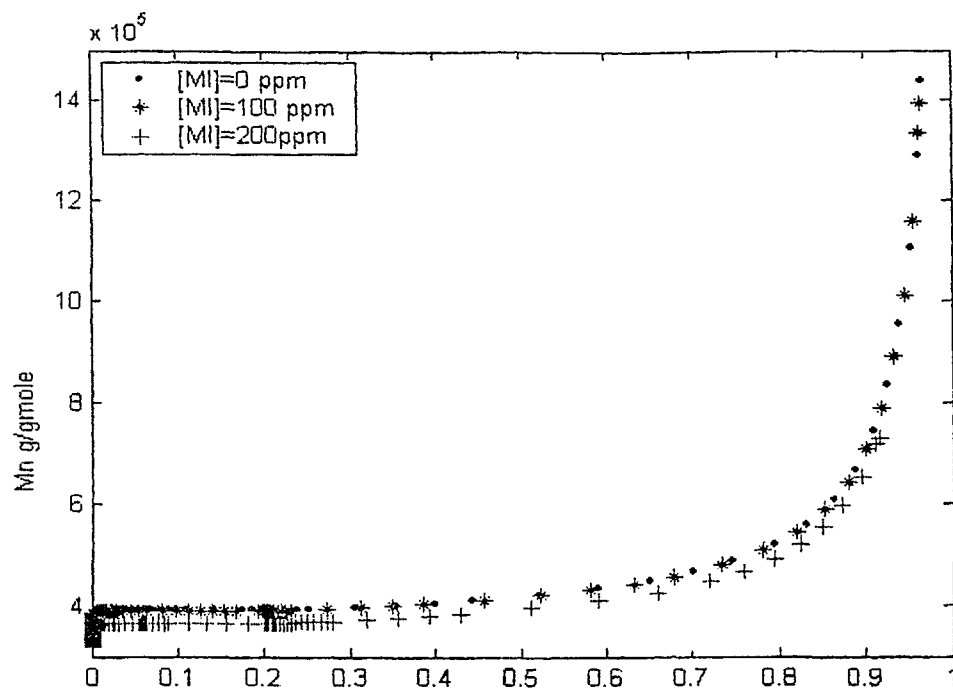
Figure 4. 49. Case 2. Effect of Impurity on Mn
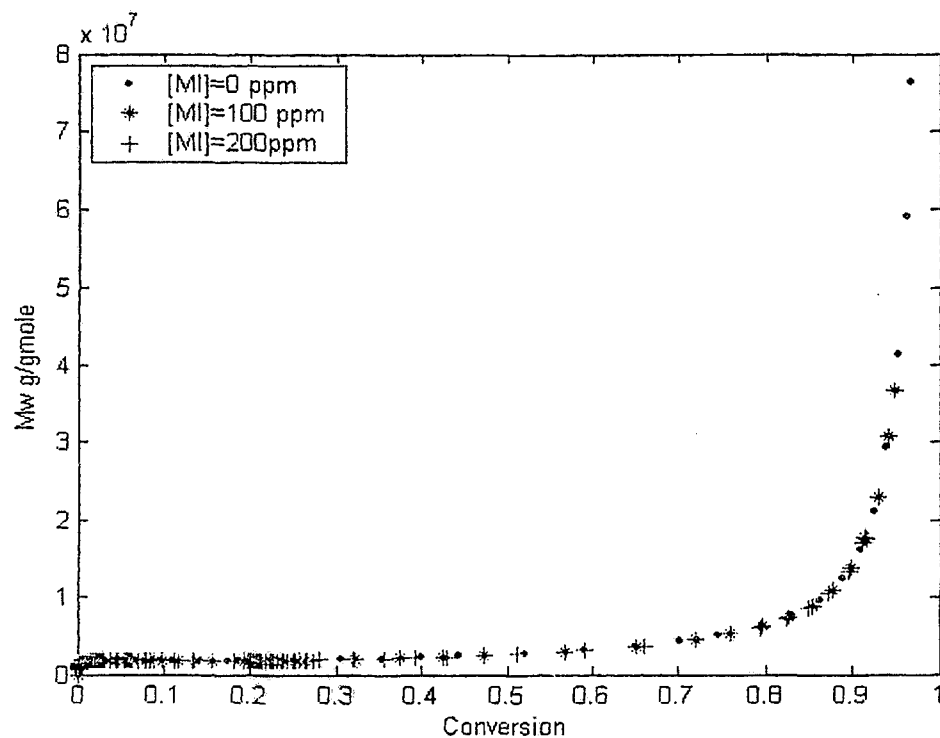
Figure 4. 50. Case 2. Effect of Impurity on Mw

68
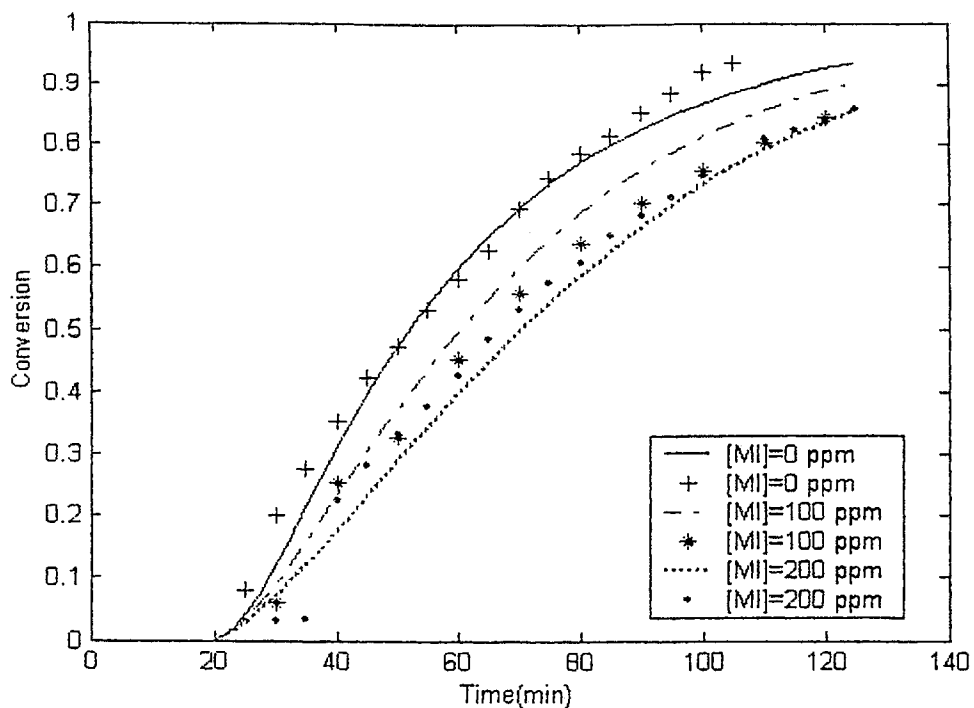
Figure 4. 51. Case 2. Comparison of Model Prediction with Experimental Data
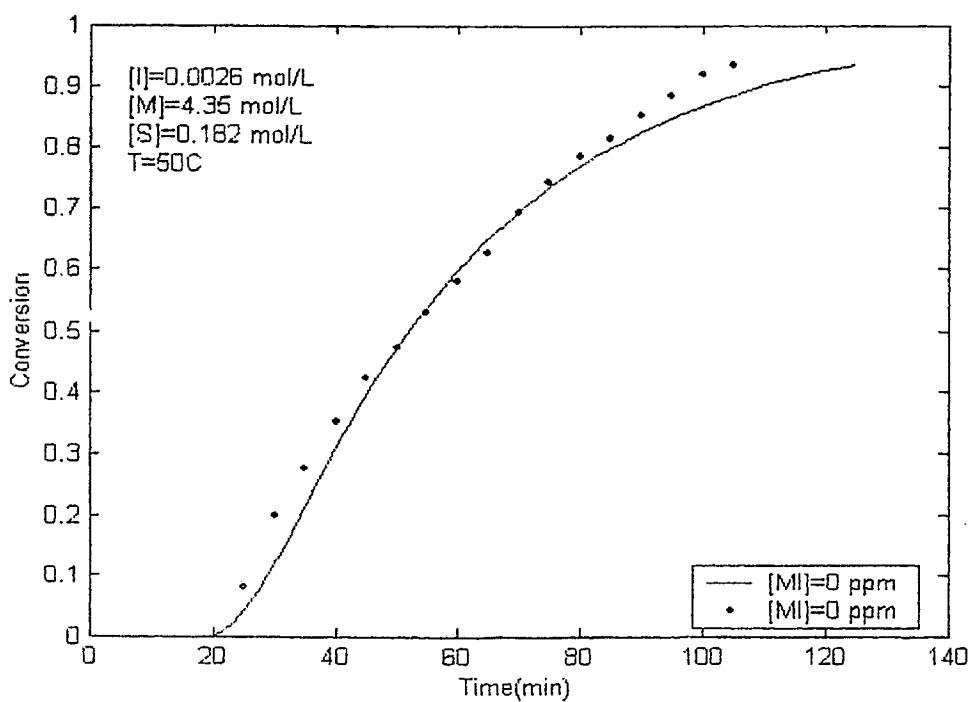
Figure 4. 52. Case 2. Comparison of Model Prediction with Experimental Data

69
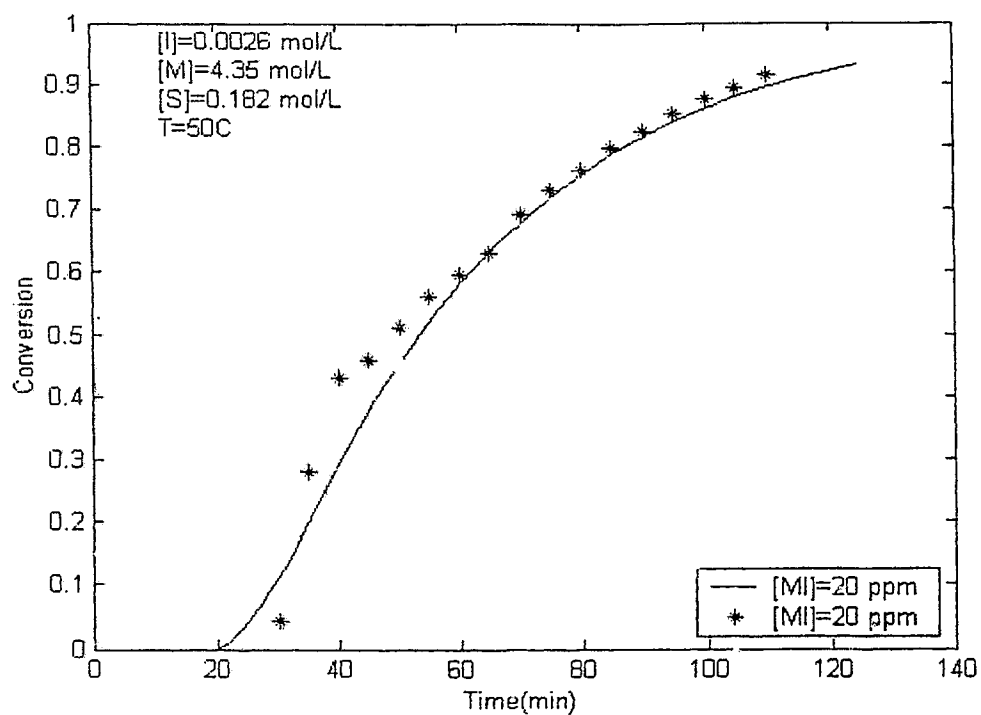
Figure 4. 53. Case 2. Comparison of Model Prediction with Experimental Data
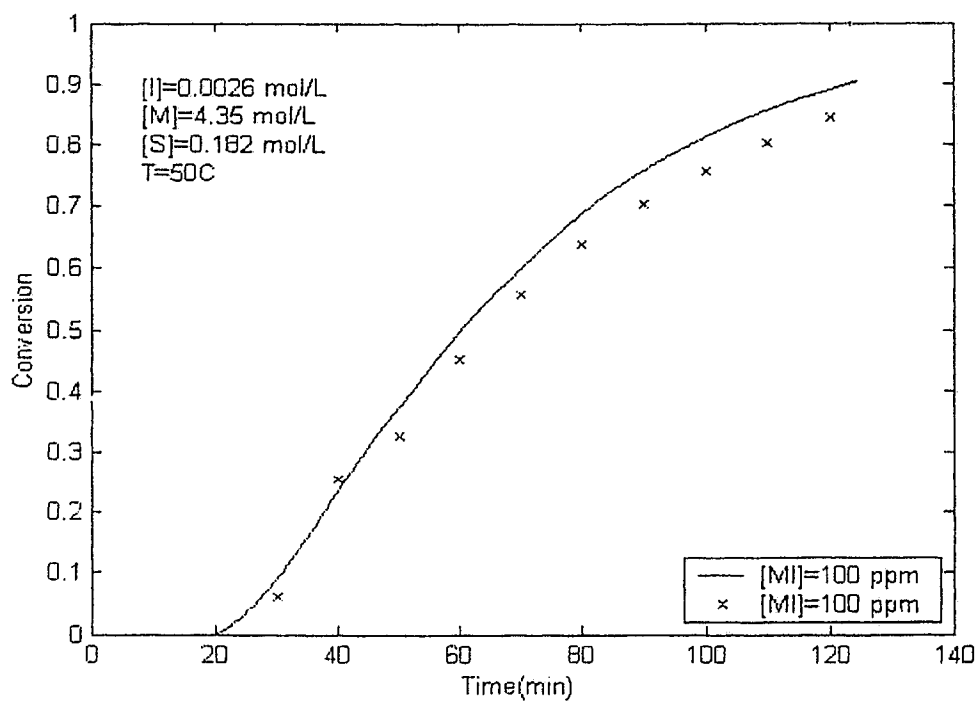

Figure 4. 54. Case 2. Comparison of Model Prediction with Experimental Data

70
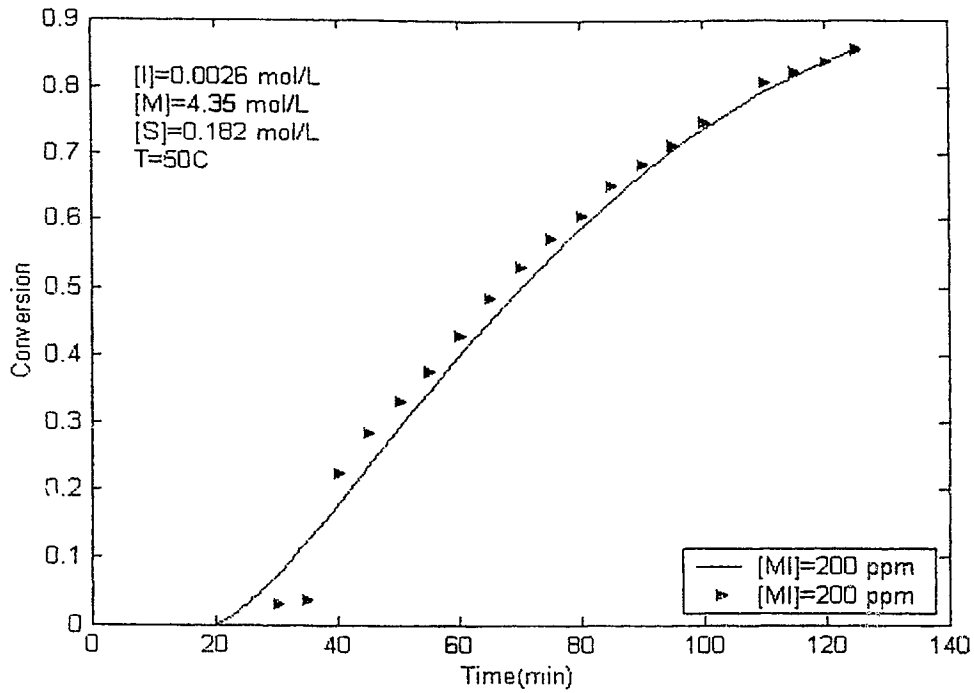
Figure 4. 55. Case 2. Comparison of Model Prediction with Experimental Data
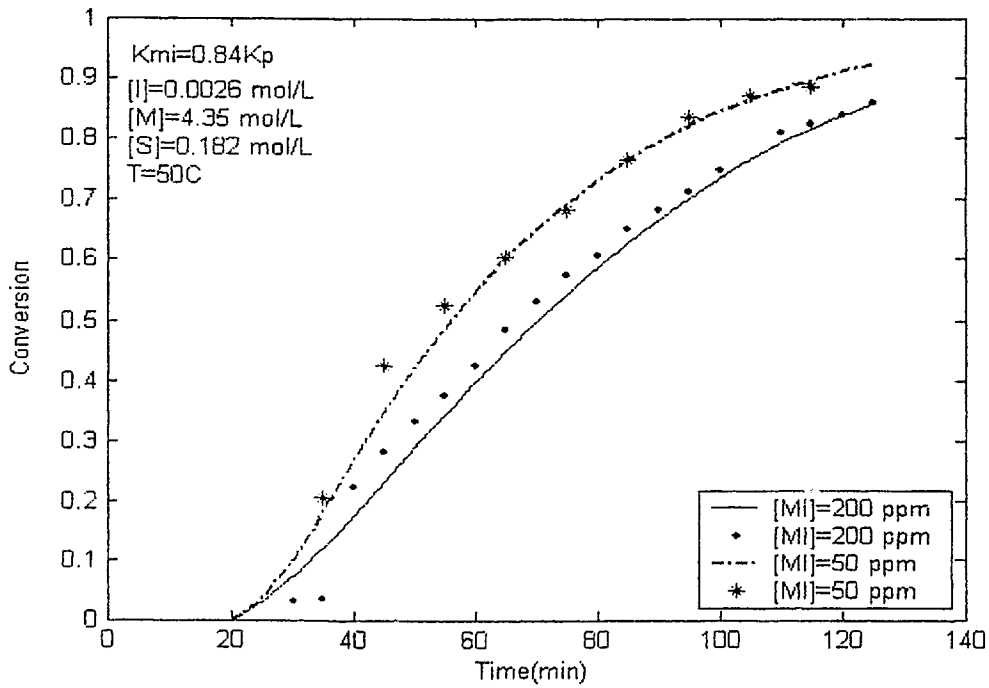
Figure 4. 56. Case 2. Effect of k_{MI} on Conversion

71

4.1.2 Semi-batch emulsion polymerization reactor

Generally, semi-batch polymerization reactors involve a continuous or intermittent addition of one or more ingredients to the batch while the reaction is in progress. Addition of monomer during emulsion polymerization reaction leads to higher rate of polymerization and also easier control of the reaction rate. One effective strategy of controlling polymer particle size is to control the polymer particle nucleation time. From the developed equations which show the rate of particle generation, it is evident that manipulation of initiator or emulsifier concentration or flow rate can have significant effect on polymer particle nucleation. As it is shown in Figures 4.3, most of the nucleation happens in stage 1, which for case 1 monomers is less than two minutes. Therefore, in a very short time almost all polymer particles are formed and subsequently start to grow during stage 2. It means that properties of the final product dependent on the polymer particle number and defined in stage 1 and 2, which are both completed in less than 10 minutes. In the vinyl acetate case, the droplets disappear at low concentration ($x_c=20\%$), which makes the situation complicated.

Previous studies showed that the number of polymer particles generated is almost independent of initiator concentration while the emulsifier concentration can affect the number of formed particles; hence it may be used to extend the nucleation time. The emulsifier can be feed in pulses or at a very slow constant feed rate to cause a series of consecutive particles generation. Each particle generation lasts until the free emulsifier level in the reaction become less than the critical micelles concentration (CMC). Previous studies (Penlidis, 1986) revealed that the system is extremely sensitive to emulsifier flow rate and development of feed policies for emulsifier was not very easy to realize due to high sensitivity of the particle generation period to internal small changes. Another proposed approach is to manipulate $A_m(t)$, the free emulsifier area in the reactor, to monitor the desired number of particles. Based on the value of $A_m(t)$, three partitions may exist:

$A_m(t) < 0$: No micelles exist in the system and the micellar nucleation is zero.

$A_m(t) = 0$: The amount of total emulsifier in the system brings the micellar concentration up to the CMC level and covers the existing polymer particles.

72

$A_m(t) > 0$: The total emulsifier is partially used to completely cover the surface of the existing polymer particles and the remainder to exceed the CMC level and form new micelles. New micelles generate new polymer particles and finally increase the total particle surface area.

Figure 4.57 shows the adjustment of $A_m(t)$ to give the three particle generations. This adjustment drives the process to generate micelles three times during the reaction, every time the area of the micelles positive. If no emulsifier is added in during the reaction, the micellar area decays to zero in very short time, as shown in the same plot. Figure 4.58 shows the growth of number of polymer particles. All three consecutive generations can be detected in this plot. As a result, the effect on the duration of stage 1 is considerable. This stage is extended to about 20 minutes by application of new feed policy. The emulsifier feed policy needed to give $A_m(t)$ was solved and is shown in Figure 4.60.

Since manipulation of $A_m(t)$ for extension of the nucleation time is not easy in practice because it is difficult to be followed during the reaction. So it is necessary to find the emulsifier feed rate policy which gives the desired $A_m(t)$ versus time history. The emulsifier feed rate policy has also a positive effect on the size of particles. Since more micelles are present in the system, the size of polymer particles increases (Figure 4.59).

73
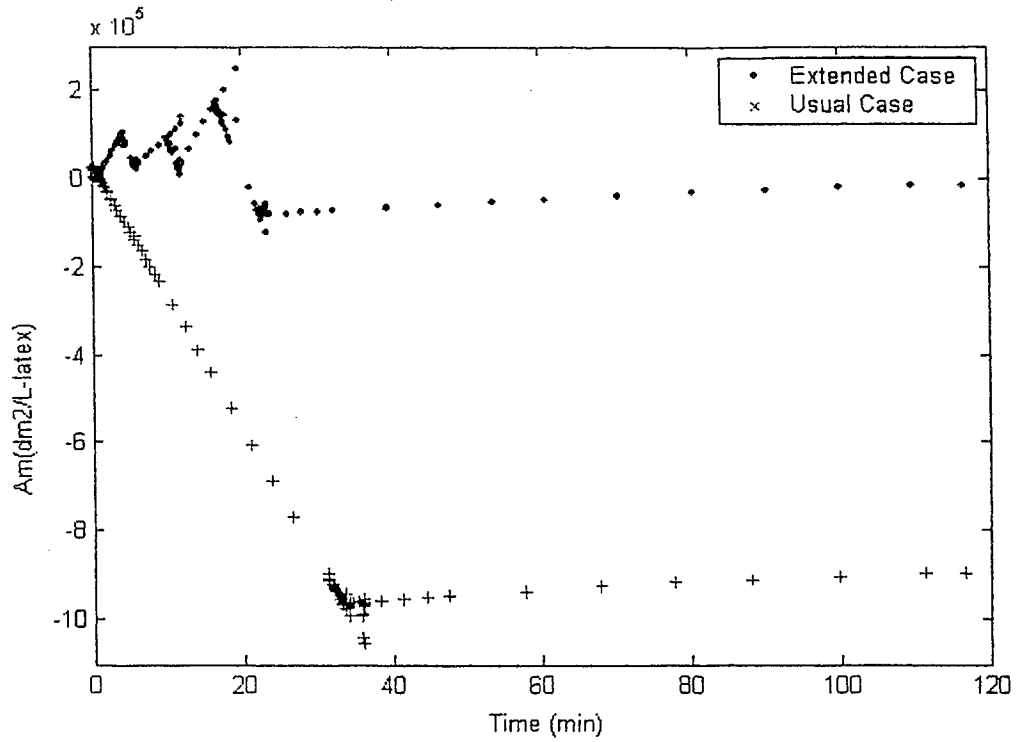
Figure 4. 57. Comparison of $A_m(t)$,Usual Case and Extended Case
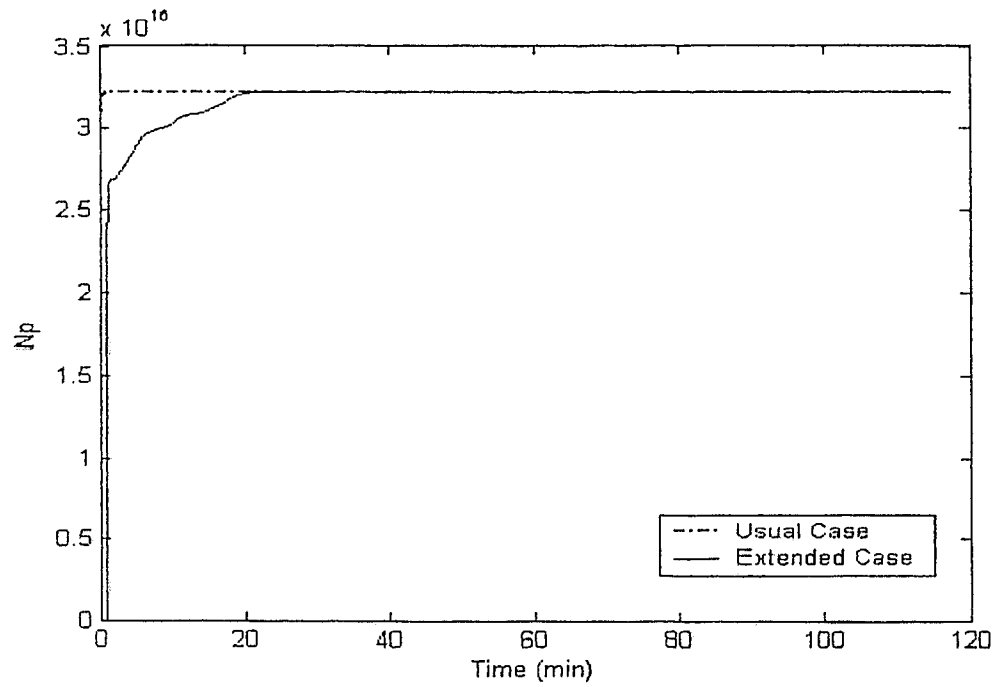

Figure 4. 58. Comparison of Np(t) between the Usual and the Extended Case

74
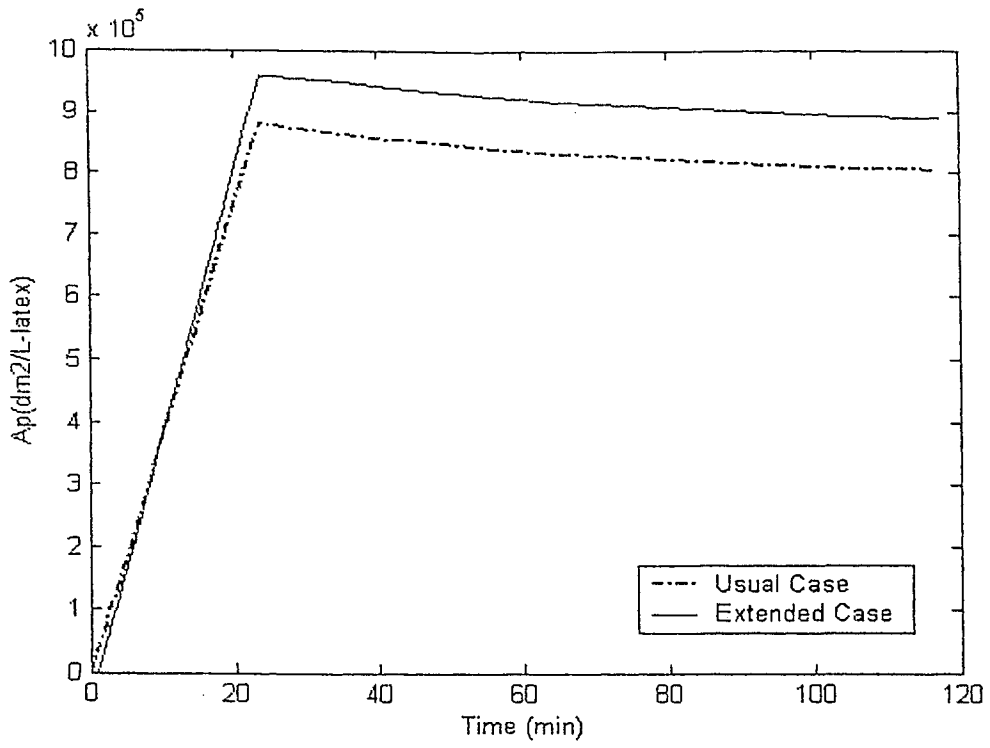
Figure 4. 59. Total Polymer Particle Surface Area Corresponding to Figure 4.58
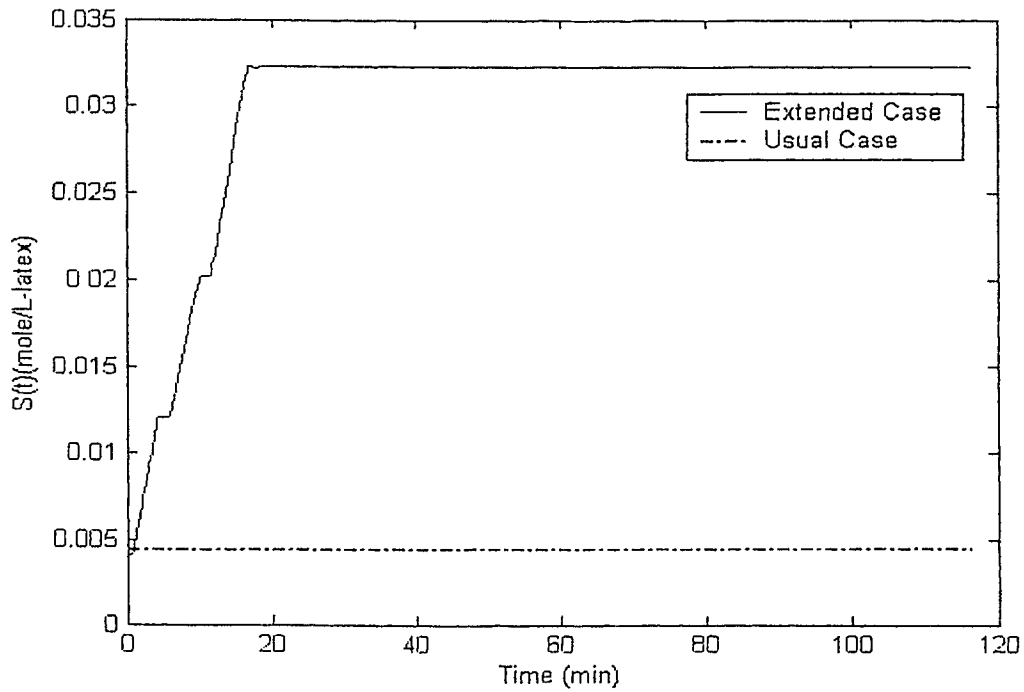
Figure 4. 60. Total Emulsifier Level in the Reactor Corresponding to Figure 4.58

75

4.1.3 Continuous stirred tank reactor (CSTR)

Batch and semi-batch reactors are mostly used in industrial latex production. Continuous polymerization reactors can offer several advantages such as lower operating costs, better heat removal capabilities and more consistency in product quality. Continuous emulsion polymerization in a CSTR is much more complex than batch polymerizations and often exhibits large and sustained oscillation in particle concentration, size and conversion. The oscillation is particularly true for case 1 monomers because of the rapid generation of a large number of particles due to periodic particle nucleation.

At the beginning of the reaction, a large number of particles is generated by particle nucleation leading to an increase in the surface area of the growing particles. The surface area is covered with emulsion molecules. When the area of particles becomes great enough, the total surface area of micelles becomes negative means there is no surfactant available in the reactor. As a result, the particle generation rate is low or even zero. After a while with a new emulsifier being fed to the reactor, emulsifier's concentration becomes sufficient to form new micelles and eventually start another stage of particle nucleation.

The pronounced oscillation was studied by Kiparissides (1978) in great details. Furthermore, he worked on the effect of feed condition (initiator and emulsifier concentration) and residence time in a single reactor. The same experimental condition was used in this study and Figures 4.61-4.65 represent simulation results using the presently developed model. The discussed process is easily revealed in these results too. In each interval when $A_m(t)$ becomes greater than zero, a new particle generation occurs until all the micellar area is used up by this new particles. As shown in figure 4.64, the rate of polymerization also goes to zero when there is no micelle available in the reactor, and then it increases very fast when the particle generation starts again.

The mean residence time of the reactor is an important factor that affects the process conversion. Figures 4.66-4.68 show another run under the same condition but lower residence time ($\theta=20$ min). The conversion remains below 30% while in the previous run ($\theta=30$ min), the conversion was about 45%. The reactants need more time in the reactor, long enough to be absorbed by the micelles and to start the reaction. When the residence time is reduced, these components don't have enough time to properly so most of them may come out of reactor unreacted. There is also a great difference in the number of

76

generated particles. The faster the reactants come out of the reactor, the fewer the generated particles are. Therefore defining a good residence time is an important factor in continuous polymerization reactors. If the residence time is too high, it may result in accumulation in the system and on the other hand, low values of residence time may decreases the monomer conversion as shown in Figures 4.66-4.68.

In the next step, the same reaction is run under a nonisothermal condition, which results in a reduction in R_p, N_p and conversion due to high sensitivity of the reaction to temperature variation (Figures 4.69-4.71). The plotted results until now pointed out the importance of designing a proper residence time and reactor control policy in order to avoid producing polymer with undesired properties. The next concern is about the effect of feed composition and its variation on the emulsion polymerization process.

During the operation of CSTRs, it is assumed that the feed is continuously fed to the reactor with a constant composition. This assumption is not very close to reality since in real processes there might be some variation in feed condition for different reasons. Figures 4.72-4.76 represent the effect of step changes in initiator concentration. The concentration of initiator is decreased to 0.005 mol/L after 160 min of reactor operation. The number of generated particles, polymerization rate and reaction conversion will decrease consequently because there are fewer radicals available in the reactor. The second step change is implemented at t=320 min and the initiator concentration is increased to 0.015 mol/L, which results in a higher particle generation and higher reaction conversion.

The same thing is done for the effect of variation of emulsifier concentration. At time t=160 min the emulsifier concentration is increased to 0.02 mol/L and at time t=320 min, is reduced to 0.008 mol/L. The results of this variation are shown in Figures 4.77-4.81.

Model testing is repeated for emulsifier concentration changes and effects on the process state out that when the emulsifier concentration in the system increases by any chance, the micelles will be available in the reactor for more time (Figure 4.80) therefore the influence of this reactant on decreasing the reactor oscillation should be considered.

Generally the effect of feed composition and implementation of any step change in feed condition beside the effect of residence time has been studied for a continuous stirred

tank reactor. More Figures can be found in appendix A, displaying the effect of operating conditions on some other reaction variables such as: R_p, $A_m(t)$, etc.

Furthermore, it was shown that the nonisothermal runs of the program results in lower particle generation and conversion. According to the results, it can be concluded that if it is desired to produce latex with high qualities, the control and optimization of operating conditions should be in the first priority.

A primary consideration in the operation of continuous reactors is the elimination of the oscillation phenomenon that is highly undesirable in industry due to probable serious implication like reactor runaway. Since in case 1 monomers a rapid generation of particles (particle nucleation) happens in a very short time, the rate of polymerization may become very high and the designed cooling capacity of the reactor's jacket might not be adequate to remove the released heat from the reactor. A remedy for this problem is proposed in the following section.

Furthermore, oscillation can increase coagulation of latex particles in the reactor and cause extensive long chain branching during the high conversion portion of the oscillation.
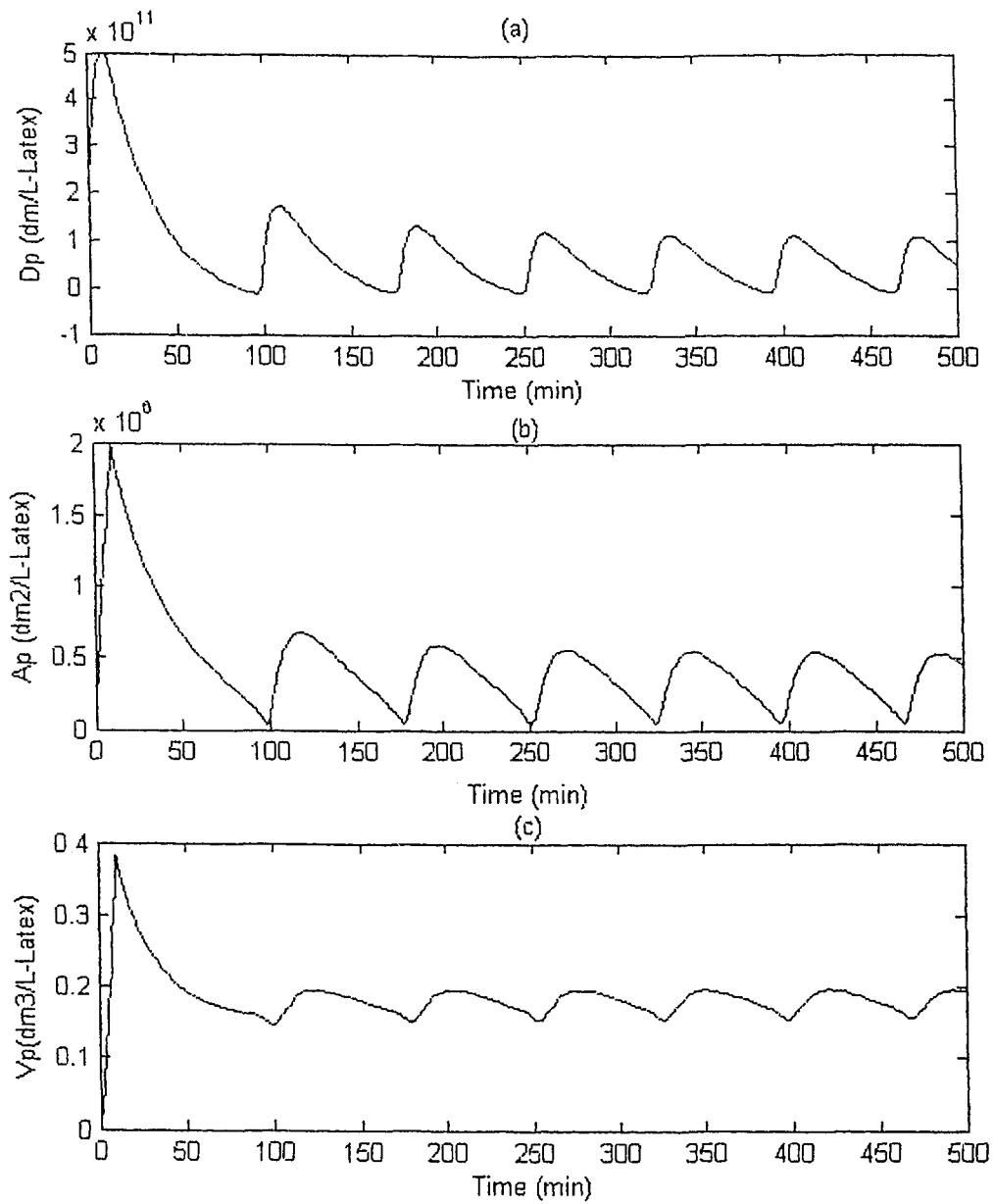
Figure 4. 61. Case 3. Model Prediction for Particle (a) Diameter, (b) Surface Area, and
(c) Volume
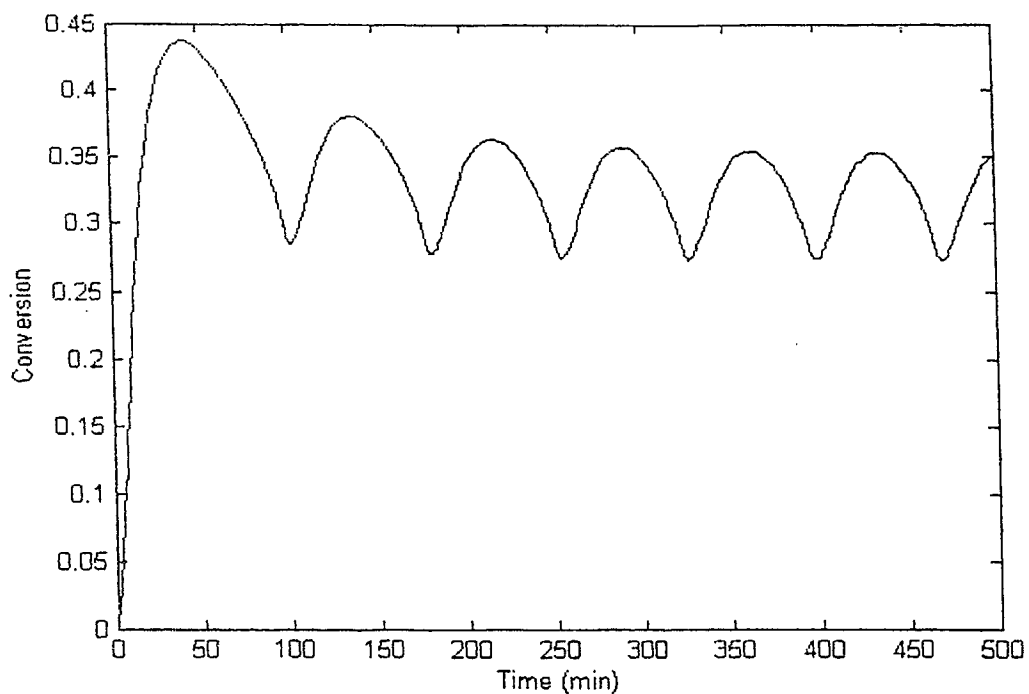
Figure 4. 62. Case 3. Model Prediction for Conversion Versus Time
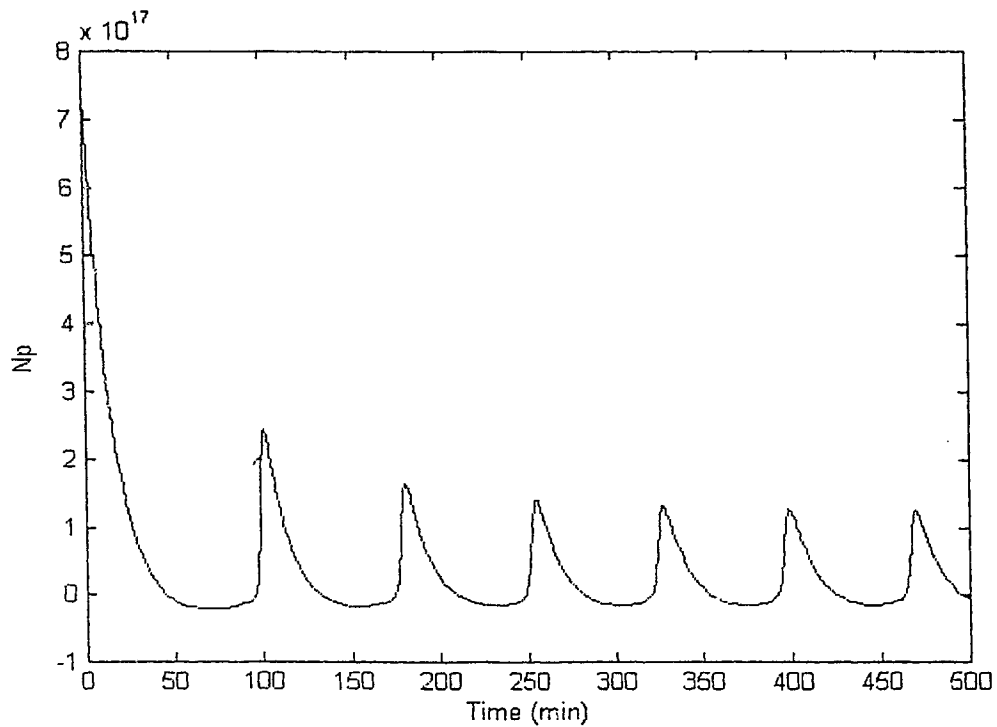
Figure 4. 63. Case 3. Model Prediction for Number of Particles Versus Time

80
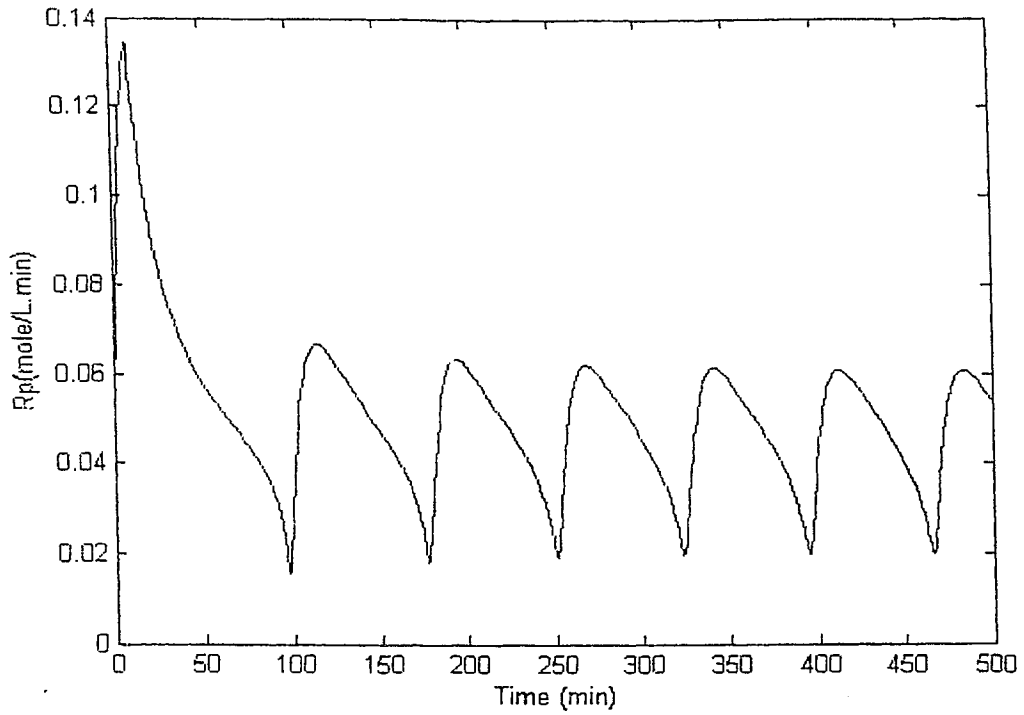
Figure 4. 64. Case 3. Model Prediction for Rp Versus Time
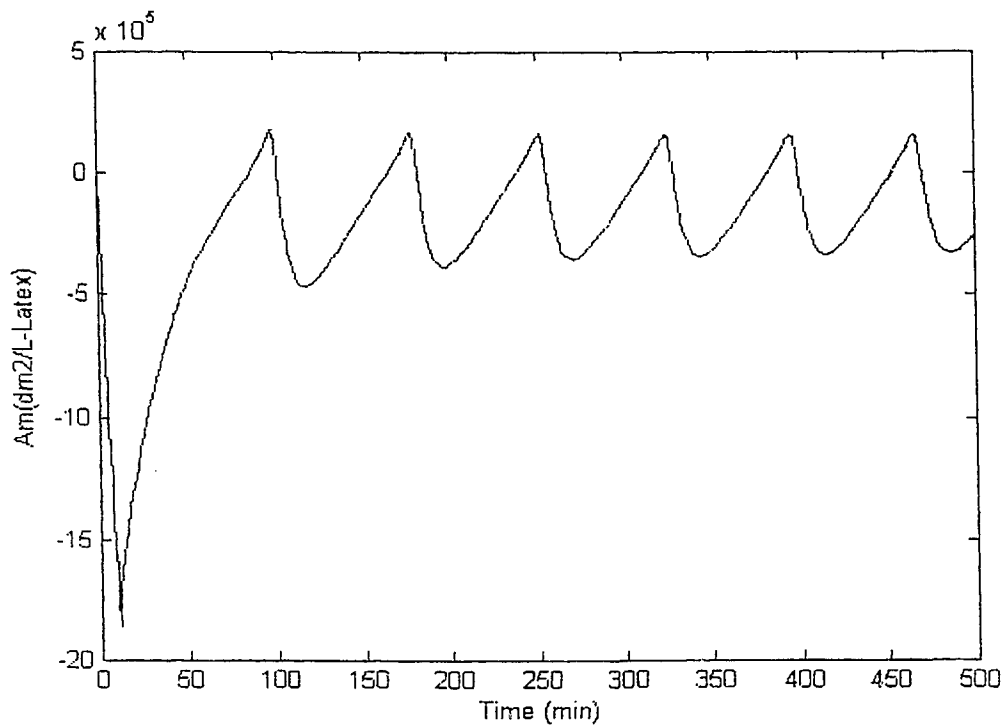
Figure 4. 65. Case 3. Model Prediction for Micellar Area Versus Time

81
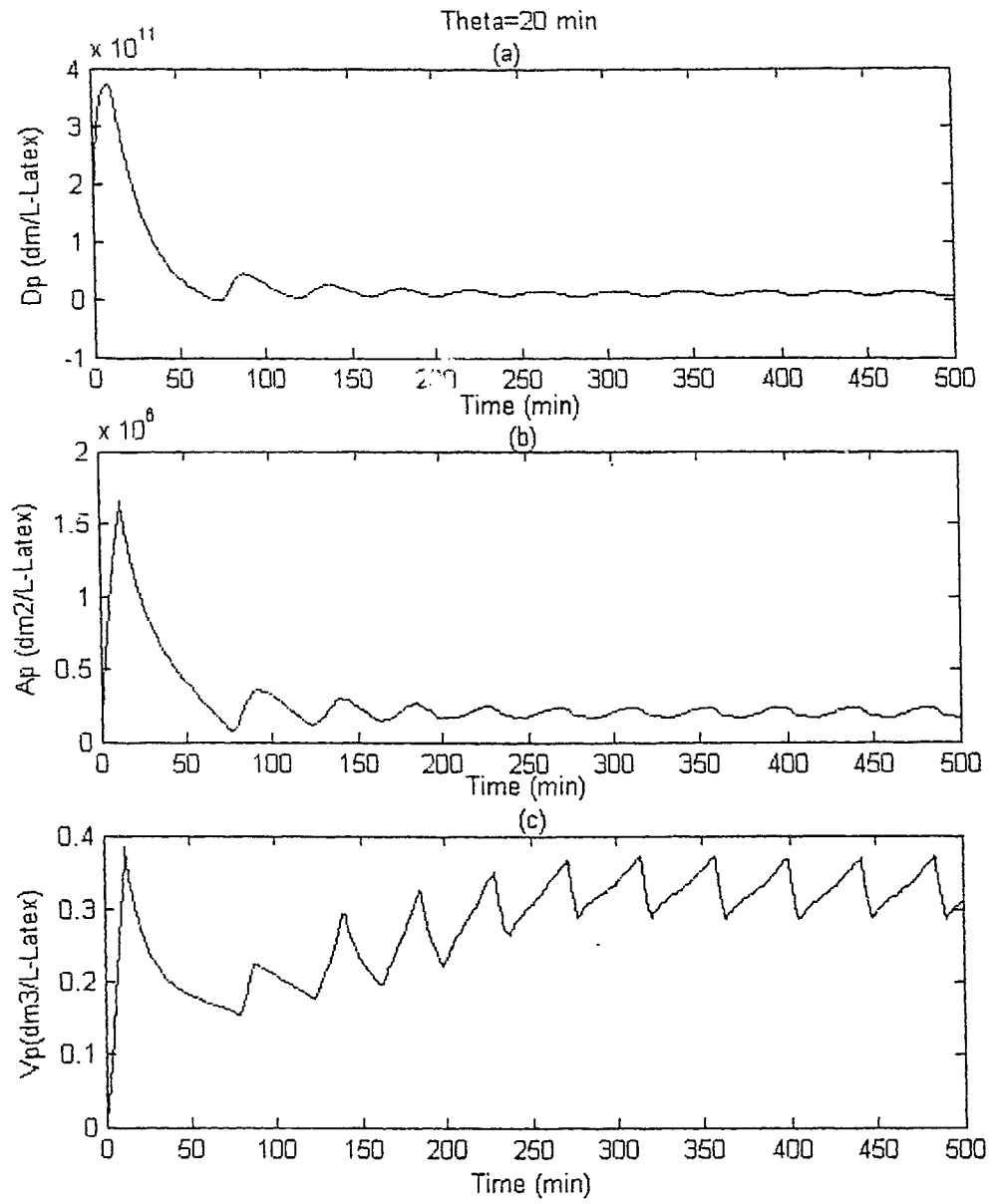
Figure 4. 66. Case 3. Effect of Residence Time on Particle (a) Diameter, (b) Surface Area, and (c) Volume
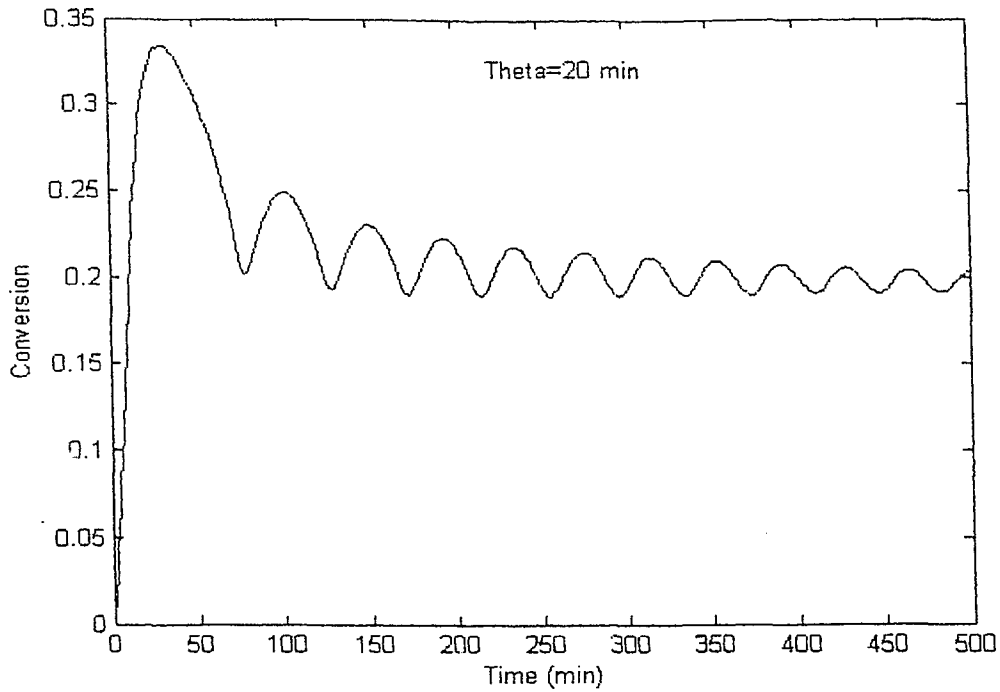
Figure 4. 67. Case 3. Effect of Residence Time on Conversion
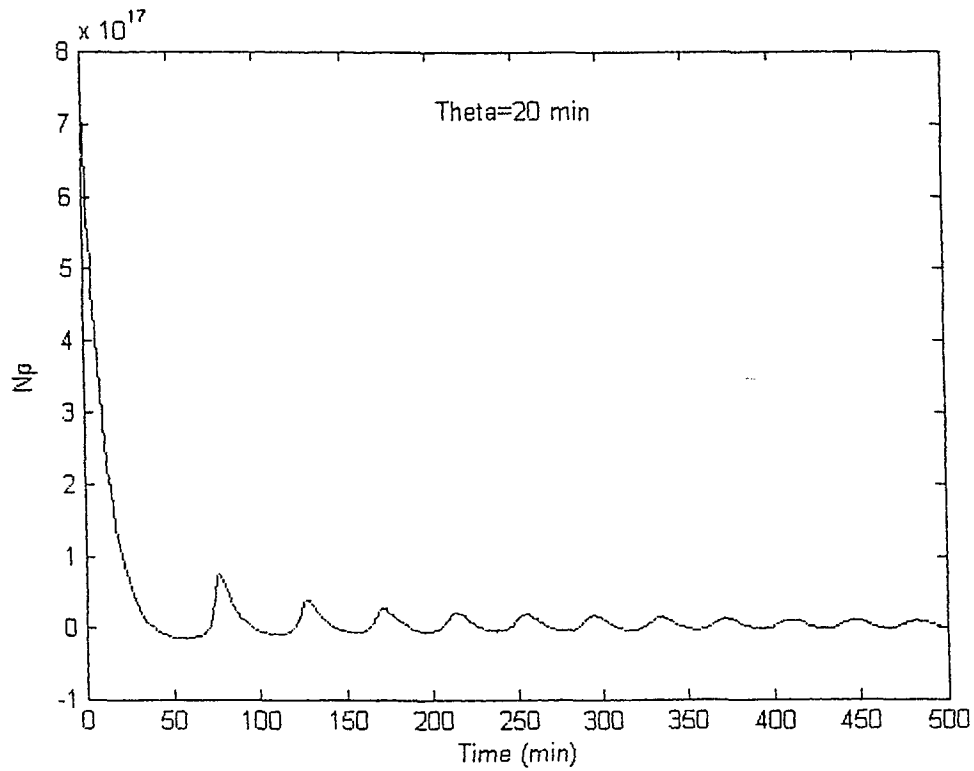
Figure 4. 68. Case 3. Effect of Residence Time on Number of Particles

83
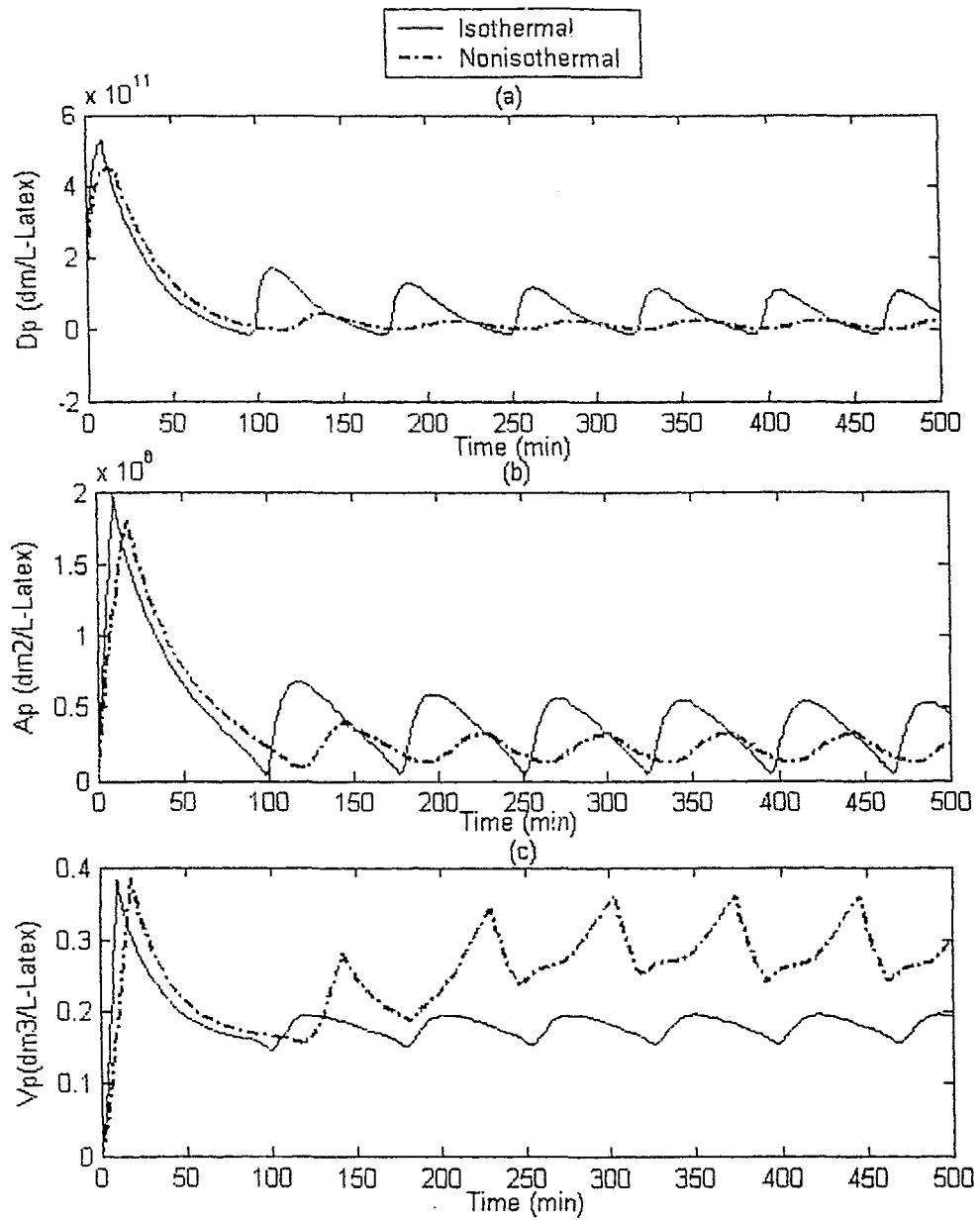
Figure 4. 69. Case 3. Effect of Nonisothermal Condition on (a) Particle Diameter, (b) Surface Area, and (c) Particle Volume
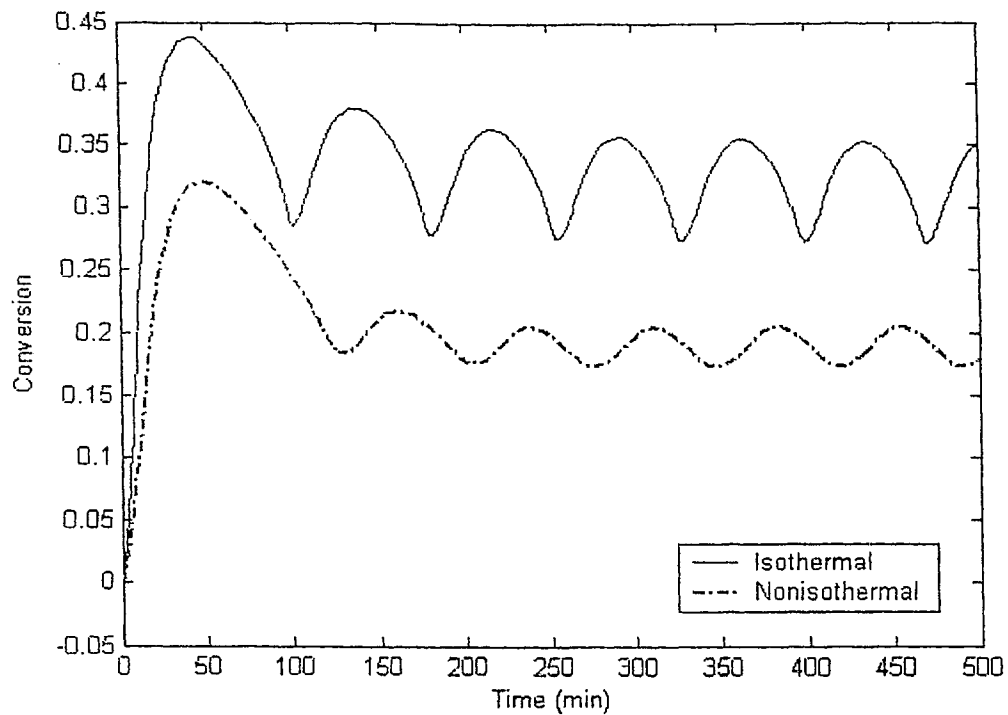
Figure 4. 70. Case 3. Effect of Nonisothermal Condition on Conversion
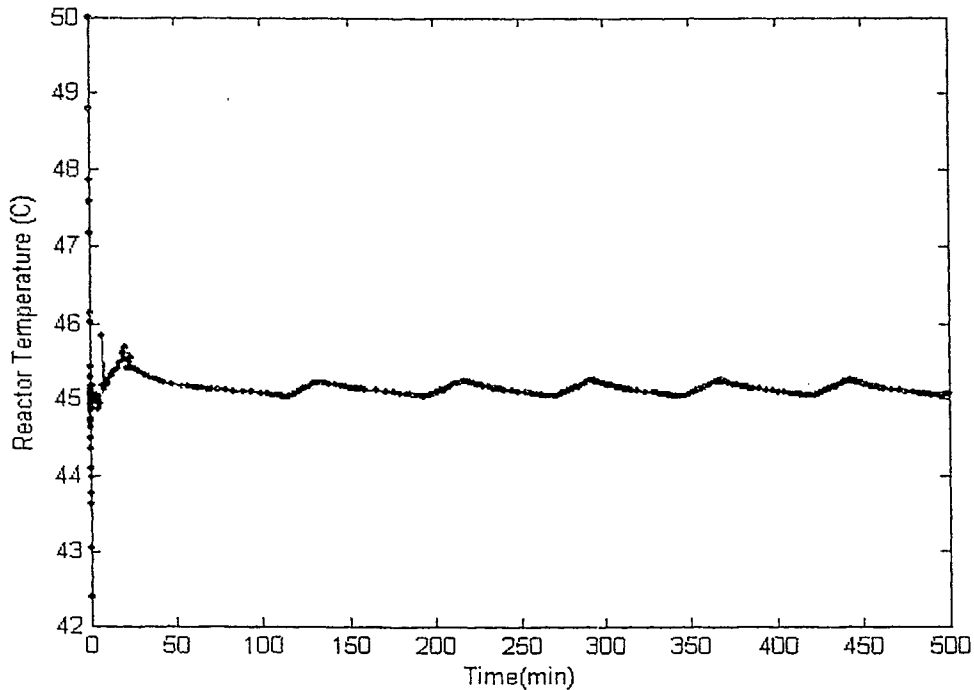
Figure 4. 71. Case 3. Variation of Reactor Temperature under Nonisothermal Condition

85
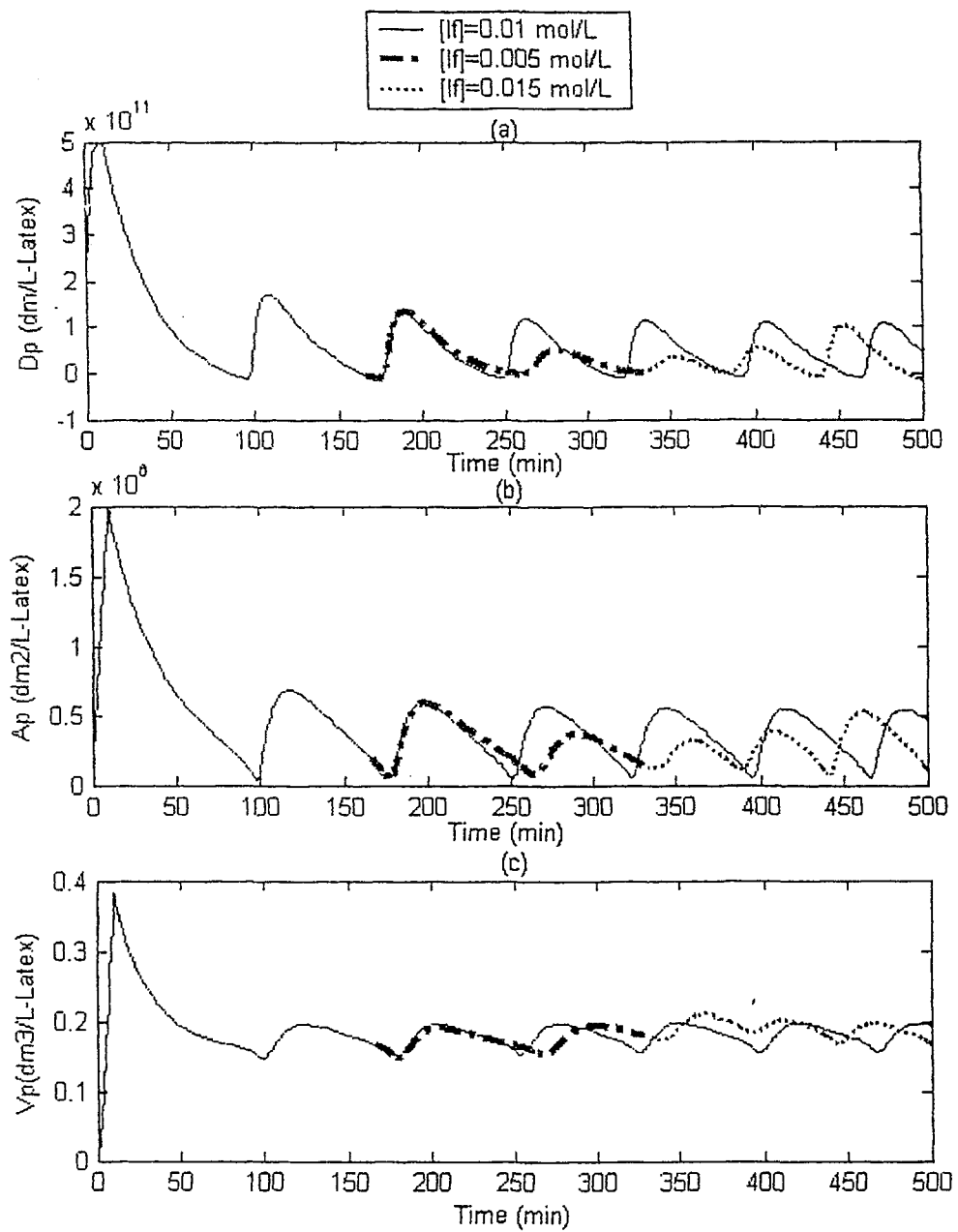
Figure 4. 72. Case 3. Effect of Step Change in Initiator Concentration on Particle (a) Diameter, (b) Surface Area, and (c) Volume

86
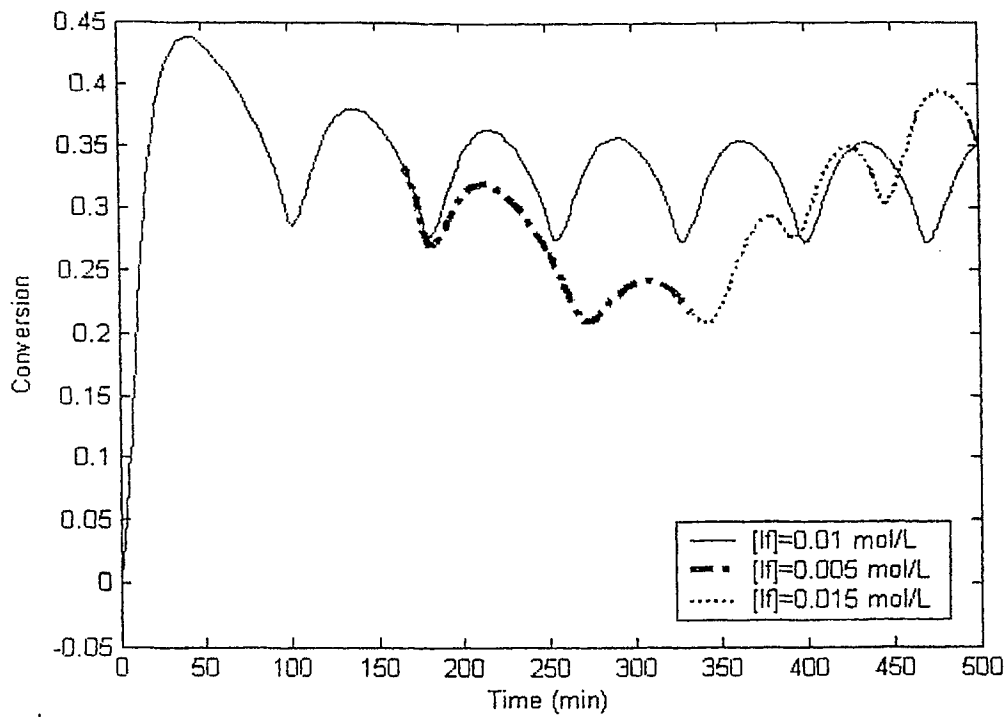
Figure 4. 73. Case 3. Effect of Step Change in Initiator Concentration on Conversion
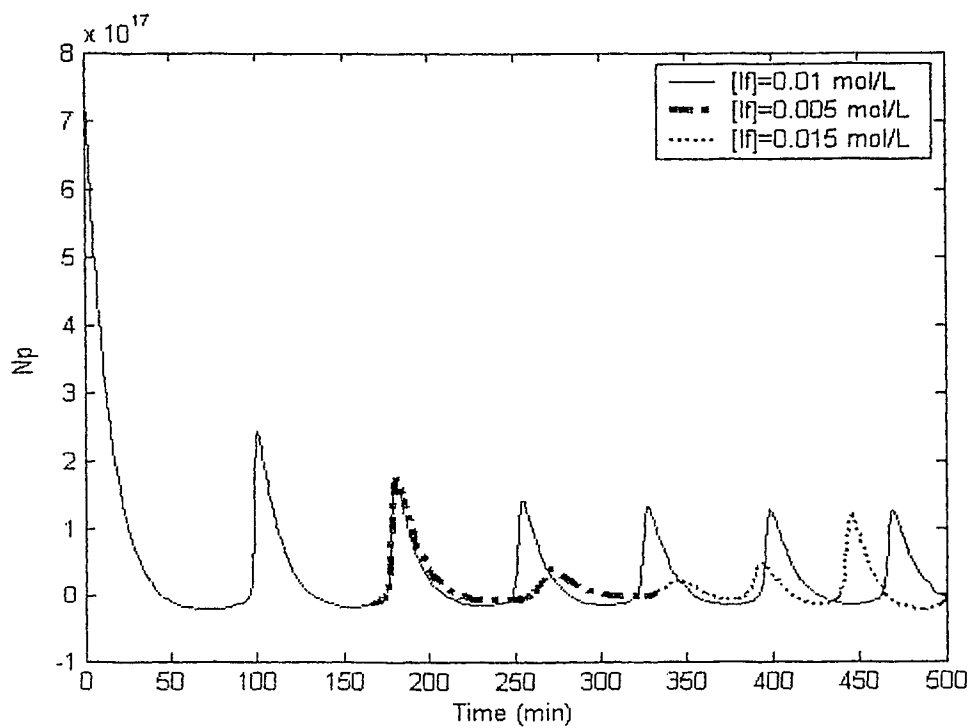

Figure 4. 74. Case 3. Effect of Step Change in Initiator Concentration on Np

87
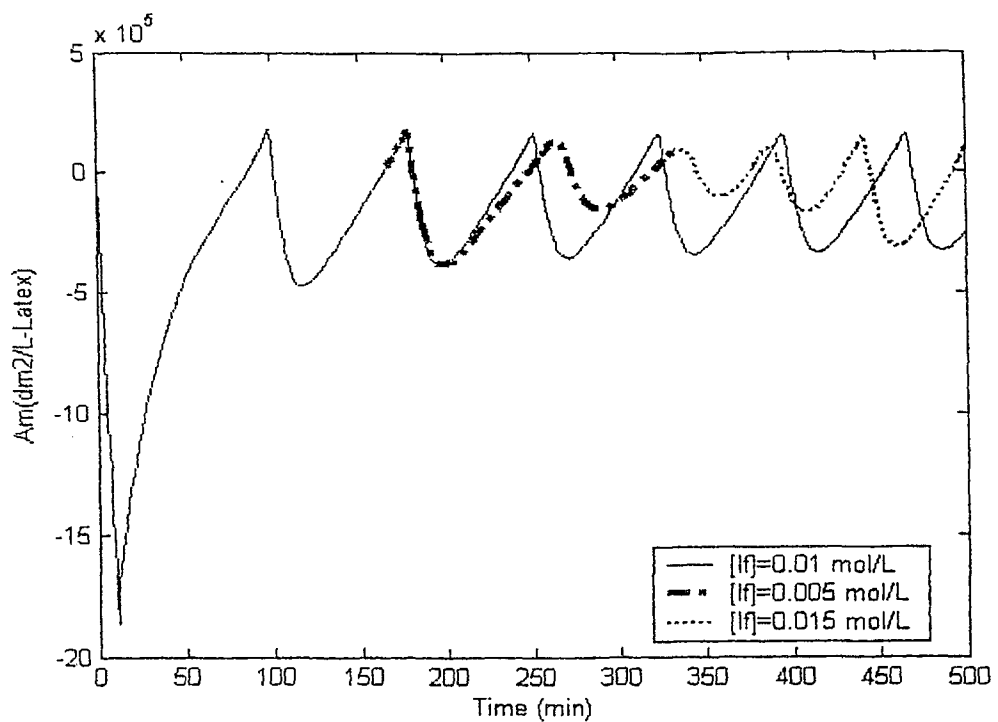
Figure 4. 75. Case 3. Effect of Step Change in Initiator Concentration on Am
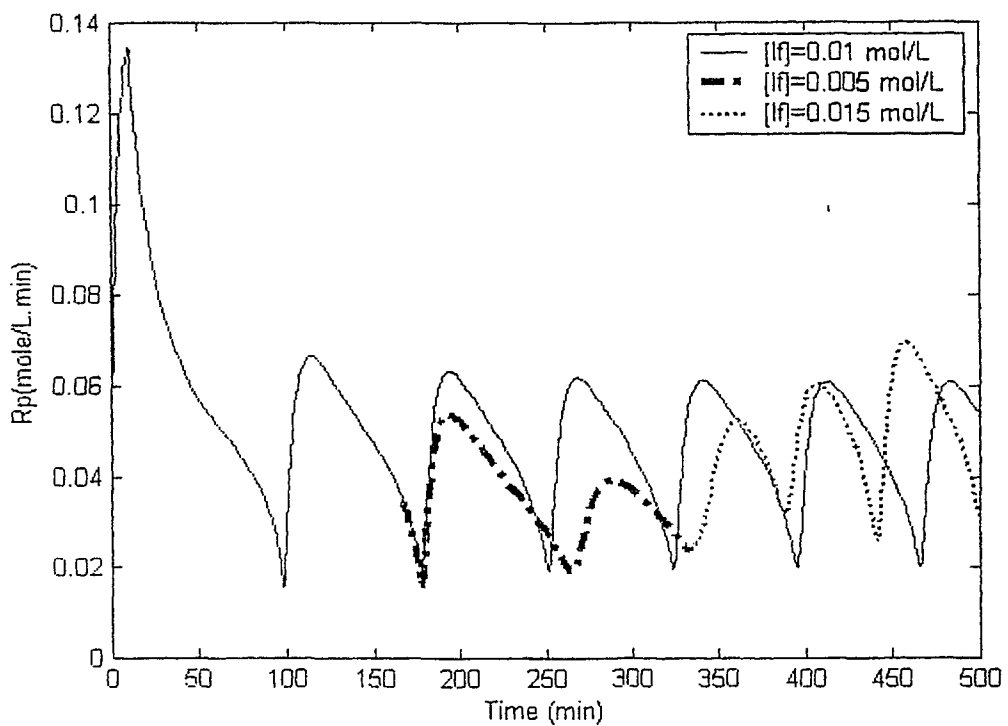
Figure 4. 76. Case 3. Effect of Step Change in Initiator Concentration on Rp

88
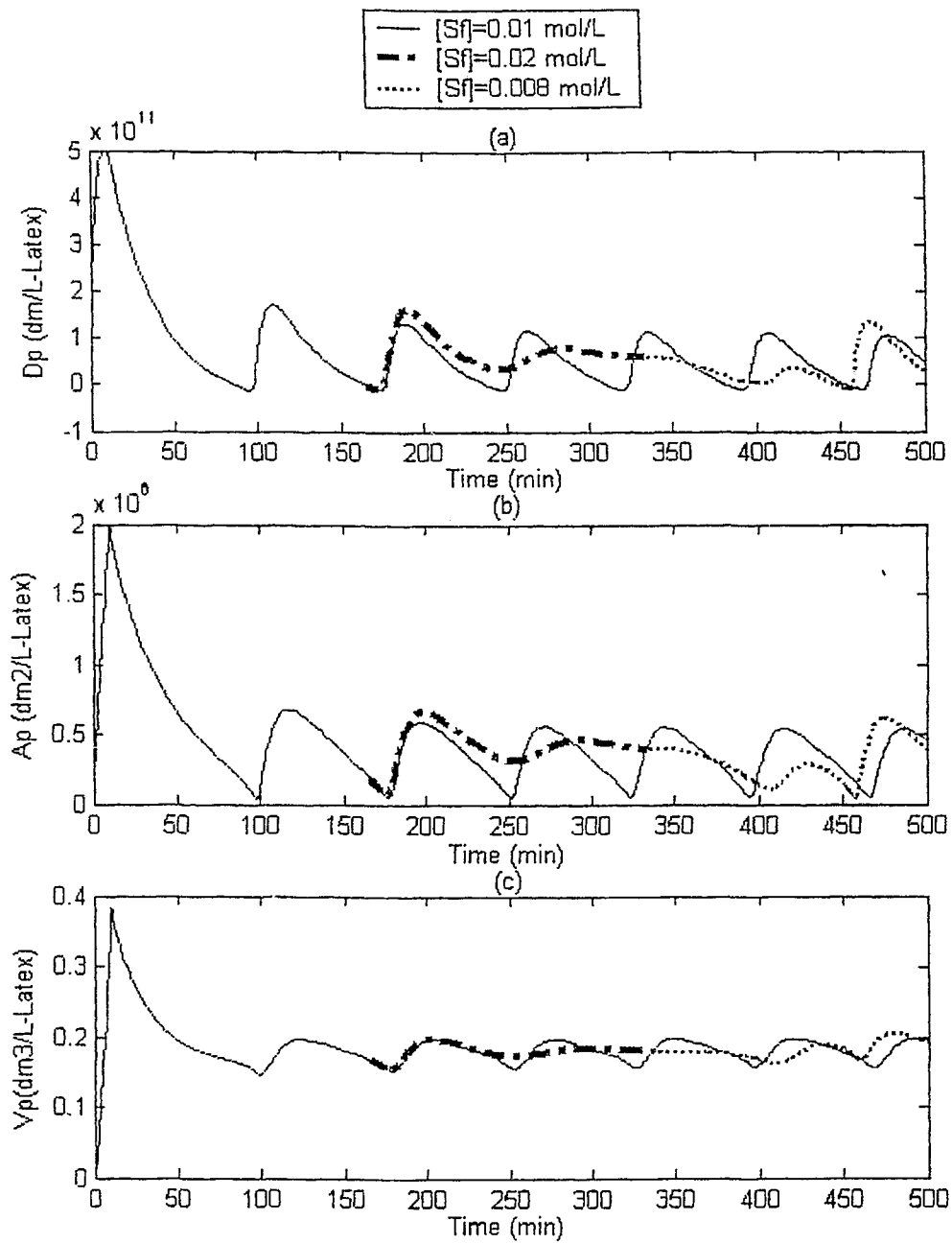
Figure 4. 77. Case 3. Effect of Step Change in Emulsifier Concentration on Particle (a)

Diameter, (b) Surface Area, and (c) Volume

89
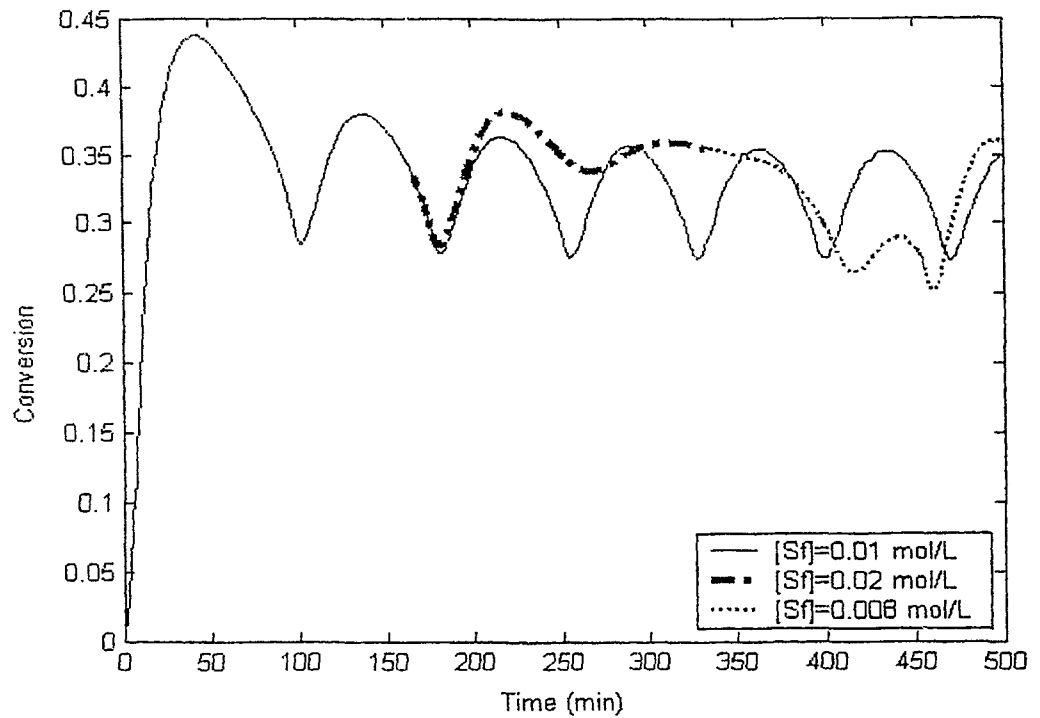
Figure 4. 78. Case 3. Effect of Step Change in Emulsifier Concentration on Conversion
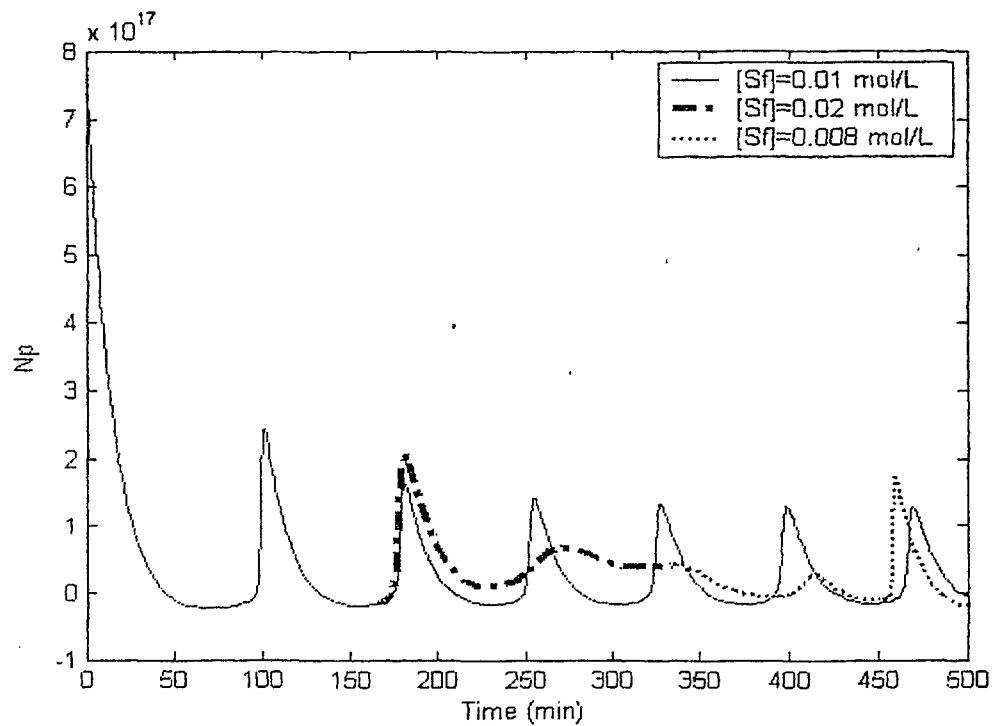
Figure 4. 79. Case 3. Effect of Step Change in Emulsifier Concentration on Np

90
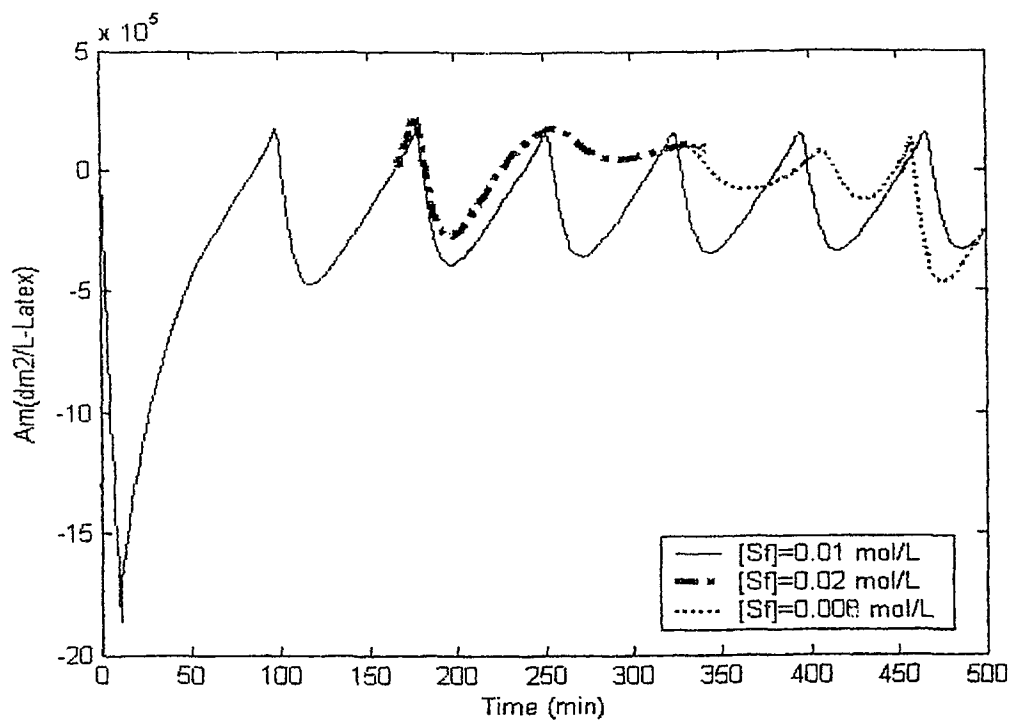
Figure 4. 80. Case 3. Effect of Step Change in Emulsifier Concentration on Am
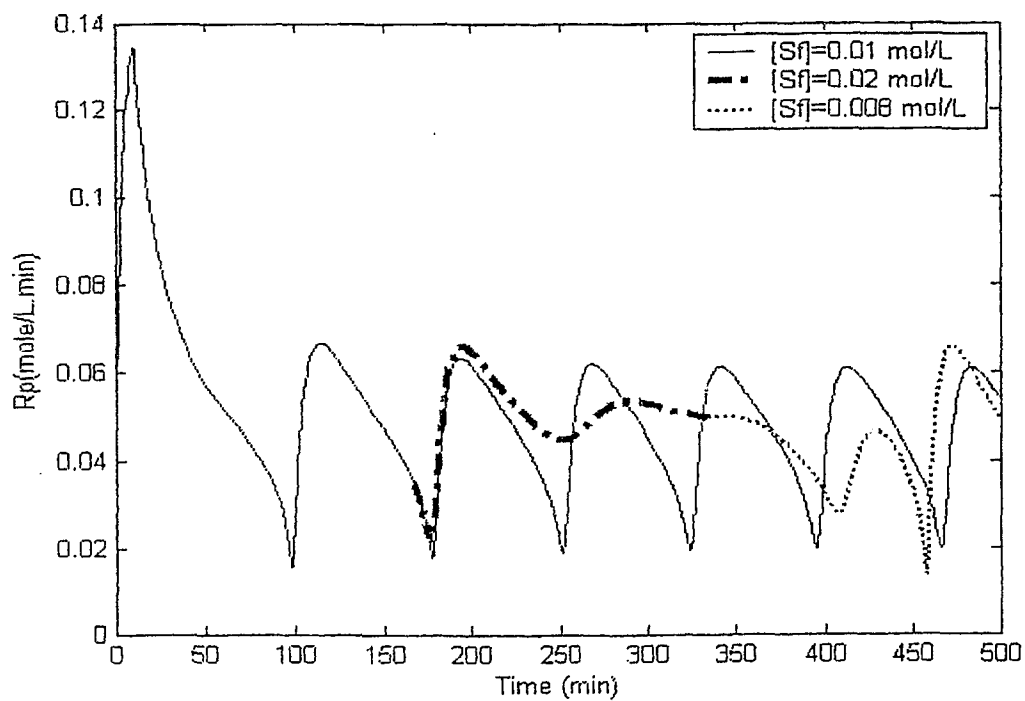
Figure 4. 81. Case 3. Effect of Step Change in Emulsifier Concentration on Rp

91

4.2 Optimization Results

Generally the next step after modeling a process is to optimize its operation. The model should be derived to describe the changes of state variables as they are affected by manipulation of input variables. Dynamic optimization of polymerization reactors usually deals with finding the optimal dynamic operation of batch or semi-batch reactors and also start-up policies for continuous reactors.

4.2.1 Batch reactor optimization

Operation of a typical batch reactor can be optimized in different ways based on the objective function and control variables. Mostly, the objective function is defined in the squared form of some difference. In this study different objective functions are defined for both isothermal and non-isothermal conditions of a batch reactor and results are discussed later. The objective functions for nine different cases are tabulated in Table 4.2.

The optimization toolbox in Matlab has been used to optimize the operation of batch emulsion polymerization reactor. Generally, optimization methods are divided to two main classes: direct search methods and indirect search methods. For instance, the Nelder-Mead method falls in the general class of direct search methods, which attempts to minimize a nonlinear function of n real variables using only function values, without any derivative information. In this method a simplex in n-dimensional space is characterized by the $n+1$ distinct vectors that are its vertices. In two-space, a simplex is a triangle; in three-space, it is a pyramid. At each step of the search, a new point in or near the current simplex is generated. The function value at the new point is compared with the function values at the vertices of the simplex and usually, one of the vertices is replaced by the new point, giving a new simplex. This step is repeated until the diameter of the simplex is less than a pre-specified tolerance.

92

Table 4. 2 Optimization Data

No	Objective Function (J_{min})	Control Variables	Reactor Condition	Figure
1	$J_{min} = (\text{Conversion} - 1)^2$	$T = 351.4\ K$	Isothermal	4.82
2	$J_{min} = (\text{Conversion} - 1)^2$	$\begin{cases} T_j = 343.75 \quad K \\ I_F = 0.0026\ mol\,/\,L \\ S_F = 0.041\ mol\,/\,L \end{cases}$	Non-Isothermal	4.83
3	$J_{min} = (\text{Conversion} - 1)^2$	$\begin{cases} T = 353.16 \quad K \\ I_F = 0.0023\ mol\,/\,L \\ S_F = 0.041\ mol\,/\,L \end{cases}$	Isothermal	4.84
4	$J_{min} = \dfrac{1}{10^{13}}(\overline{Mw} - 8 \times 10^6)^2$ $+ (\text{Conversion} - 0.91)^2$	$\begin{cases} T = 323.13 \quad K \\ I_F = 0.0022\ mol\,/\,L \\ S_F = 0.042\ mol\,/\,L \\ CTA = 0.03\ mol\,/\,L \end{cases}$	Isothermal	4.85
5	$J_{min} = \dfrac{1}{10^{13}}(\overline{Mw} - 4 \times 10^6)^2$ $+ (\text{Conversion} - 0.75)^2$	$\begin{cases} T_j = 318.21 \quad K \\ I_F = 0.0022\ mol\,/\,L \\ S_F = 0.043\ mol\,/\,L \\ CTA = 0.02\ mol\,/\,L \end{cases}$	Non-Isothermal	4.86
6	$J_{min} = \dfrac{1}{10^{13}}(\overline{Mw} - 8 \times 10^6)^2$ $+ (\text{Conversion} - 1)^2$	$\begin{cases} T = 325.1 \quad K \\ I_F = 0.0035\ mol\,/\,L \\ S_F = 0.053\ mol\,/\,L \\ CTA = 0.18\ mol\,/\,L \end{cases}$	Isothermal	4.87
7	$J_{min} = \dfrac{1}{10^{13}}(\overline{Mw} - 4 \times 10^6)^2$ $+ (\text{Conversion} - 1)^2$	$\begin{cases} T = 326.1 \quad K \\ I_F = 0.0025\ mol\,/\,L \\ S_F = 0.040\ mol\,/\,L \\ CTA = 0.21\ mol\,/\,L \end{cases}$	Non-Isothermal	4.88
8	$J_{min} = (\text{Conversion} - 1)^2$	$\begin{cases} T = 325.91 \quad K \\ I_F = 0.0027\ mol\,/\,L \\ S_F = 0.187\ mol\,/\,L \end{cases}$	Isothermal with Impurity	4.89 (a)
9	$J_{min} = \dfrac{1}{10^{13}}(\overline{Mw} - \overline{Mw}_{x=0.82})^2$ $+ \dfrac{1}{10^{10}}(\overline{Mn} - \overline{Mn}_{x=0.82})^2$ $+ (\text{Conversion} - 0.91)^2$	$\begin{cases} T = 322 \quad K \\ I_F = 0.0022\ mol\,/\,L \\ S_F = 0.0422\ mol\,/\,L \\ CTA = 0.207\ mol\,/\,L \end{cases}$	Isothermal	4.89 (b)

93

In the first set of runs, the objective is to maximize the monomer conversion in the reactor using feed temperature as the optimization variable. The reactor is run under isothermal condition. If polymerization starts under previous condition (case 1) to polymerize 4.32 mol/L of vinyl acetate, the final monomer conversion will be about 90% but by using the optimization toolbox and implementing new reactor temperature, the monomer conversion reaches to 100% much faster. The effect of new reactor temperature policy on the number of generated particles is shown in part (a) of Figure (4.82). Higher temperature yields in lower number of particles. Therefore, there is not a great reduction in the property of the product and does not have significant effect on the product quality. The phenomenon is due to higher rate of polymerization.

Higher temperatures speed up reaction rates, which in turn generate particles to grow faster based on equation (3.23) ($A_m(t) = ([S(t)] - [S(t)]_{CMC})S_a N_A - A_p(t)$), where the micelle area falls under its critical point (end of stage 1). As a result, lower number of particles are generated. The effect of optimal operating condition on molecular weight averages is displayed in parts (c) and (d) of Figure (4.83). With higher temperature, lower molecular weight averages are produced than the standard case. Similar results were achieved in the previous section (modeling and simulation results), when the effect of reactor temperature on molecular weight averages was investigated. Figures 4.82(e) and 4.82(f) show the number of branching points and polydispersity index. The final number of branching points and polydispersity index obtained are higher in the case of optimal operating temperature. Therefore, for higher conversion with no change in product quality, there should be some conditions on the molecular weight averages of product.

In the next set of runs a non-isothermal reactor is studied working under the same operating condition of case 1. As Figure 4.83, the final conversion is lower than with the isothermal case. Thus it is important to find a good feed policy beside proper cooling medium temperature, which gives higher monomer conversion. Running the reactor under new operating condition calculated by the optimization toolbox can solve this problem and bring the reactor conversion to full. The start-up temperature was set to 50°C but after that the cooling jacket is employed to control the reactor temperature in order to reach higher monomer conversion. This new optimization policy produces similar effects on the product

94

properties (higher molecular weight averages, number of branching points and polydispersity index).

During run #3, the goal is the same as run #1 but it was desired to know if the concentrations of emulsifier and initiator in the feed are enough to polymerize *4.32 mol/L* vinyl acetate monomer. Since, usually one of the most important aspects of any industrial process is its economical point of view. So it is important to make using the lowest amount of initiator and emulsifier for polymerization possible. In this part, three variables are considered and if one compares the optimization results with those of case 1, it can be seen that the initiator and emulsifier concentrations in case 1 are almost the same as optimal values and it is just recommended to run the reactor under higher temperature (the same as run #1). The effect of higher reactor temperature on product can be again seen in Figure 4.84.

Runs #4 and #5 deal with optimizing the system to get the desired weight average molecular weight, $\overline{Mw}$. So if in any condition, one wants to have lower molecular weight averages, this optimization package can calculate better feed policies. As discussed in part 4.1.1, one of the solutions to decrease the molecular weight averages is to add a certain amount of chain transfer agent (CTA) to the reactor. In this section, the best amount of required CTA is calculated for both isothermal and non-isothermal cases. The final conversion is the same as standard case because the objective is defined to decrease the weight average molecular weight in the same conversion as standard case.

Polymerization of vinyl acetate under case 1 condition results in weight average molecular weights of about $1.8 \times 10^7 \, g / mole$ and $6 \times 10^6 \, g / mole$ for isothermal and non-isothermal conditions respectively. But by application of optimal feed policy and addition of some CTA, the weight average molecular weight of the product can be kept on some desired value ($8 \times 10^6 \, g / mole$ and $4 \times 10^6 \, g / mole$) while the monomer conversion won't change (Figures 4.85-4.86).

In the next runs (#6 and #7), the objective functions consist of two parts, the first part deals with keeping the weight average molecular weight on some desired value and the second part works on increasing the monomer conversion to its highest value. Based on this new defined objective function, new feed policies are found for isothermal/non-isothermal conditions. Figures 4.87-4.88 display the optimization results, which present the

95

advantages of newly defined objective function, which is able to increase the monomer conversion without deteriorating the product quality. In other words, by this method the monomer conversion and product properties can be controlled simultaneously.

Generally, runs #1-#5 were preliminary approaches for investigation of optimal operating conditions effecting the monomer conversion and product properties. They are helpful to understand the process behaviour under each objective function separately and then combine them in one multi objective function to find a more general optimal policy which can optimize the system from both points of view.

As discussed before, monomer conversion of industrial scale emulsion polymerization reactors has some deviation (usually reduction) from the laboratory scale results. Usually purified monomers are employed for experimental purposes while in industrial operations; unpurified, partially purified or even recycled monomers are used in which the presence of impurities is very probable. The effect of impurities on reduction of monomer conversion has been studied in modeling and simulation part and here in run #8, the objective function is defined to maximize the monomer conversion while there is 200 *ppm* of impurity in the reactor. In the presence of impurity, the final reactor conversion reaches 90% but application of optimal feed policy the conversion can goes to 100%. In order to increase the conversion, it is required to feed more emulsifier and initiator to the reactor since some part of generated radicals is consumed by the impurities.

A large number of properties depend on the molecular weight distribution of the polymer. The higher the conversion, the wider the graph. This phenomenon is due to an increase in the number of branching in higher conversion. Since it is usually desired to have higher conversion with less branching, the optimization toolbox can be employed to find the best feed policy which gives a narrower distribution in the same conversion. As shown in Figure 4.89 part (a), the distribution for 91% of conversion is wider than that for 82%. So if one selects the solid line (x=0.82) as the desired line and optimizes the system in order to get it in higher conversion (x=0.91), the optimization toolbox is able to find the best policy. The objective function in this part (run #9) consists of summation of three parts. The distribution (equation 3.124) is a function of molecular weight averages, the optimization method for the conditions that giving the final molecular weight averages (previously obtained at 82%) but having higher conversion of 91%, which is incorporated

96

in the objective function. In the other words, the set points for molecular weight averages are the same as those with 82% of conversion. The optimization results show good performance as shown in Figure 4.89 (b), MWD becomes narrower in comparison with that obtained with 91% of monomer conversion.

In this part the Matlab optimization toolbox was employed to find optimal operating conditions for vinyl acetate polymerization reactor. The results recommend good feed policies. The next step of this study deals with optimization of CSTRs. As it was shown in section 4.1.1, due to periodic generation of micelles, these reactors have oscillatory behaviour so the next concern is to find some remedies to suppress the oscillation.

97
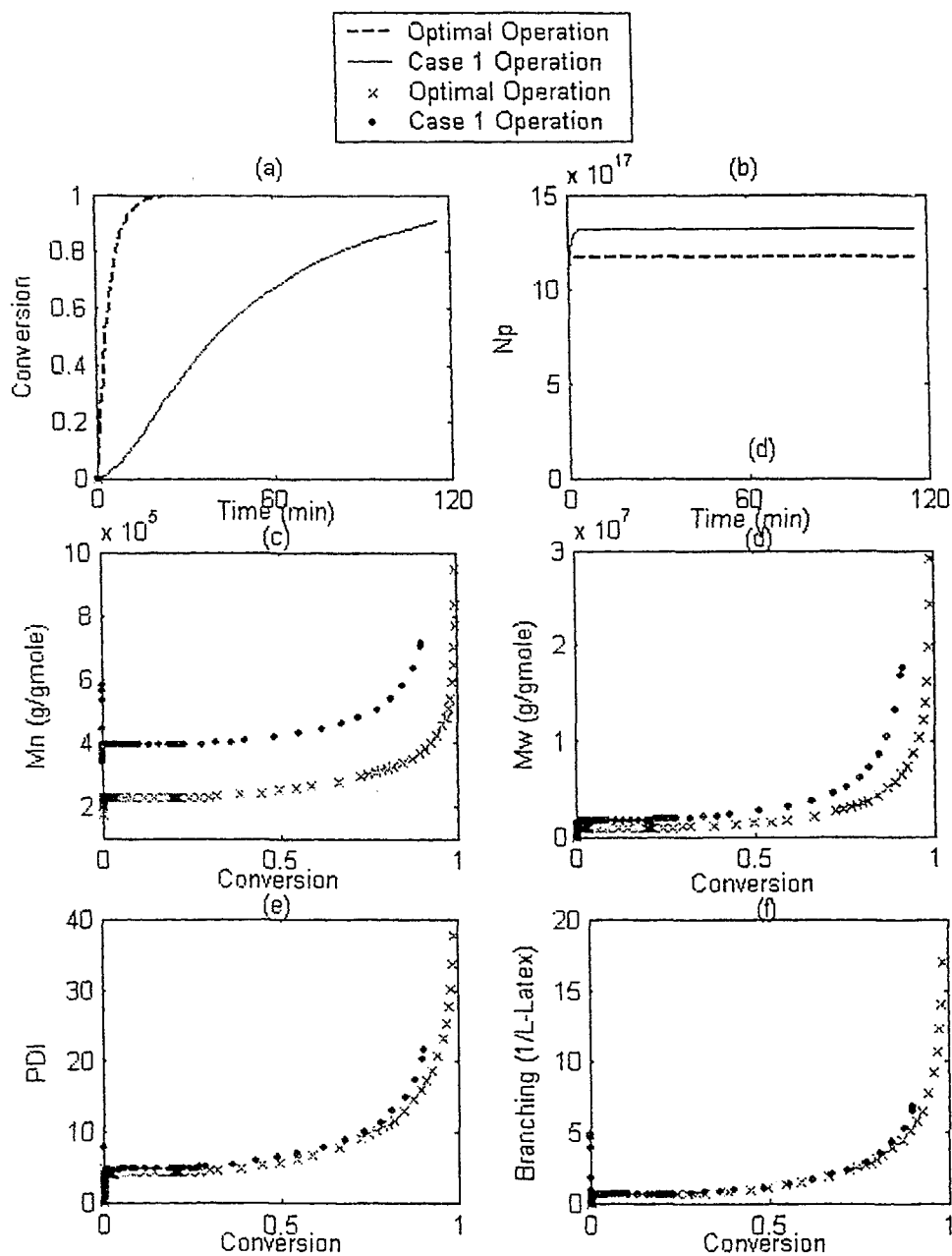
Figure 4. 82. Run #1, Effect of Optimal Policy on Different State Variables
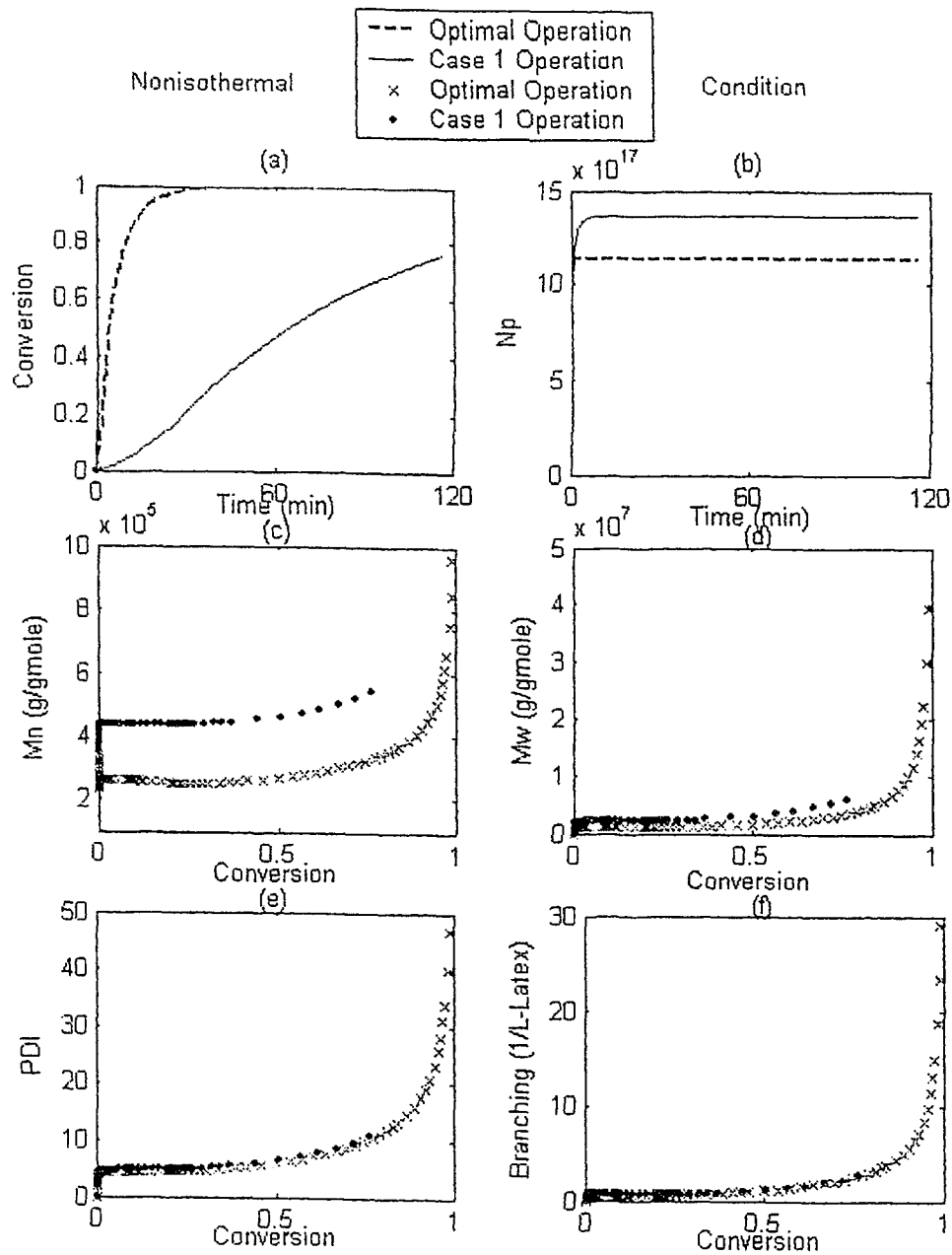
Figure 4. 83. Run #2. Effect of Optimal Policy on Different State Variables

99
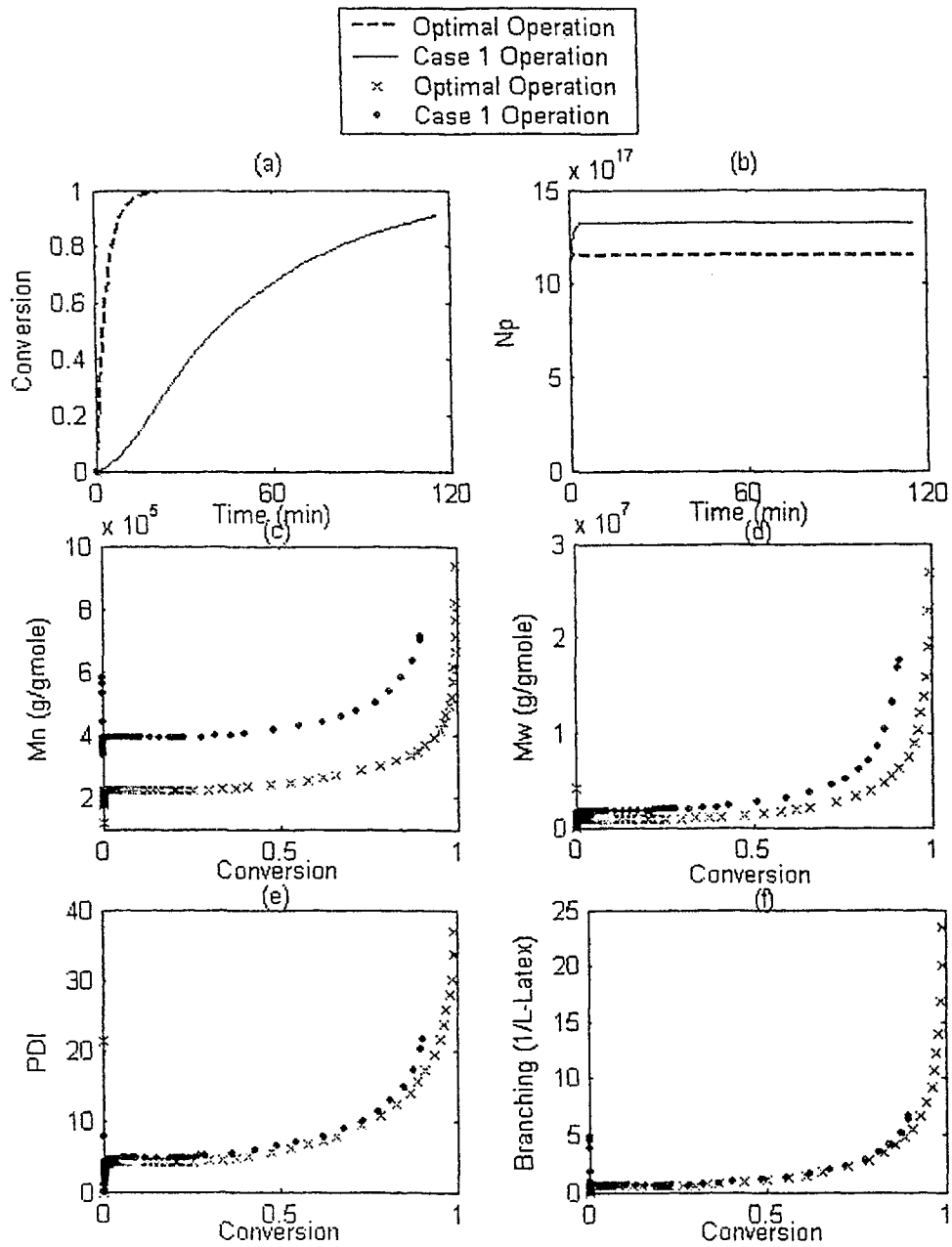
Figure 4. 84. Run #3, Effect of Optimal Policy on Different State Variables

100
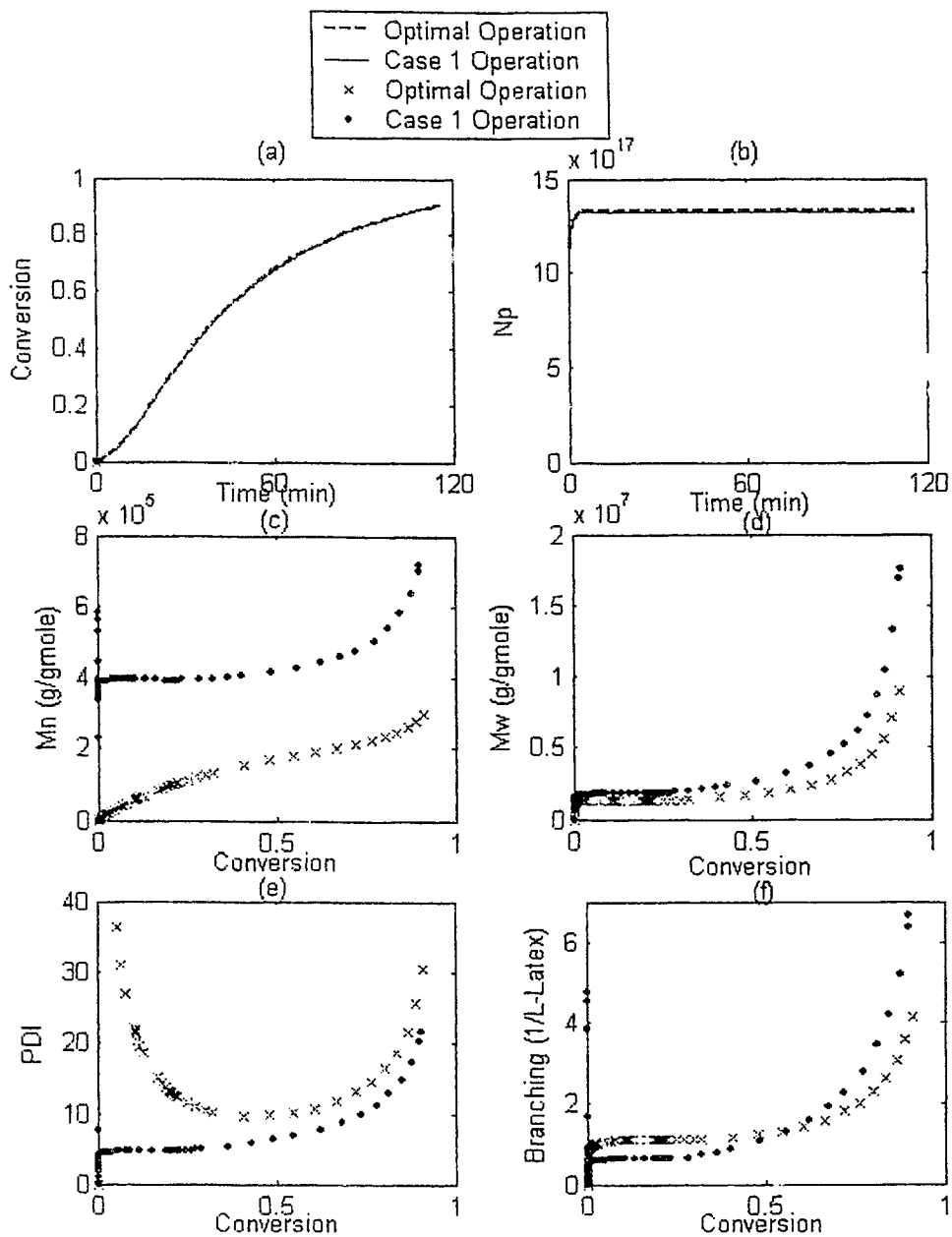
Figure 4. 85. Run #4, Effect of Optimal Policy on Different State Variables
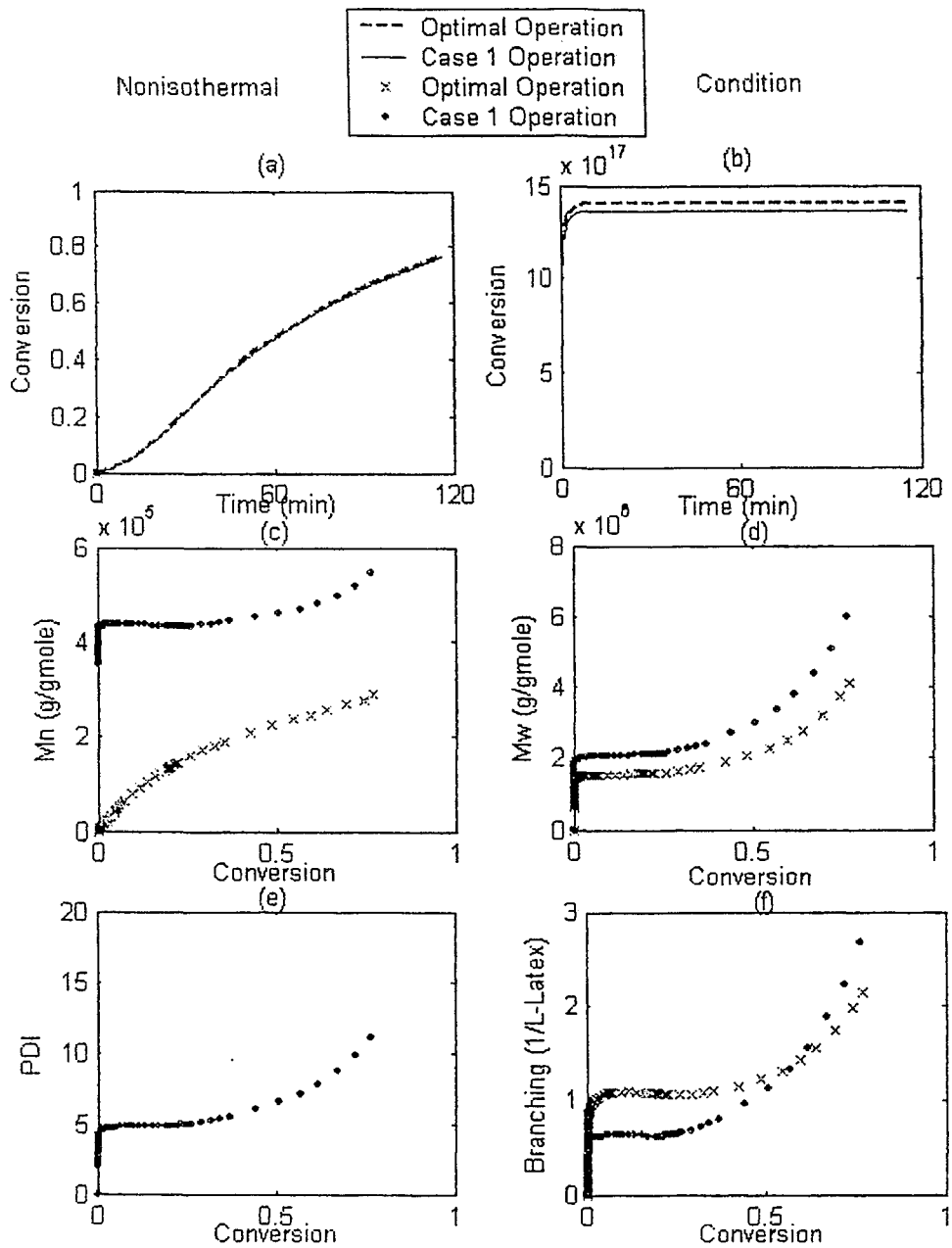
Figure 4. 86. Run #5, Effect of Optimal Policy on Different State Variables

102
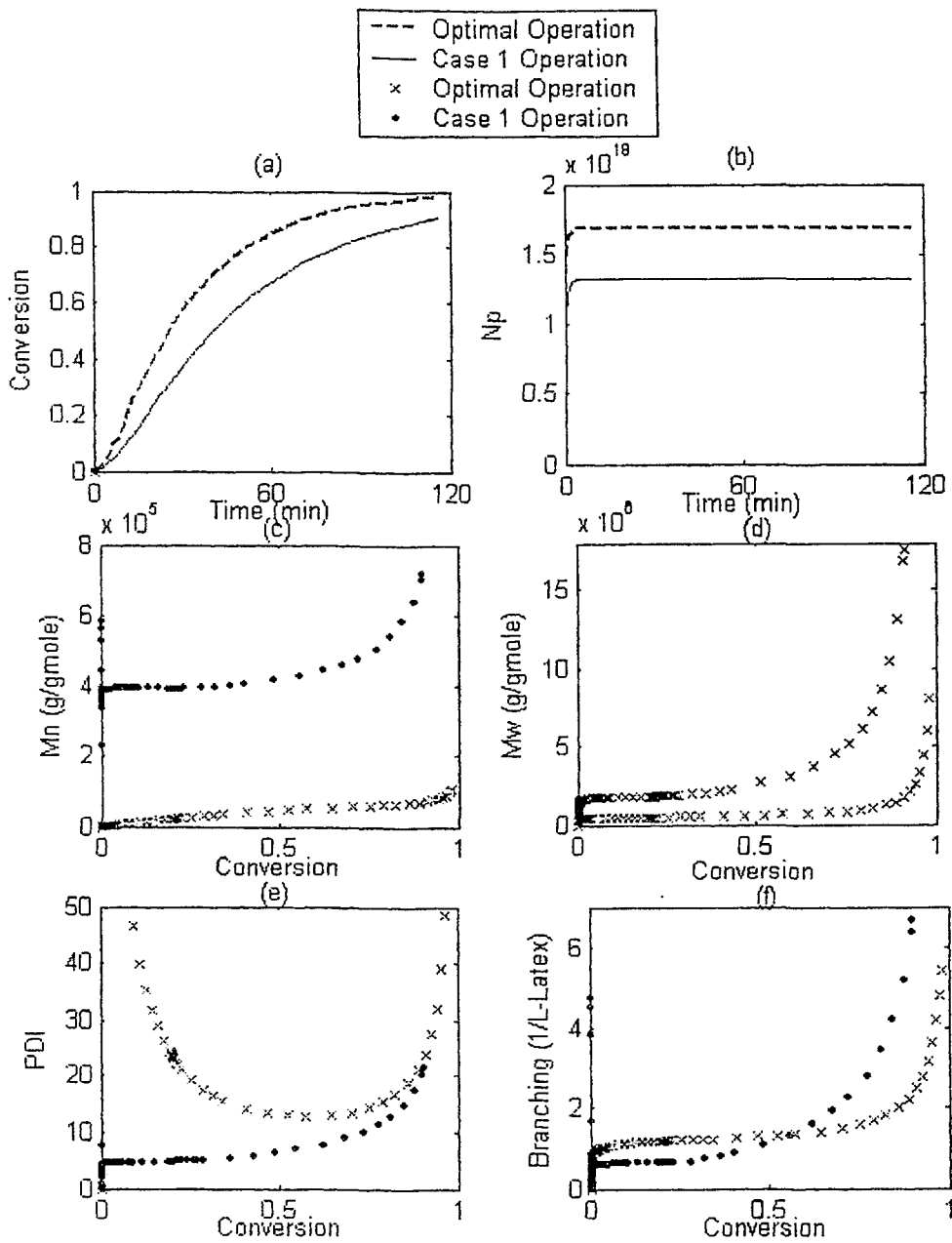
Figure 4. 87. Run #6, Effect of Optimal Policy on Different State Variables

103
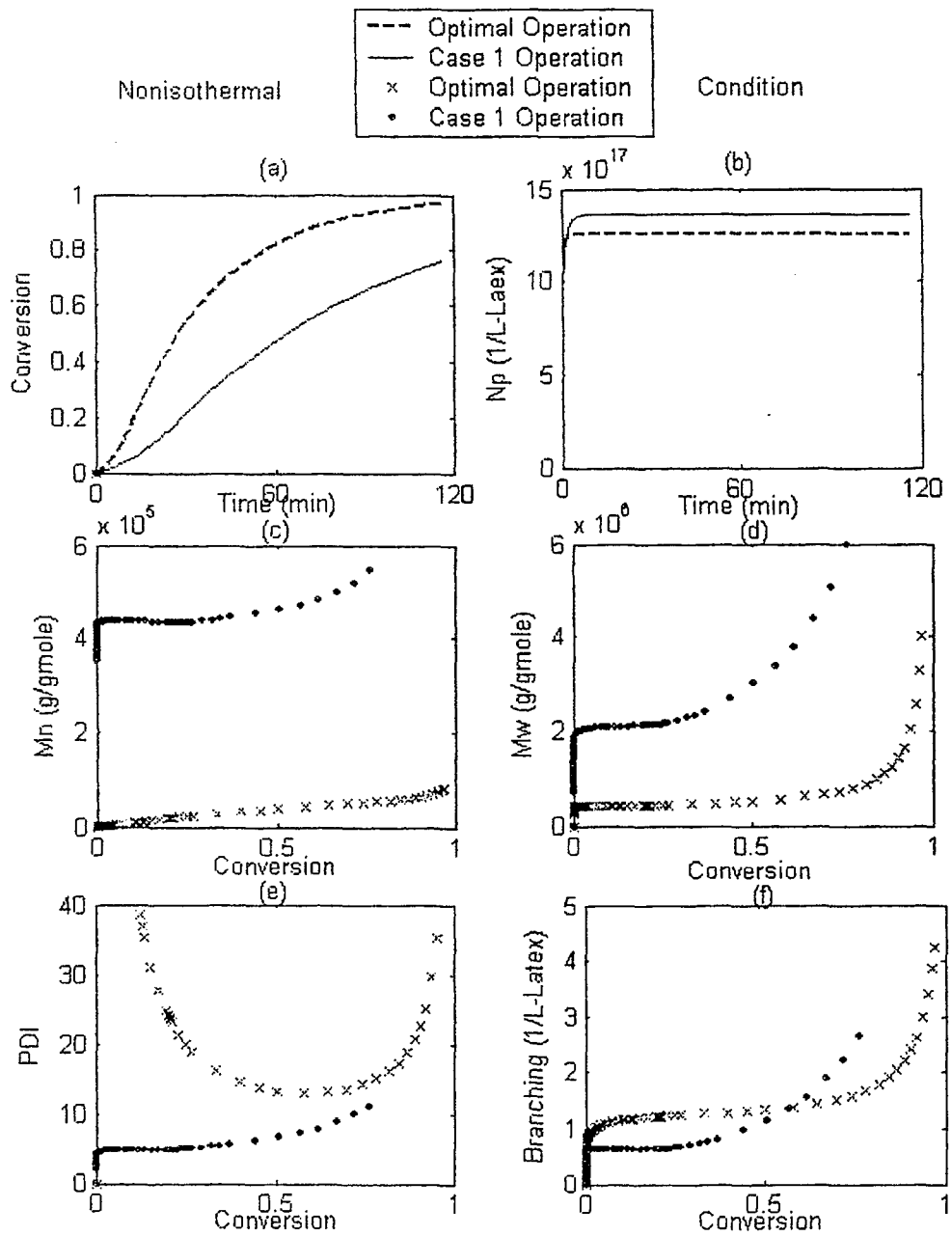
Figure 4. 88. Run #7, Effect of Optimal Policy on Different State Variables

104
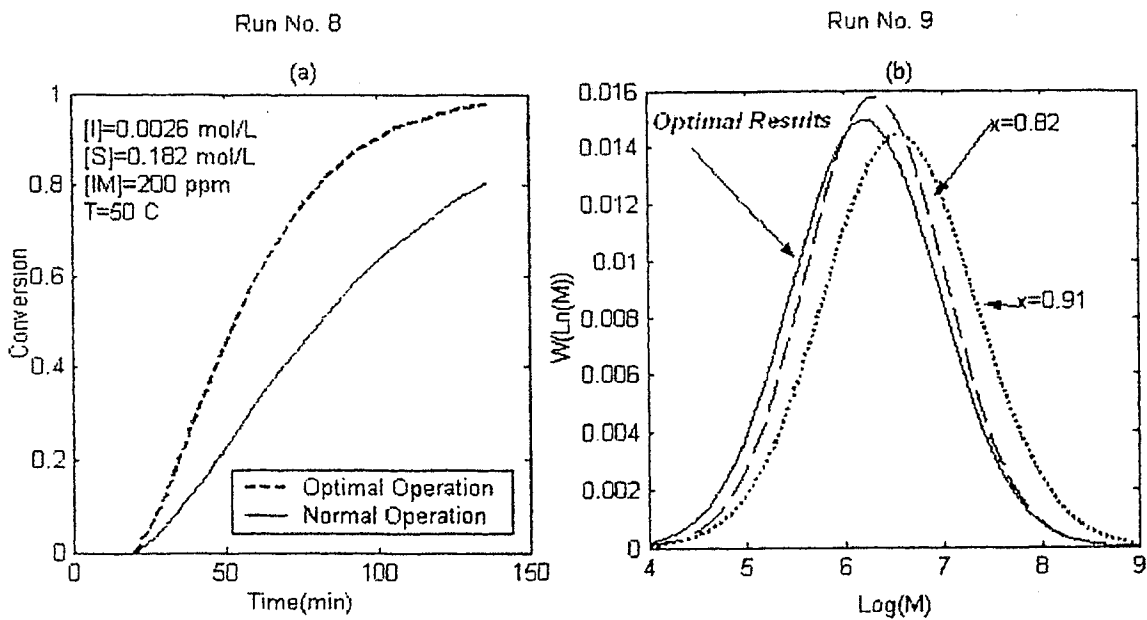
Figure 4. 89. (a) Run #8, Effect of Optimal Policy on Conversion, (a) Run #9, Effect of Optimal Policy on MWD

4.2.2 Continuous reactor optimization

Possible solutions to the oscillation problem

The problems encountered when operating emulsion continuous reactors show the importance of finding possible solutions to overdamp the oscillatory behaviour of the process. The oscillatory behaviour of a single CSTR was widely investigated experimentally by Penlidis (1986).

The first and common remedy is to run the process with higher emulsifier concentration (Penlidis, 1984; Nomura et el., 2002). The oscillation will be eliminated as the high soap concentration hinders on-off nucleation of polymer particle (Figures 4.91-4-92). As long as, the concentration of emulsifier is higher than its critical value, $A_m(t)$ will be greater than zero.

Nomura et al. (2002) also carried out continuous emulsion polymerization of vinyl acetate and investigated the effect of residence time and initiator concentration on the oscillatory behaviour of the reactor. Similar conditions are applied in the present simulation procedure and the results are in agreement with their study. Model testing results are shown in Figures 4.93-4.95.

Lower residence time leads to lower oscillation since the monomer conversion is low. Besides, running the reactor under lower concentration of initiator decreases the unsteady behaviour but the low number of radicals result in lower monomer conversion and lower number of generated particles. Elimination of the oscillations, using higher concentration of emulsifier is not a practical solution from a standpoint of both experimental and product quality. More emulsifier means more expensive operation, larger number of generated particles and reduced capability to control particle size.

Controllability of the polymer particle size and its distribution by taking advantage of the self-sustained oscillations of monomer conversion was examined by Ohmura et al. (1998) in continuous emulsion polymerization of vinyl acetate. He stated that due to the dependence of particle size distribution on operating conditions, this distribution and also monomer conversion can be controlled by varying the emulsifier concentration under its CMC level. In their recent study, application of novel operating method was studied for

106

controlling the particle size distribution. The mean residence time was switched between two values, which can affect the size of particles.

Another possible remedy to this problem can be done by feeding a stream of seed particles to the reactor continuously. The continuous addition of seed particles prevents new particle formation. The results, Figures 4.97-4.98, show that the conversion and the number of particles are much more stable in a seeded reactor in comparison those in unseeded reactor. Besides, the monomer conversion is high and results in high productivity of the process.

The next design consideration focuses on the way of seeding the reactor. Batch wise production of seeds is costly and also is it hard to keep a consistent seed property from batch to batch operation. A short plug flow tubular reactor (PFTR) can be employed as a seeder to accomplish the nucleation but it may cause operational and cleaning problems due to agglomeration, wall fouling and plugging. Since, a small PFTR is similar to a small CSTR, it is more recommended to employ a small CSTR for a better mixing, operation and cleaning.

A Split Feed Seeding Reactor Design

A reactor configuration for a non-oscillatory production of PVAc in continuous emulsion reactors was suggested by Pollock et al. (1981). In the design procedure, the first large reactor is preceded by a very small initial CSTR (approximately one tenth or less of the size of the subsequent reactor in the train). In order to keep emulsifier and initiator concentrations high in the small reactor, almost all of the initiator and emulsifier were fed into it. With this configuration, the initiator and emulsifier concentration in the seed reactor plus the degree of split of monomer and water can be controlled to produce PVAc with desired properties. Usually 10-40 percent of monomer and water are fed to the small CSTR, therefore it can operate under high concentration of initiator and emulsifier. As a result, generation of most polymer particles can be entirely accomplished in the first reactor and the second reactor be used only for particle growth. Figure 4.90 presents the reactor configuration.

Monomer
Water

60%-90%

Recycle

10%-40%

Initiator

Emulsifier

Small
Seeding
Reactor

Large
Reactor
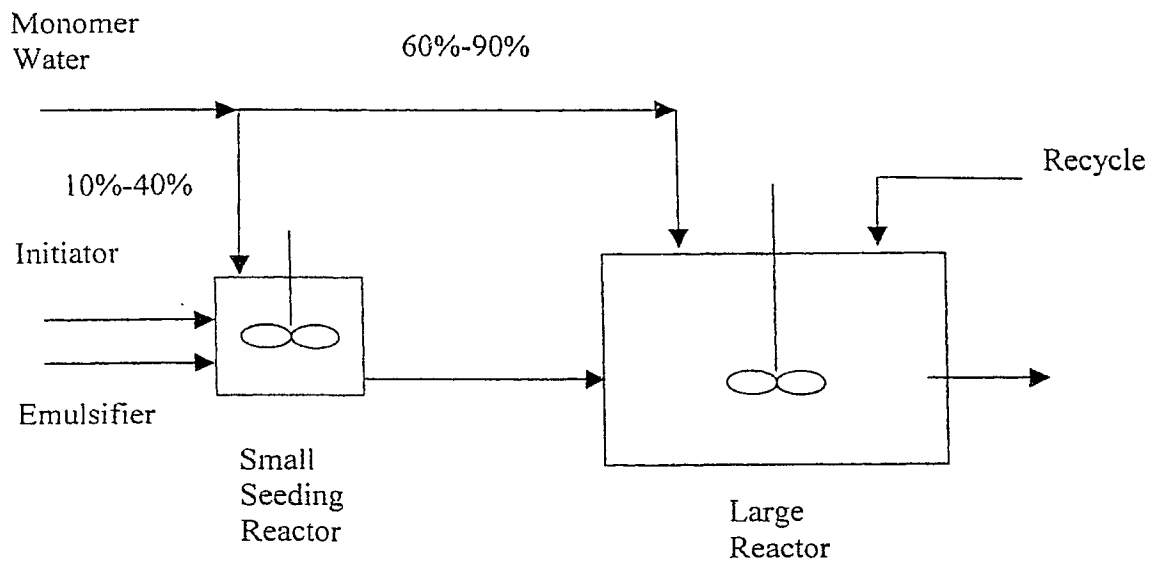
Figure 4. 90. Continuous Reactor Train Configuration

A definition of flow split was proposed by Penlidis (1986), which is more easily applicable for on-line measurements.

Split Definition

The split defined by Penlidis (1986) is as follows:

$$S_p = \frac{M_1 + W_1^{Tot}}{FT}$$ (4.1)

Where M_1 denotes the flow rate of monomer to the first reactor (R_1) and W_1^{Tot} is defined as:

$$W_1^{Tot} = W_1 + I_{R_1} + S_{R_1}$$ (4.2)

FT is the total volumetric flow rate to the second reactor which will be :

$$FT = M_1 + W_1 + I_{R_1} + S_{R_1} + M_2 + W_2$$ (4.3)

Table 4.3 shows the flow rate profiles of this run. Initiator flow rate and split are changed to show their effect on conversion. The conversion behaviour for parts A, B and C is shown in Figures 4.99-4.101.

108

Table 4. 3 Continuous Run Operating Condition

Flow Rate (mL/min)	A	B	C
M_1	10	10	10
M_2	38	38	70
W_1	16	16	0
W_2	63	63	63
I	10	10	10
S	30	30	14
Split	0	0.395	0.204
C_I=0.167 mol/L	C_S=0.139 mol/L	k_v=1.4	θ_2=30 minutes
V_2=5000mL	V_1=500 mL	T=50°C	

During part A, no initiator is fed to the seed reactor, so this reactor acts like an emulsifying vessel with zero conversion. In this part when all initiator is diverted to the second reactor, the oscillatory behaviour is evident which verifies the usual unstable behaviour of conventional CSTRs once more. In parts B and C, the polymerization starts by feeding some amount of initiator to the first reactor. Although this reactor has oscillatory behaviour, the second reactor reaches its steady behaviour soon after start-up and does not show any oscillation. These results again show the stable behaviour of the new train in the presence of the seeding reactor (Figures 4.99-4.101).

The solid line in Figure 4.102 shows the model prediction, which is close to experimental data (Penlidis, 1986). The decrease in conversion of part C (experimental data) is due to problem happened during running the experiments such as: leakage or inconsistency in emulsifier and monomer flow rate to the first reactor. These problems usually mean lower polymerization rate and number of polymer particles.

Generally the two-reactor configuration presented its superiority to the conventional reactor in overdamping the oscillation. If the emulsion polymerization is carried out in these reactors, the main focus can be on controlling the operating conditions to produce high quality latex since the reactor operates under stable condition. The splitted amount of defined split can affect the product properties so it is important to apply control scheme to

109

have the optimal split. Obviously, any other controller must be considered mainly for the seeding reactor and what is just important about the second reactor it trying to keep the emulsifier concentration under its CMC level throughout the reaction in order to avoid any more particle generation which results in overshoots in its behaviour.
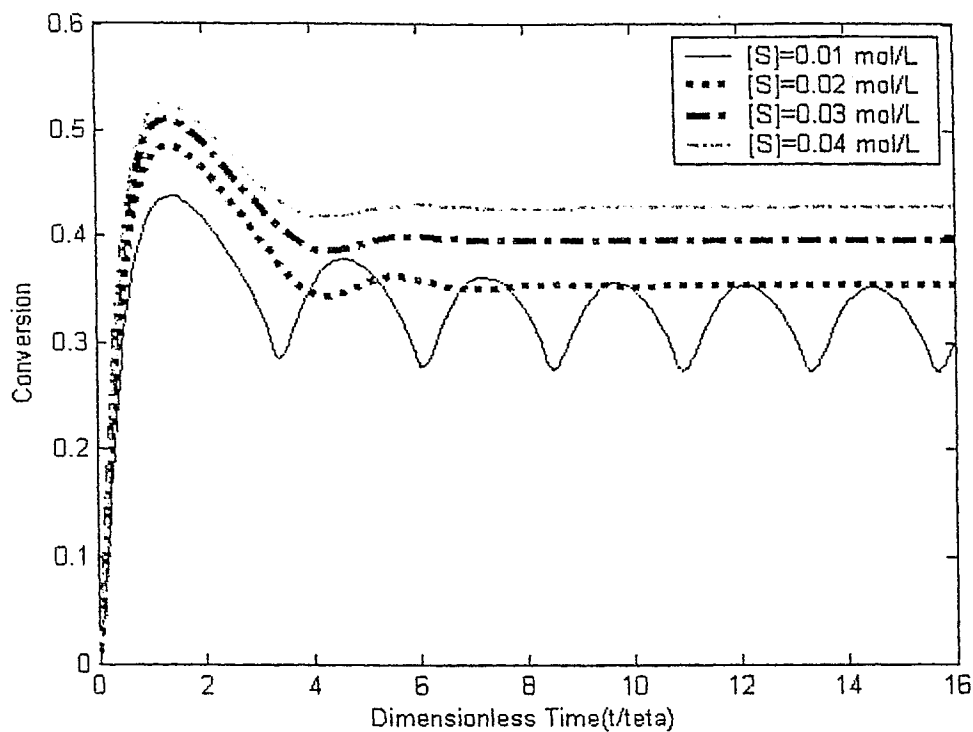
Figure 4. 91. Effect of Emulsifier Concentration on Conversion
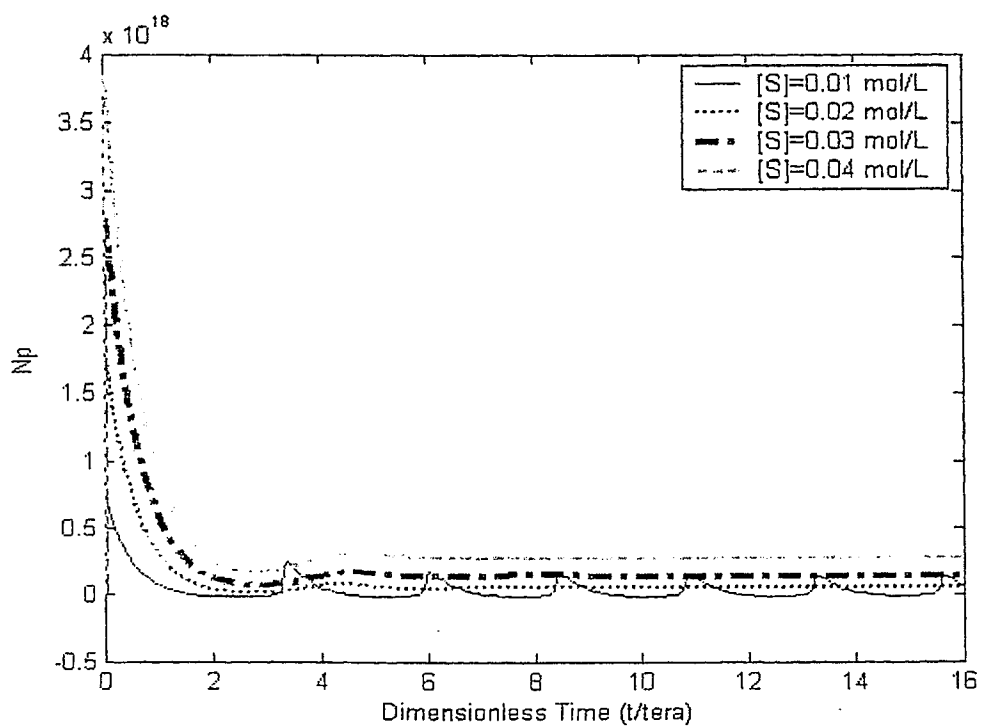

Figure 4. 92. Effect of Emulsifier Concentration on Np

111
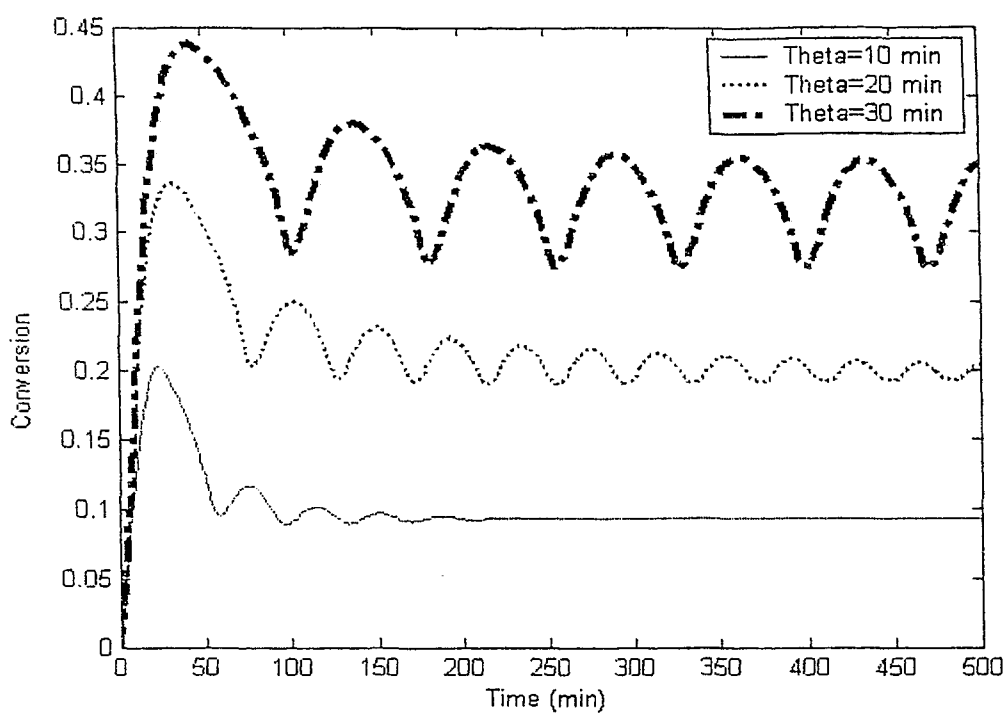
Figure 4. 93. Effect of Mean Residence time on Conversion
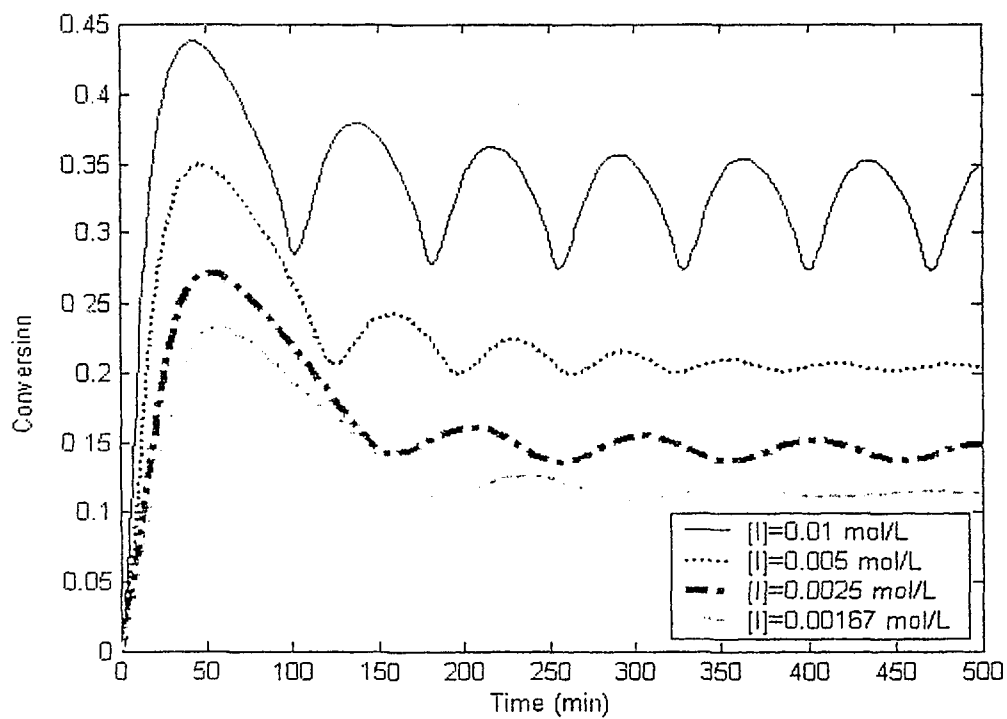
Figure 4. 94. Effect of Initiator Concentration on Conversion

112
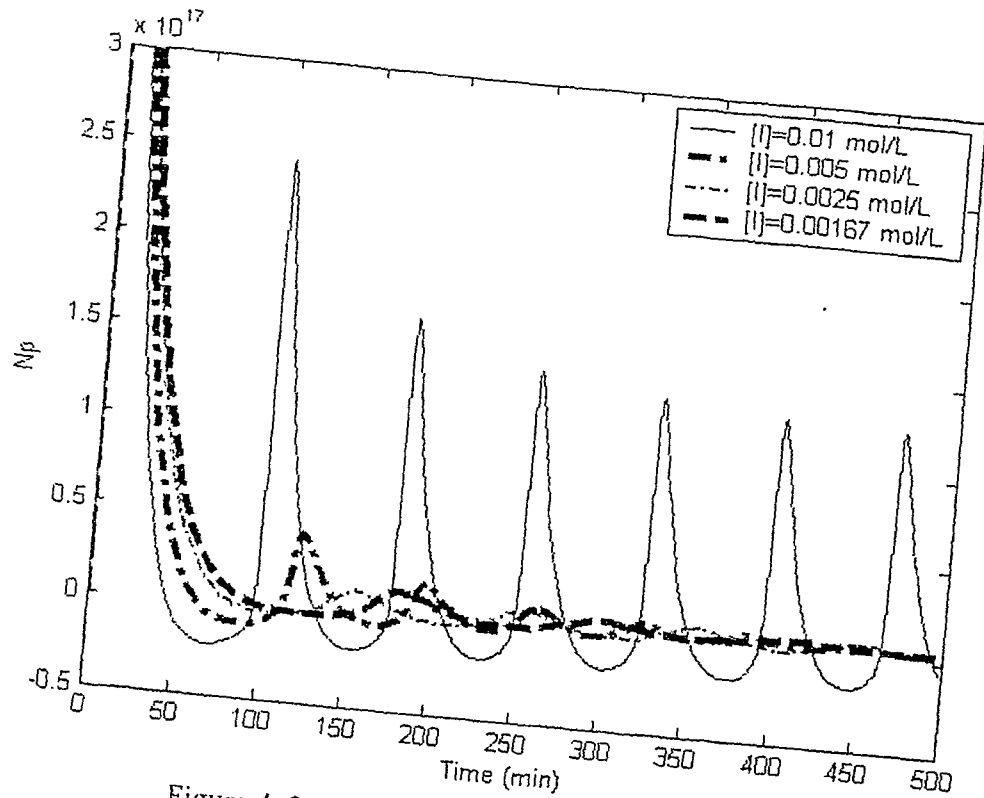
Figure 4. 95. Effect of Initiator Concentration on Np
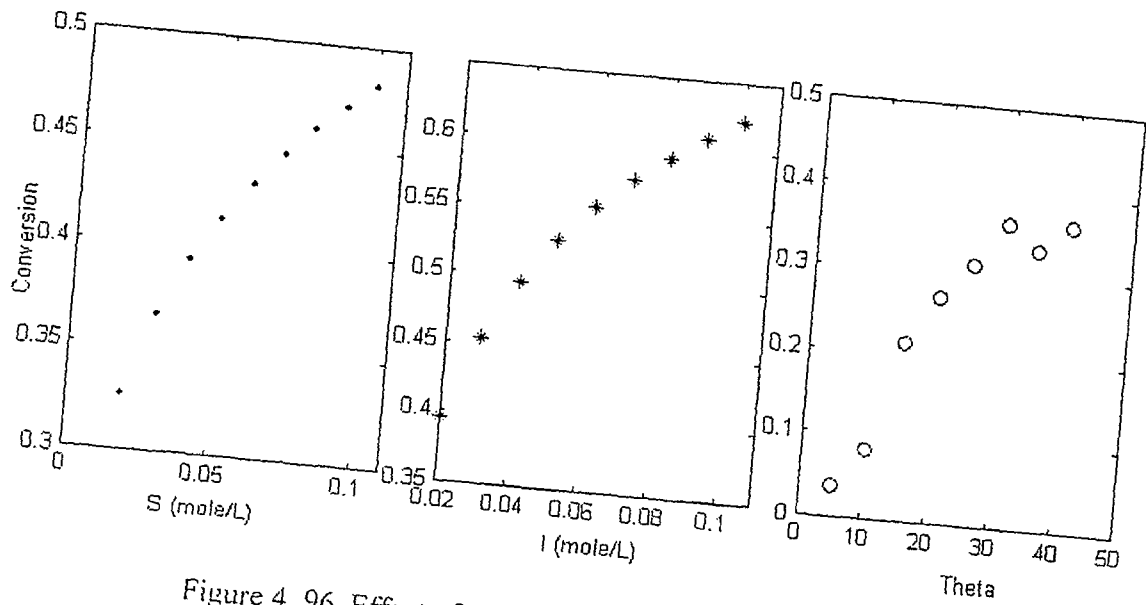
Figure 4. 96. Effect of Operating Condition on Conversion

113
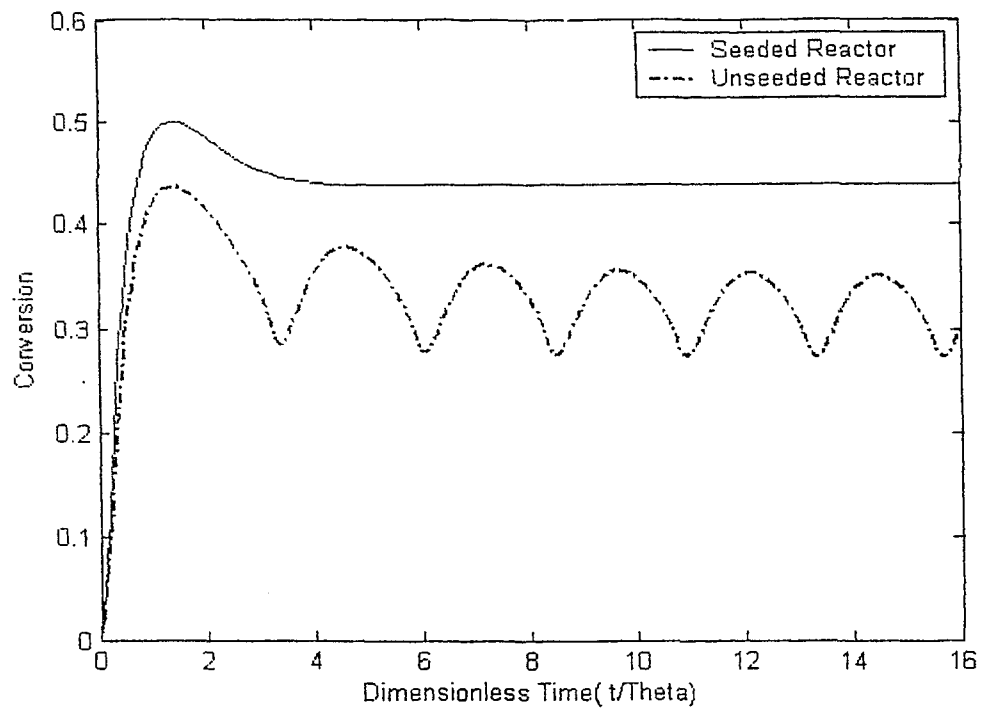
Figure 4. 97. Seeded Reactor Performance in Elimination of Oscillation
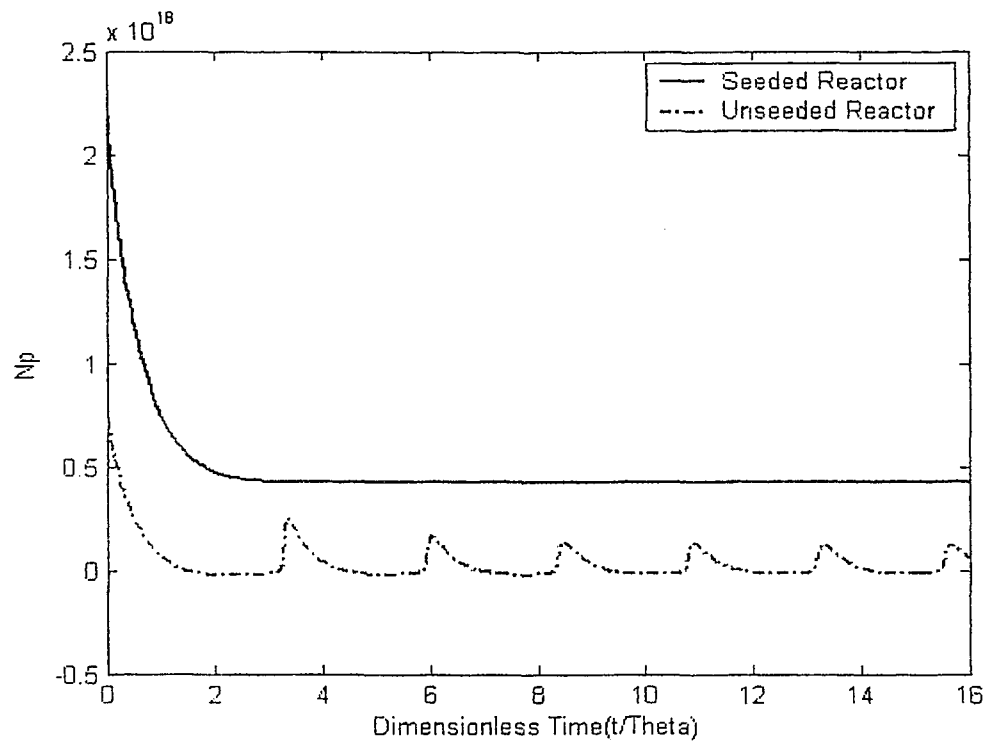

Figure 4. 98. Seeded Reactor Performance in Elimination of Oscillation

114
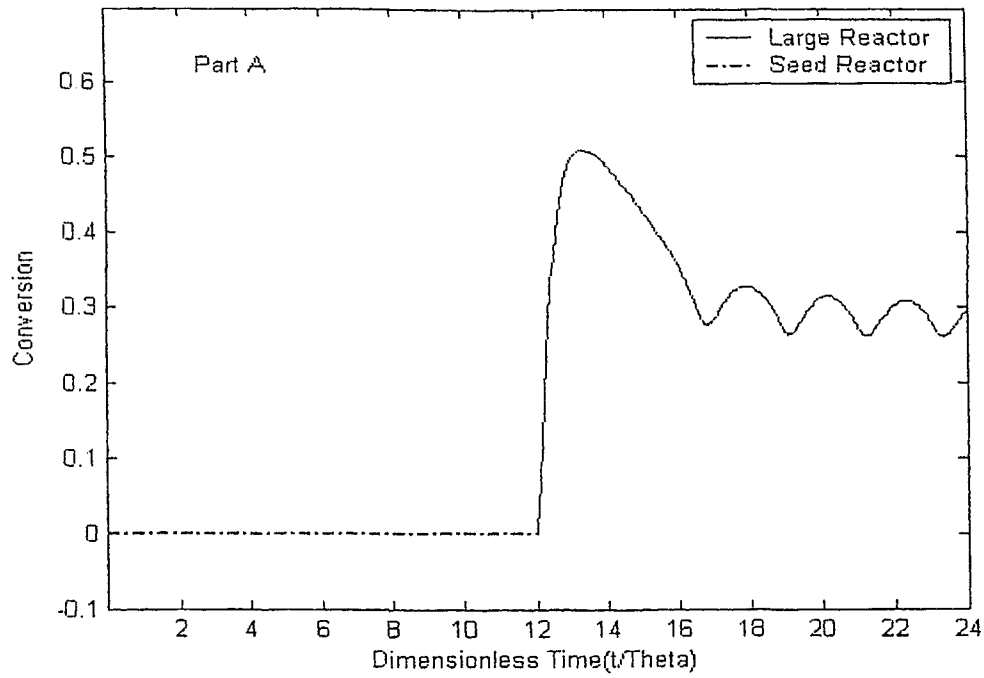
Figure 4. 99. Conversion Versus Time in the New Configuration
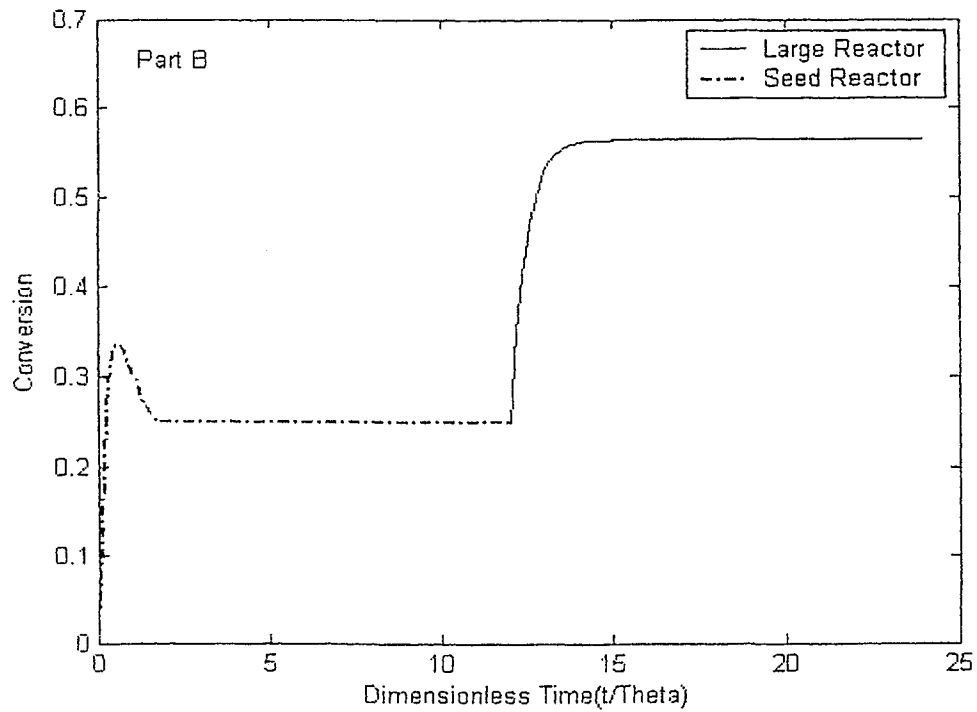
Figure 4. 100. Conversion Versus Time in the New Configuration

115
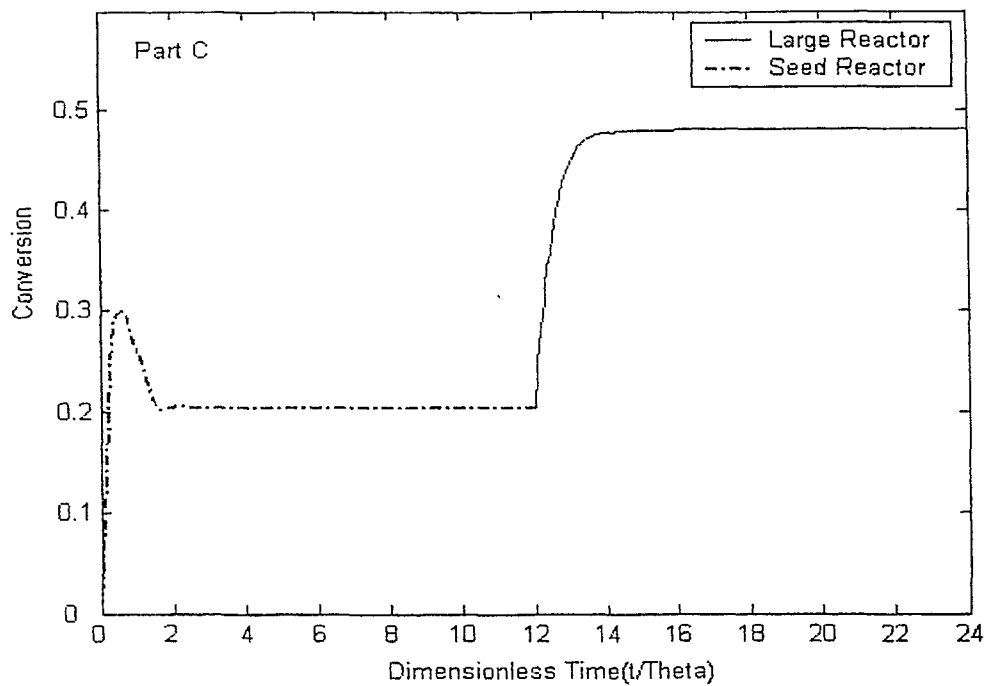
Figure 4. 101. Conversion Versus Time in the New Configuration
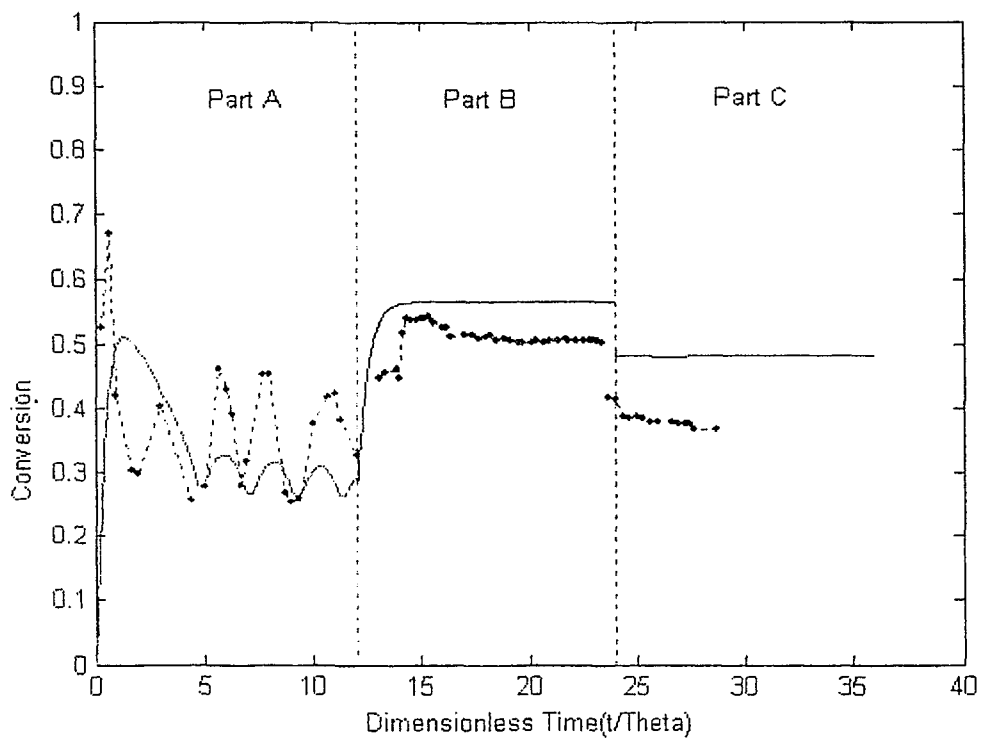
Figure 4. 102. Comparison of Model Prediction with experimental Data

116

Chapter 5

Conclusions

The reaction mechanism of emulsion polymerization was described in detail in this study. A mathematical model was developed for emulsion polymerization and applied on batch, semi-batch and continuous reactors. The probability of presence of monomer soluble impurities was also considered in this model since in industrial scale plants, it is very common to have some impurity in monomer. The model was tested for polymerization of vinyl acetate. Moreover, the effects of initiator and emulsifier concentrations as well as reactor temperature on monomer conversion and product properties have been investigated in detail. The results revealed the sensitivity of the process to these variables. The simulation results were compared with experimental data and the model successfully followed these data in most of the conditions.

The next section of this study deals with optimization of the process in both batch and continuous reactors. The optimization of batch reactor was carried out mainly with the aim of increasing the monomer conversion as well as producing polymer with desired properties. Some suggestions were proposed to enhance the quality of the polymer in the continuous reactor mode, the main problem as shown in chapter 4 is reactor's oscillatory behaviour, therefore some remedies have been suggested and the results were also in good agreement with experimental data.

117

Chapter 6

Recommendations

Since this study was only a theoretical research paper, there can be some recommendation considered in future works.

- Set up a small emulsion polymerization reactor and perform some lab-scale experiments

- Performance of some experiments to test the validity of proposed optimization policies for batch and continuous reactors.

- Application of the same study on emulsion copolymerization with the aim of enhancing polymer properties

118

References

Asua, M. J., M. Vicente and J. R. Leiza, "Control Of Microstructural Properties In Emulsion Polymerization Systems", Macromol. Symp. **182**, 291-303 (2002).

Broadhead, T. O., A. E. Hamielec and J. F. Macgregor, "Dynamic Modelling Of The Batch, Semi-Batch And Continuous Production Of Styrene/Butadiene Copolymerization By Emulsion Polymerization", Makromol. Chem. Suppl. **10/11**, 105-128 (1985).

Chiu, W. and C. Lee, "Kinetic Study On The Poly (Methyl Methacrylate) Seeded Soapless Emulsion Polymerization Of Styrene", J. Appl. Polym. Sci. **65**, 425-438 (1997).

Choi, K. Y. and T. J. Crowley, "Calculation Of Molecular Weight Distribution From Molecular Weight Moments In Free Radical Polymerization", Ind. Eng. Chem. Res. **36**, 1419-1423 (1997).

Corriou, J. P., C., Gentric, F. Pla and M. A. Latifi, "Optimization And Non-Linear Control Of A Batch Emulsion Polymerization Reactor", Chem. Eng. J. **75**, 31-46 (1999).

Doyle III, F. J., C. D. Immanuel, C. F. Cordeiro and S. S. Sundaram, "Population Balance PSD Model For Emulsion Polymerization With Steric Stabilizers", AICHE J. **49/6**, 1392-1404 (2003).

Fitch, R. M. and C. H. Tsai, "Particle Formation In Polymer Colloids. III. Prediction Of The Number Of Particles By A Homogeneous Nucleation Theory", In: Fitch RM, editor. Polymer colloids. New York: Plenum Press, 73-102 (1971).

Friis, N. and A. E. Hamielec, "Kinetics Of Vinyl Chloride And Vinyl Acetate Emulsion Polymerization", J. Appl. Polym Sci. **19**,97 (1975).

Gao, J. and A. Penlidis, "Mathematical Modeling And Computer Simulator/Database For Emulsion Polymerizations", Prog. Polym. Sci. **27**, 403-535 (2002).

Gao, J., K. D. Hungenberg and A. Penlidis, "Process Modeling And Optimization Of Styrene Polymerizations", Macromol. Symp. **206**,509-522 (2004).

Ghadi, N., "Modeling of an Emulsion Polymerization Reactor", Internal Report, Department of Chemical Engineering, Ryerson University, Ontario, March (2004).

Hamielec, A. E., J. F. Macgregor and A. Penlidis, "Multicomponent Free-Radical Polymerization In Batch, Semi-Batch And Continuous Reactors", Makromol. Chem., Macromol. Symp. **10/11**, 521-570 (1987).

Harada, M., M. Nomura, W. Eguchi and S. Nagata, "Studies of The Effect of Polymer Particles on Emulsion Polymerization of Vinyl Acetate", J. Chem. Eng. Of Japan **4**, 54-60 (1971).

Harkins, W. D., "A General Theory Of The Mechanism Of Emulsion Polymerization", J. Am. Chem. Soc. **69**,1428 (1947).

Jang, S. S. and P .H. Lin, "Discontinuous Minimum End-Time Temperature/Initiator Policies For Batch Emulsion Polymerization Of Vinyl Acetate", Chem. Eng. Sci. **46/12**, 3153-3163 (1991).

Jang, S. S. and W. L. Yang, "Dynamic Optimization Of Batch Emulsion Polymerization Of Vinyl Acetate-An Orthogonal Polynomial Initiator Policy", Chem. Eng. Sci. **44/3**, 515-528 (1989).

Kiparissides, C., Ph.D. Thesis, Dept of Chemical Engineering, McMaster University, Hamilton, Ontario (1978).

Kiparissides, C., D. S. Achilias and C. E. Frantzikinakis, "The Effect Of Oxygen On The Kinetics And Particle Size Distribution In Vinyl Chloride Emulsion Polymerization", Ind. Eng. Chem. Res. **41**, 3097-3109 (2002).

Kumar, A. and R. K. Gupta, "Fundamentals Of Polymers", McGraw-Hill, 224-257 (1998).

Leiza, J. R., G. Arzamendi and J. M. Asua, "Copolymer Composition Control in Emulsion Polymerization Using Technical Grade Monomers", Polym Int. **30**, 455 (1993).

Liang, W. R., D. N. Butala and K. Y. Choi, "Multiobjective Dynamic Optimization Of Batch Free Radical Polymerization Process Catalyzed By Mixed Initiator Systems", J. Appl. Polym. Sci. **44**, 1759-1778 (1992).

Lovell P. A., D. Britton and F. Heatley, "Chain Transfer To Polymer In Free-Radical Bulk And Emulsion Polymerization Of Vinyl Acetate Studied By NMR Spectroscopy", Macromol. **31**, 2828-2837 (1998).

Lu Y. and C. Lin, "Simulation Of Particle Size Distribution In Continuous Emulsion Polymerization Of Styrene Monomer", Polym. Eng. And Sci. **26**/2, 127-132 (1985).

Lu Y. and C. Lin, "The Effect Of Radical Desorption On The Particle Size Distribution In Vinyl Acetate Emulsion Polymerization", Polym. Eng. And Sci. **25**/1, 57-63 (1986).

Meira, G. R., A. Salazar, L. M. Gugliotta and J. R. Vega, "Molecular Weight Control In A Starved Emulsion Polymerization Of Styrene", Ind. Eng. Chem. Res. **37**, 3582-3591 (1998).

121

Nomura, M., M. Harada, K. Nakagawara, W. Eguchi and S. Nagata, "The Role Of Polymer Particles In The Emulsion Polymerization Of Vinyl Acetate", J. Chem. Eng. Jpn **26**, 17-26 (1981).

Nomura, M., X. Wei, H. Takahashi and S. Sato, "Continuous Emulsion Polymerization Of Styrene In A Single Couette-Taylor Vortex Flow Reactor", J. Appl. Polym. Sci. **80**, 1931-1942 (2001).

Nomura, M., S. Sasaki, K. Xue and W. Fujita, "Continuous Emulsion Polymerization Of Vinyl Acetate. I. Operation In A Single Continuous Stirred Tank Reactor Using Sodium Lauryl Sulfate As Emulsifier", J. Appl. Polym. Sci. **86**, 2748-2754 (2002).

Odian, G., "Pronciples Of Polymerization", A Wiley-Interscience Publication, New York, 335-355 (1991).

Ohmura, N., S. Watanabe, K. Kataoka and M. Okubo, "Controlling Particle Size By Self-Sustained Oscillations In Continuous Emulsion Polymerization Of Vinyl Acetate", Chem. Eng. Sci. **53**/12, 2129-2135 (1998).

Ohmura, N., T. Yano, K. Kataoka and K. Kitamoto, "Novel Operating Method For Controlling Latex Particle Size Distribution In Emulsion Polymerization Of Vinyl Acetate", Ind. Eng. Chem. Res. **40**, 5177-5183 (2001).

Penlidis, A., A. E. Hamielec and J. F. MacGregor, "Dynamic Modeling Of the Continuous Emulsion Polymerization Of Vinyl Chloride", J. Vinyl Tech. **6**/4, 134-142 (1984).

Penlidis, A., "Polymer Reactor Design, Optimization and Control in Latex Production Technology", Ph.D. Thesis, Dept of Chemical Engineering, McMaster University, Hamilton, Ontario (1986).

Penlidis, A., J. F. MacGregor and A. E. Hamielec, "Effect Of Impurities On Emulsion Polymerization", J. Appl. Polym. Sci. **35**, 2023-2038 (1988).

Penlidis, A., M. A. Dube, R. K. Mutha and W. R. Cluett, "Mathematical Modeling Of Emulsion Copolymerization Of Acrylonitrile/Butadiene", Ind. Eng. Chem. Res. **35**, 4434-4448 (1996).

Pinto, J. C., C. Sayer, P. H. H. Araujo, G. Arzamendi, J. M. Asua and E.L. Lima, "Modeling Molecular Weight Distribution In Emulsion Polymerization Reactions With Transfer To Polymer", J. Polym. Sci. Part A **39**, 3515-3528 (2001).

Pollock, M. J., J. F. MacGregor and A. E. Hamielec, "Computer Applications In Applied Polymer Science", ACS Symposium Series 197, Washington, D.C. (1981).

Rawlings, J. B. and W. H. Ray, "The Modelling Of Batch And Continuous Emulsion Polymerization Reactors. Part I: Model Formulation And Sensitivity To Parameters", Polym Eng. And Sci. **28/5**, 237-256 (1988).

Rawlings, J. B. and W. H. Ray, "The Modelling Of Batch And Continuous Emulsion Polymerization Reactors. Part II: Comparison With Experimental Data", Polym Eng. And Sci. **28/5**, 257-274 (1988).

Scholtens, C., J. Meuldijk and I. B. Drinkenburg, "Emulsion Copolymerization In A Pulsed Packed Column", 6th World Cong. Of Chem. Eng., Melbourne, Australia (2001).

Smith, W. V. and R. H. Ewart, "Kinetics Of Emulsion Polymerization", Chem. Phys. **16**, 592 (1948).

Tobita, H., "Kinetics Of Long-Chain Branching In Emulsion Polymerization: 2. Vinyl Acetate Polymerization", Polym. J. **35**, 3032-3038 (1994).

Wu, G. Z., L. A. Denton and R. L. Laurence, "Batch Polymerization Of Styrene-Optimal Temperature Histories", Polym. Eng. And Sci. **22**, 1-8 (1982).

Appendix A

Extra Figures

125
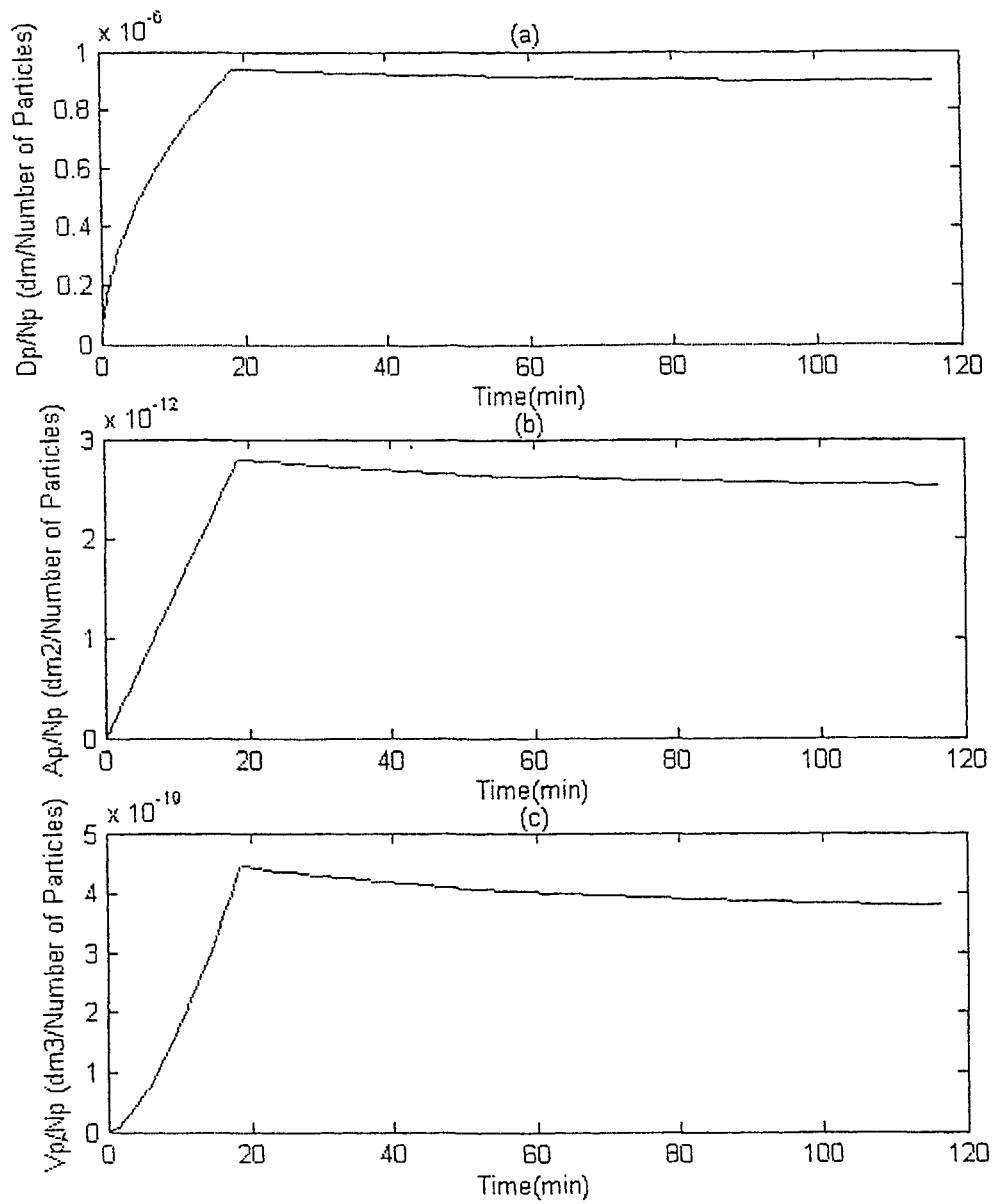
Figure A.1. Case 1. Particle (a) Diameter, (b) Surface Area, and (c) Volume Per Number of Particles

126
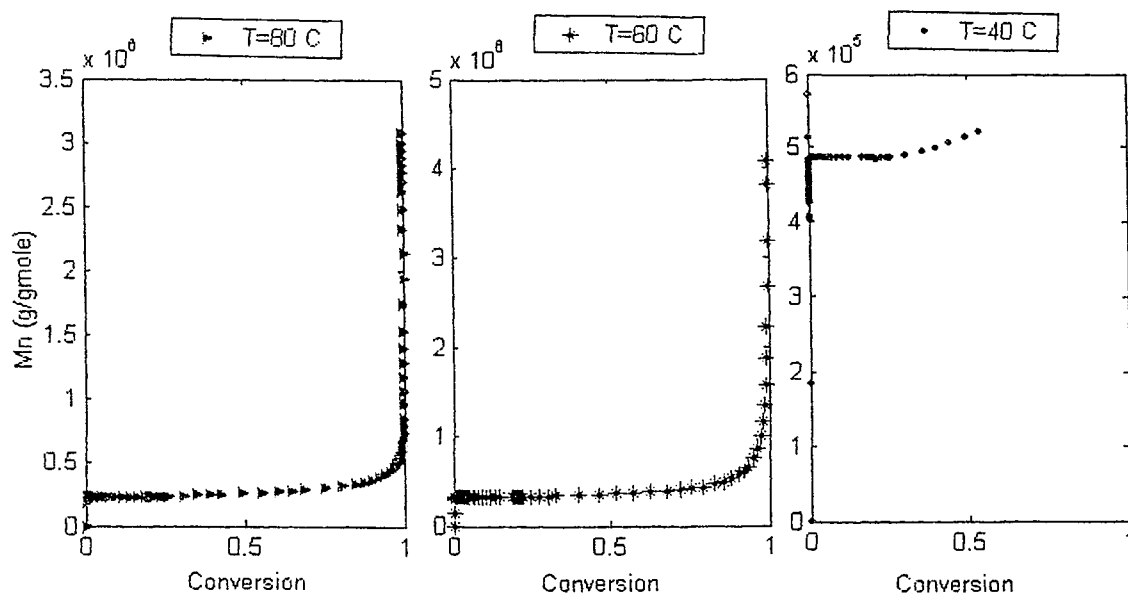
Figure A.2. Case 1. Effect of Reactor Temperature on Mn
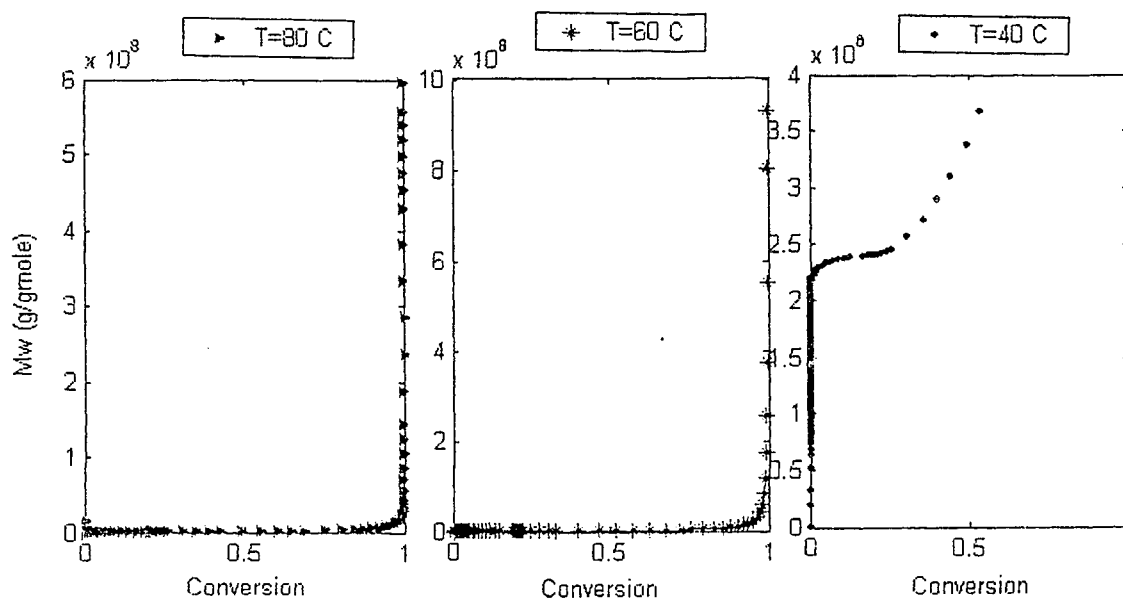
Figure A.3. Case 1. Effect of Reactor Temperature on Mw

127
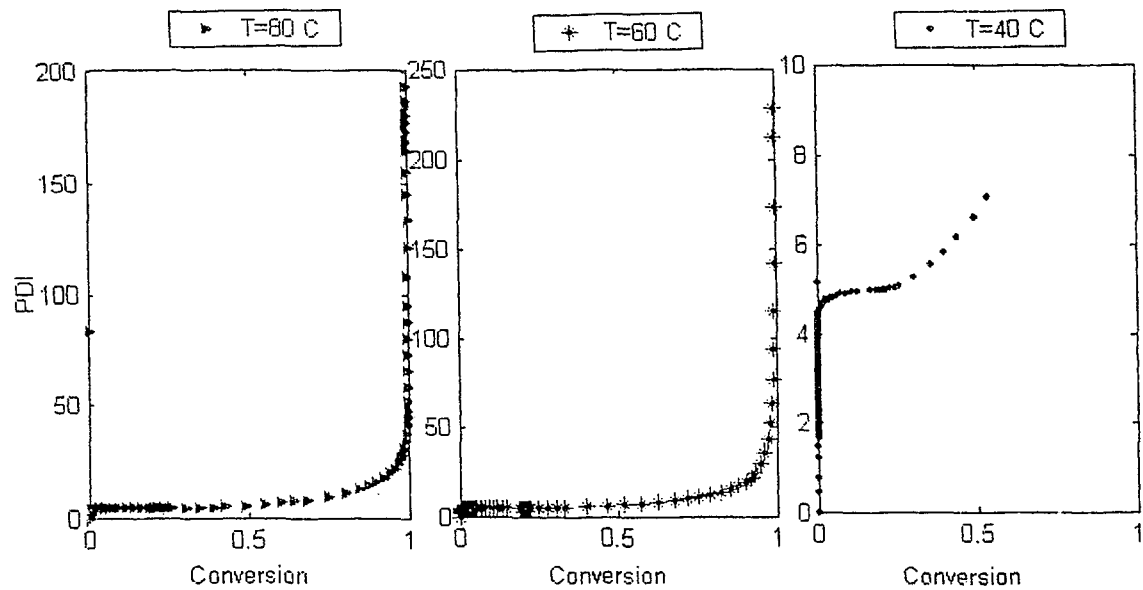
Figure A.4. Case 1. Effect of Reactor Temperature on PDI
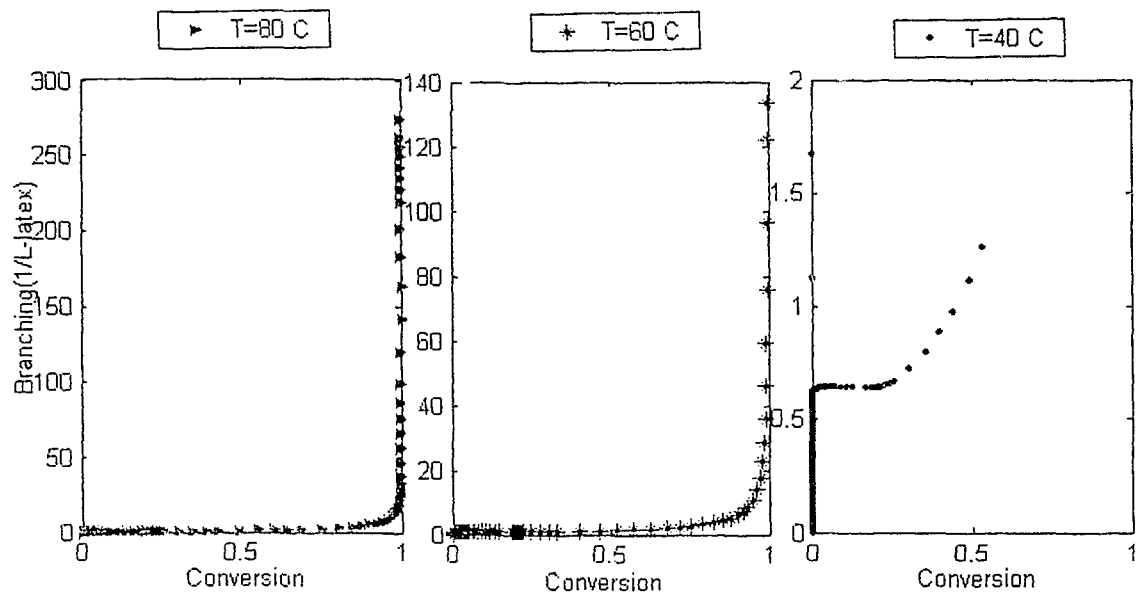
Figure A.5. Case 1. Effect of Reactor Temperature on Number of Branch Points

128
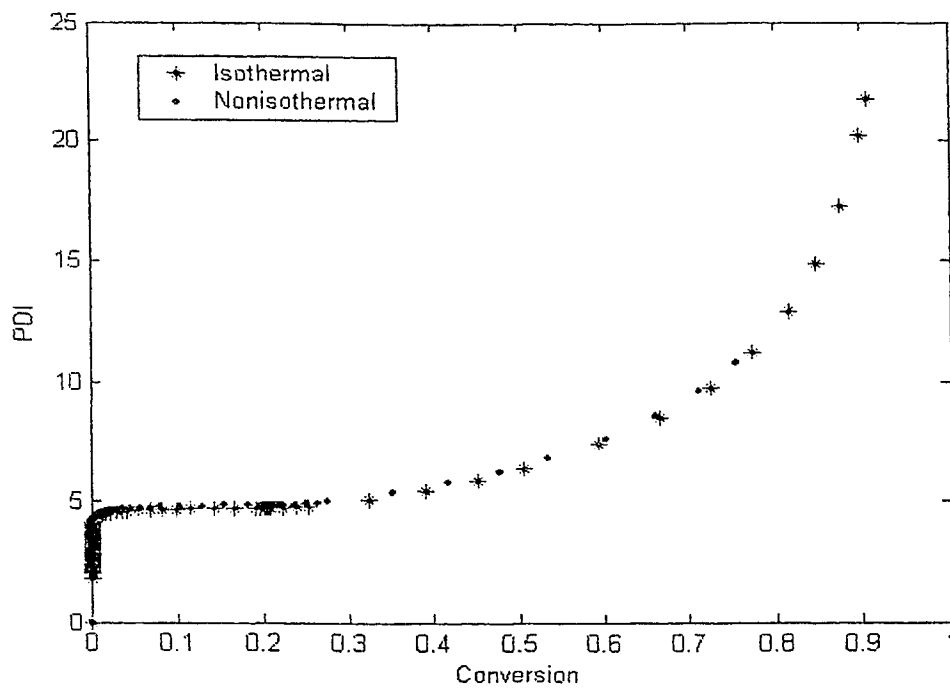
Figure A.6. Case 1. Effect of Nonisothermal Condition on PDI
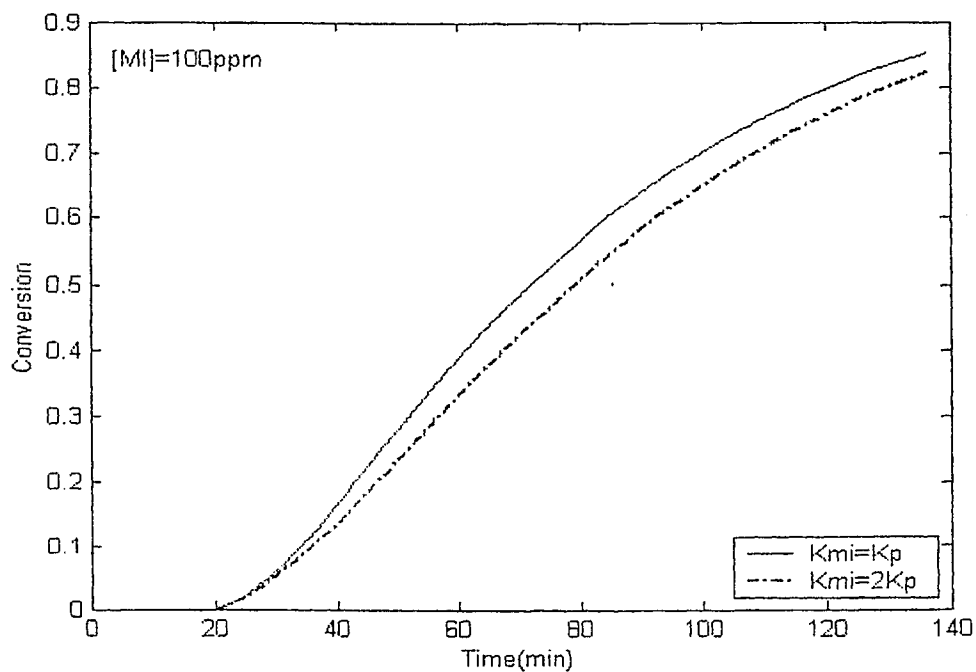
Figure A.7. Case 2. Effect of Rate constant for Transfer to Inhibitor on Conversion

129
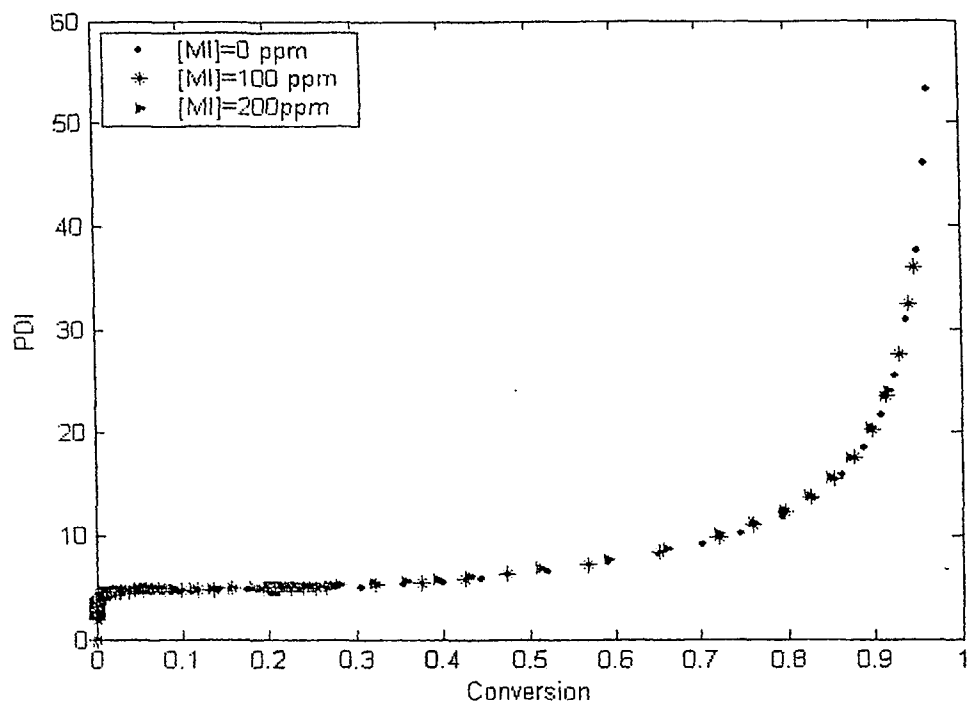
Figure A.8. Case 2. Effect of Impurity on PDI
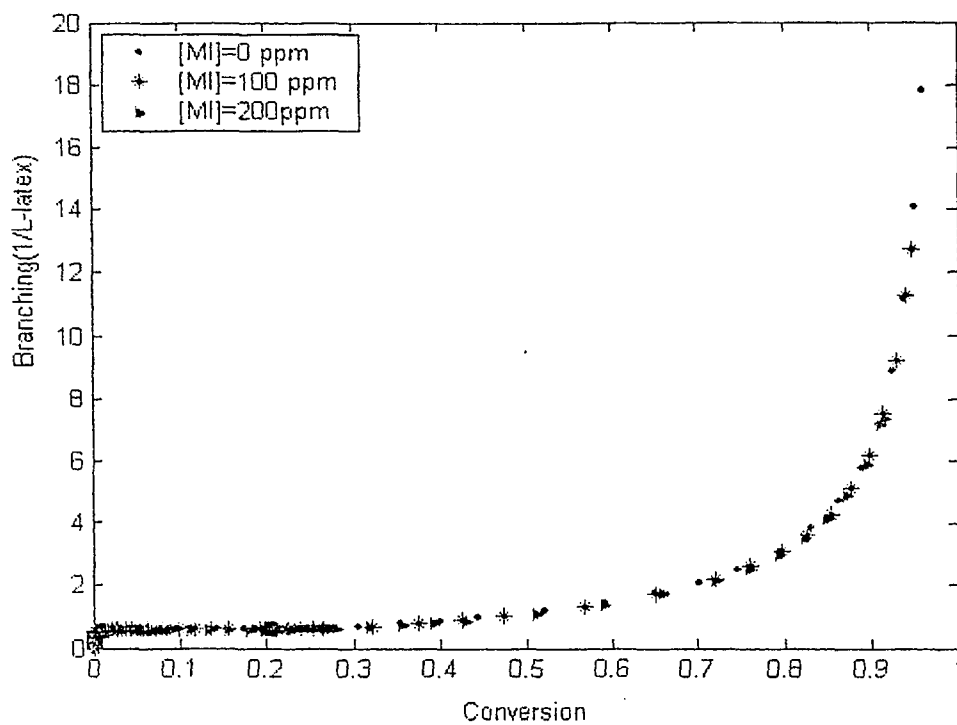
Figure A.9. Case 2. Effect of Impurity on Number of Branch Points

130
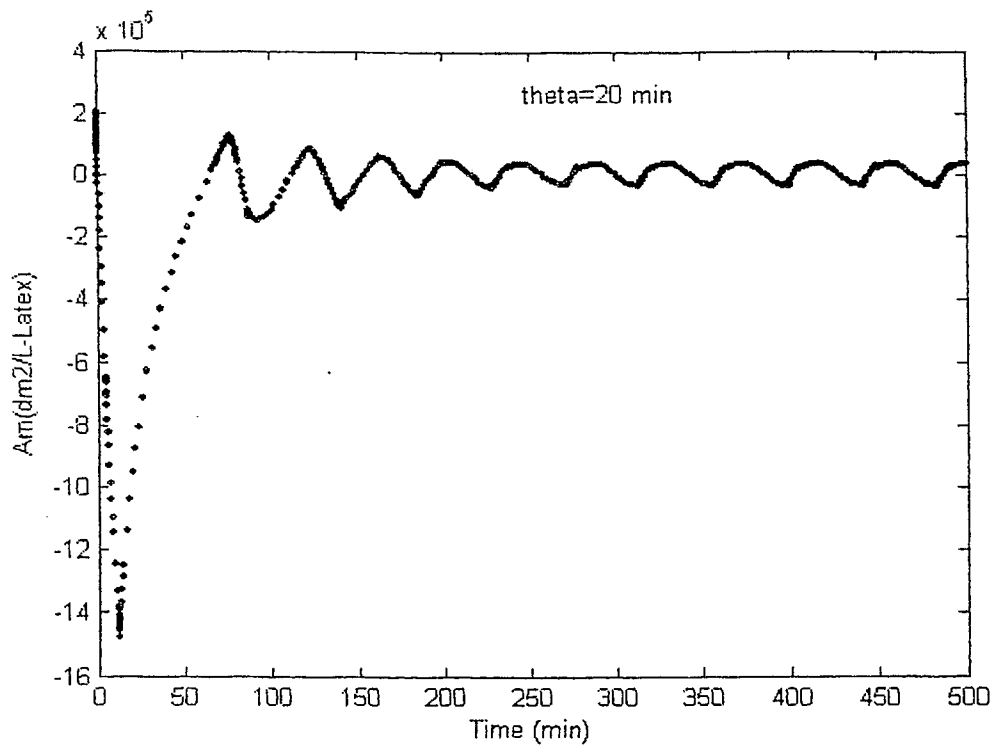
Figure A.10. Case 3. Effect of Residence time on Micellar Area
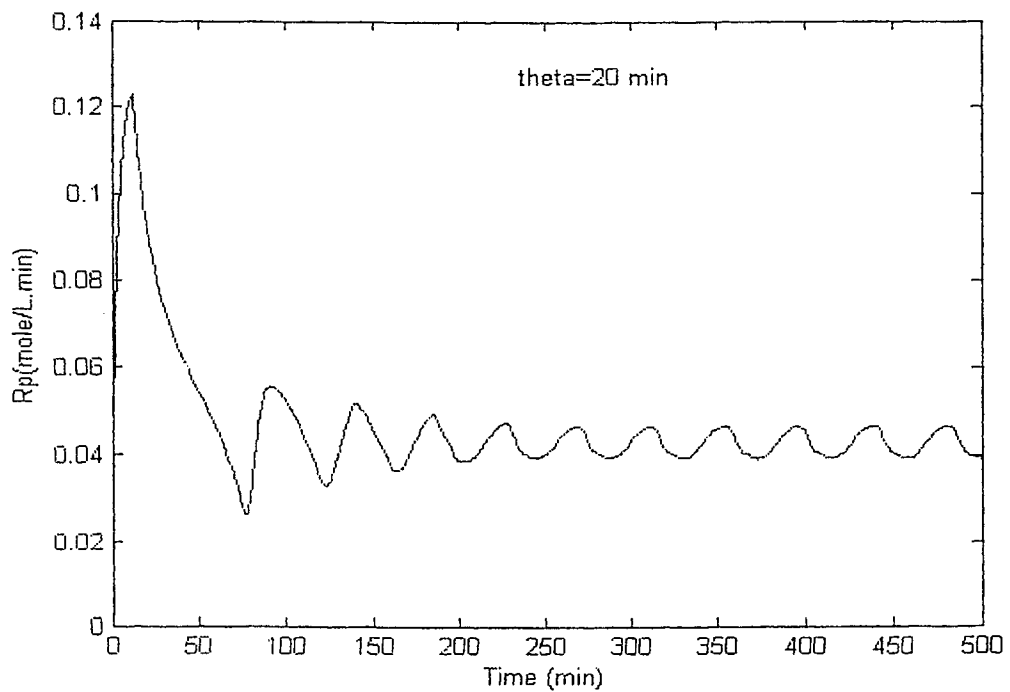
Figure A.11. Case 3. Effect of Residence time on Rp

131
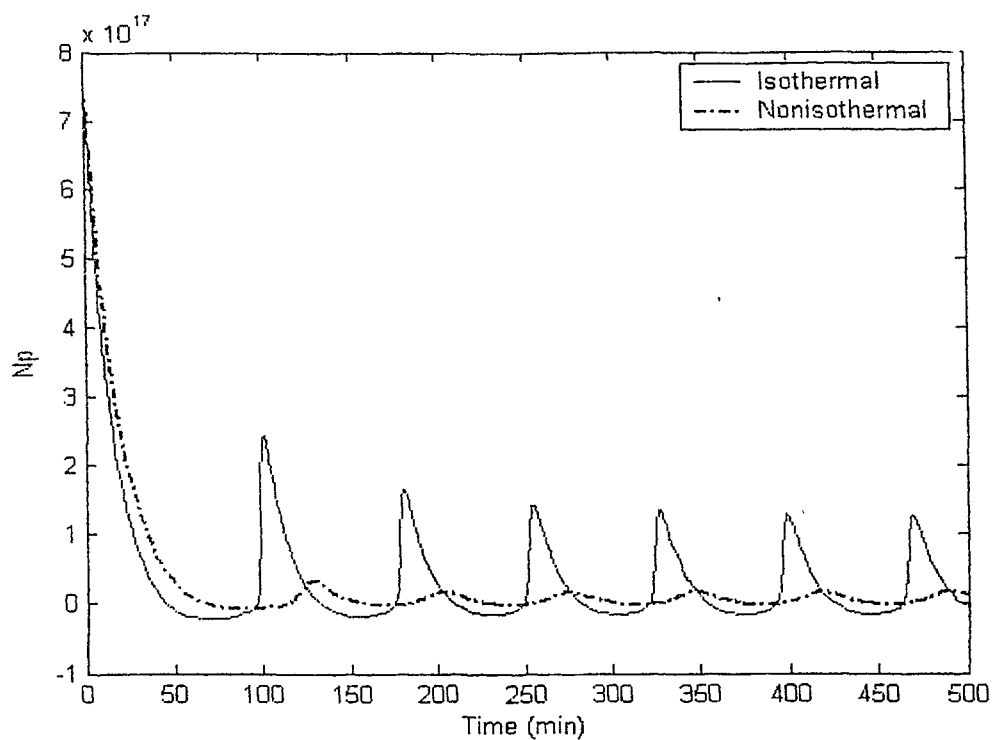
Figure A.12. Case 3. Effect of Nonisothermal Condition on Number of Particles
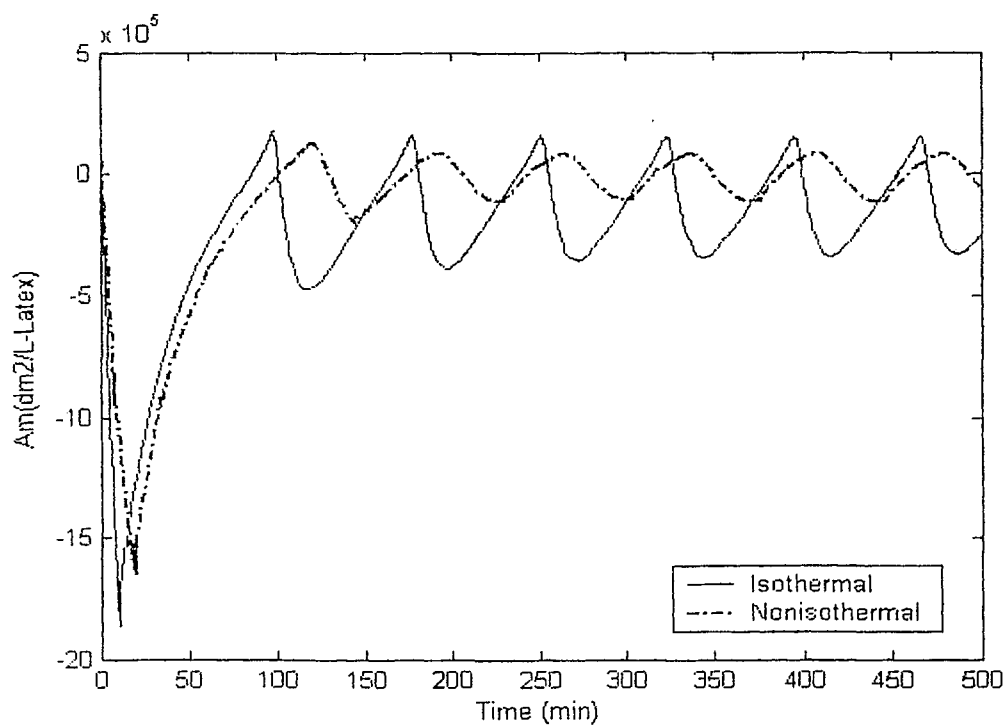

Figure A.13. Case 3. Effect of Nonisothermal Condition on Micellar Area

132
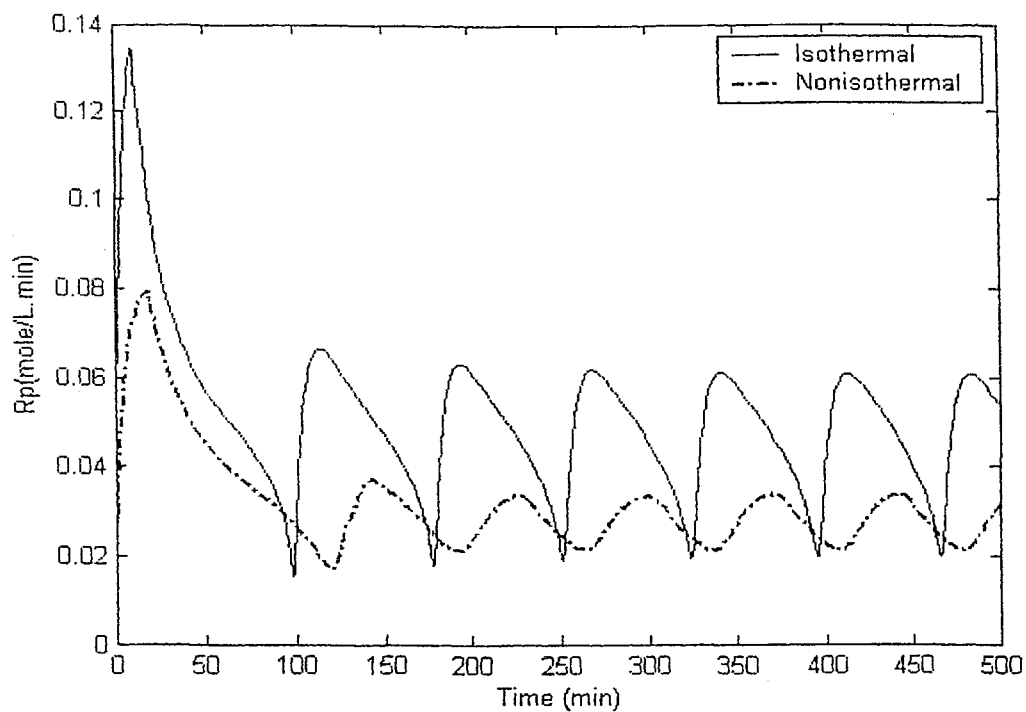
Figure A.14. Case 3. Effect of Nonisothermal Condition on Rp
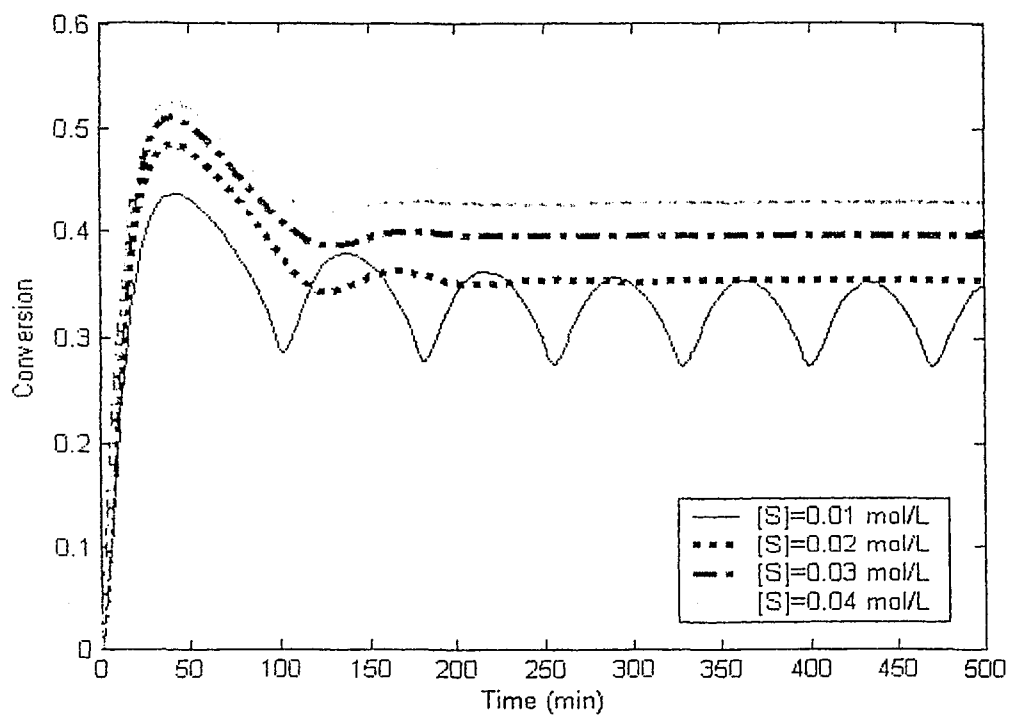

Figure A.15. Effect of Emulsifier Concentration on Conversion

133
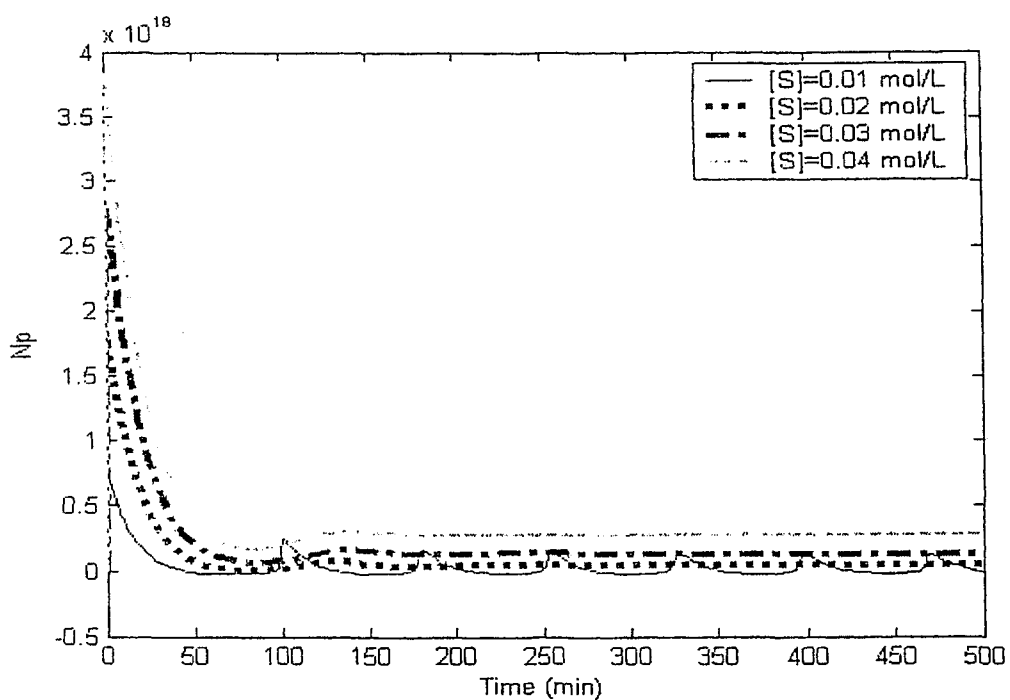
Figure A.16. Effect of Emulsifier Concentration on Np

134